Mount Isa Cu and Pb-Zn-Ag orebodies

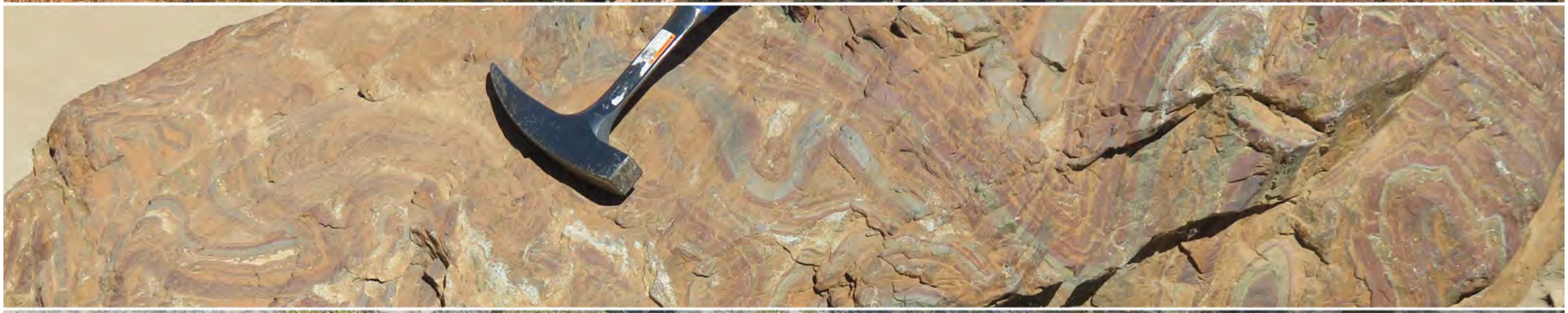

LOCATION

Geological Domain

Leichhardt River Domain

Co-ordinates

Latitude: 20° 43’ 10” S, Longitude: 139° 28’ 52” E

MGA Zone 54: 341795 E, 7707960 N

NATURE OF MINE

Mined Commodities

Cu, Zn, Pb, Ag

Mining Method

Underground (1931-present) and open pit (1957-1965) mining;

Depth of Mining

1800 m (underground); 150 m (open cut)

PRODUCTION AND DIMENSIONS

Mineralised bodies

Cu mineralisation occurs in extensive zones of silica-dolomite alteration. The main mineralised bodies include the 1100, 1900, 200, 500, 650, 3000 and 3500 orebodies.

Pb-Zn-Ag mineralisation occurs in a series of over 30 stratiform lenses occurring to the north of, and above the copper orebodies.

Dimensions

The Mount Isa copper orebody as a whole covers an extent of over 4kms and a vertical extent of 1800 metres (Lilly et al, 2017). The dimensions of the main copper orebodies at Mount Isa are as follows (Long, 2010):

Orebody	Length	Width	Vertical Extent
200	300	50	250
500	1300	230	500
650	320	30	450
1100	2330	530	700
1900N	440	80	250
1900S	470	160	300
3000	1200	290	250
3500	1340	260	500

The Zn-Pb-Ag bodies are too numerous to list their dimensions in detail. As examples:

- 5 Orebody has a strike length of approximately 2000 metres, a width of up to 35m metres, and a vertical extent of approximately 1000 metres.
- 12 orebody has a length of approximately 1500m, a width of approximately 10 metres, and a vertical extent of approximately 1000 metres.

Orientation of Mineralised bodies

The Cu orebodies fall into two broad orientation groups: the 500, 1900N and 3500 orebodies are broadly stratabound and dip west at between 60 and 80 degrees; and the 1100, 1900S, 3000, 200 and 650 orebodies dip moderately to steeply west-southwest (ie with an approximate 15 degree sinistral rotation from the orientation of bedding) (Miller, 2007). The 1100, 1900, 3000 and 3500 orebodies show local plunge variations which are broadly parallel to the intersection between bedding in the Urquhart Shale and the underlying basement contact with the Eastern Creek Volcanics. The 1100 and 1900 orebodies show a subhorizontal plunge, while the 3000 and 3500 orebodies plunge moderately to the north. The 200, 500 and 650 orebodies also show a moderate north plunge.

Pb-Zn-Ag orebodies at Mount Isa are broadly stratiform with a 60-65° westerly dip parallel to bedding in the host Urquhart Shale. The main stacked group of orebodies defines and en-echelon group of north-plunging lenses which are bounded to the south by the silica-dolomite alteration zone associated with the copper orebodies and to the north by the NNW-plunging Mount Isa Fold (Davis 2004).

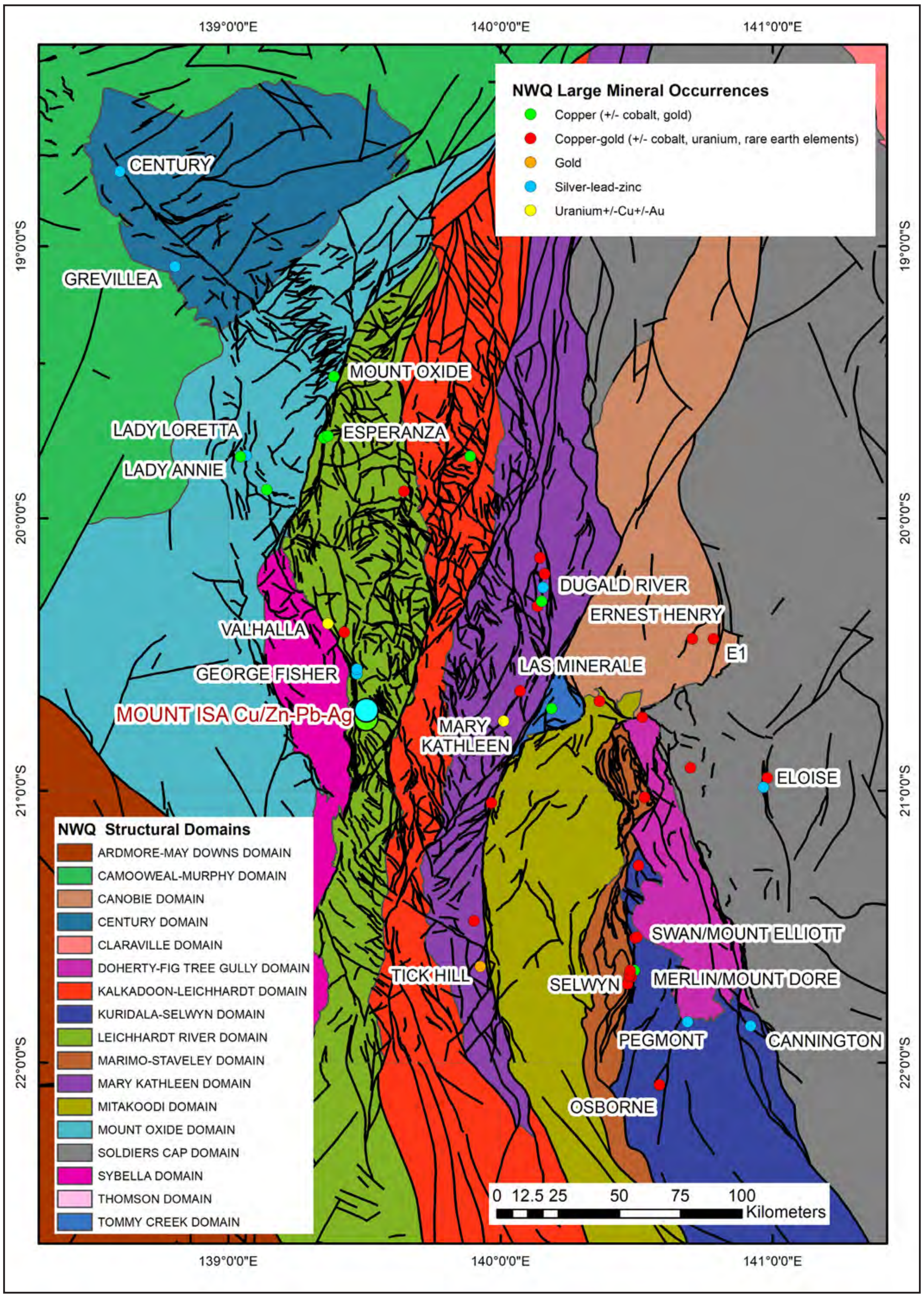

Figure 2.1. Regional location of Mount Isa shown with respect to the Mount Isa Structural Domain Map from the 2010 NWQMEP GIS

The stratiform zone of Zn-Pb-Ag and pyrite enrichment within the Urquhart Shale is much more laterally extensive than the economically-defined orebodies (Painter, 2003), extending along stratigraphically consistent zones for more than 10km north of the economic limit of mineralisation.

Historic Production

7.76mT Cu metal at 3.2% Cu (Ozmin database as of 2011)

11.58mT Pb metal at 5.8% Pb (Ozmin database as of 2011)

15.24mT Zn metal at 5.3% Zn (Ozmin database as of 2011)

118.7mOz Ag at 156g/t Ag (Ozmin database as of 2011)

Recent Production

Glencore reports combined Cu production from Mount Isa and Ernest Henry

Glencore reports combined Zn-Pb-Ag production from Mount Isa, George Fisher and McArthur River

HOST ROCKS

Mine Stratigraphy

The Mount Isa Cu and Zn-Pb-Ag deposits are hosted within the Mesoproterozoic Urquhart Shale of the 1670Ma Mount Isa Group

Major Host Rock

Variably laminated mudstones and siltstones which vary from siliceous to carbonate-rich, with significant and extensive accumulations of fine grained pyrite

Minor Host Rock

A minor amount of copper mineralisation and associated alteration occurs in the Spear Siltsone, which overlies the Urquhart Shale. Copper mineralisation and silica dolomite alteration also encroach slightly on the underlying Native Bee siltstone in the 3500 orebody.

INTRUSIVE ROCKS IN REGION

Granitoids

The Sybella Granite occurs to the West of the Mount Isa deposit, and shows U-Pb radiometric ages in the area of 1670Ma, which shortly precedes the deposition age of the Mount Isa group (Page and Bell, 1986)

Mafic Intrusives

Minor mafic dykes intrude the Mount Isa Group (eg the Spring Creek Dyke)

Other

The Urquhart Shale contains a series of thin tuff marker beds which form important stratigraphic markers for correlation of orebodies in the Mount Isa and George Fisher Mines.

METAMORPHISM

Metamorphic Grade

Regional metamorphism in the Mount Isa Mine is interpreted to be at the Upper Chlorite Zone of Greenschist Facies (Foster and Rubenach, 2006), with an estimated temperature of 300 to 350°C.

STRUCTURAL CHARACTERISTICS

Structural Setting

The Mount Isa orebodies are located in a zone of anomalously thick accumulation of sag-phase sediments of the Isa Superbasin (NWMEP, 2010), depositing in an environment of broadly N-S extension (NWMEP 2010). Early structures include NW-trending faults which mark thickness changes in the Mount Isa Group (eg the Transmitter Fault), south-dipping normal faults which juxtapose Mount Isa group and the older Eastern Creek Volcanics, and the Mount Isa basement fault (sometimes called the Paroo Fault) which also places Mount Isa group in high angle contact with the Eastern Creek Volcanics after or late during deposition of the Mount Isa Group. The Urquhart Shale in the mine area is cut by NE, NW and layer-parallel faults, and also exhibits minor asymmetric moderately NNW-plunging folds with NNW-trending axial surfaces, the most prominent of which is the Mount Isa fold.

In the Mount Isa mine area, the Mount Isa group (including the host Urquhart Shale) dips approximately 65° to the west and is westwardly younging. The Paroo fault truncates the Mount Isa group at a high angle, juxtaposing Mount Isa group against the older Eastern Creek volcanics. The fault is subhorizontal in the southern part of the mine and progresses to steeper easterly dips in the northern parts of the mine. Structural elements occurring in the

Figure 2.2. Regional location of Mount Isa overlain on an image of total magnetic intensity from the GADDS data for the region

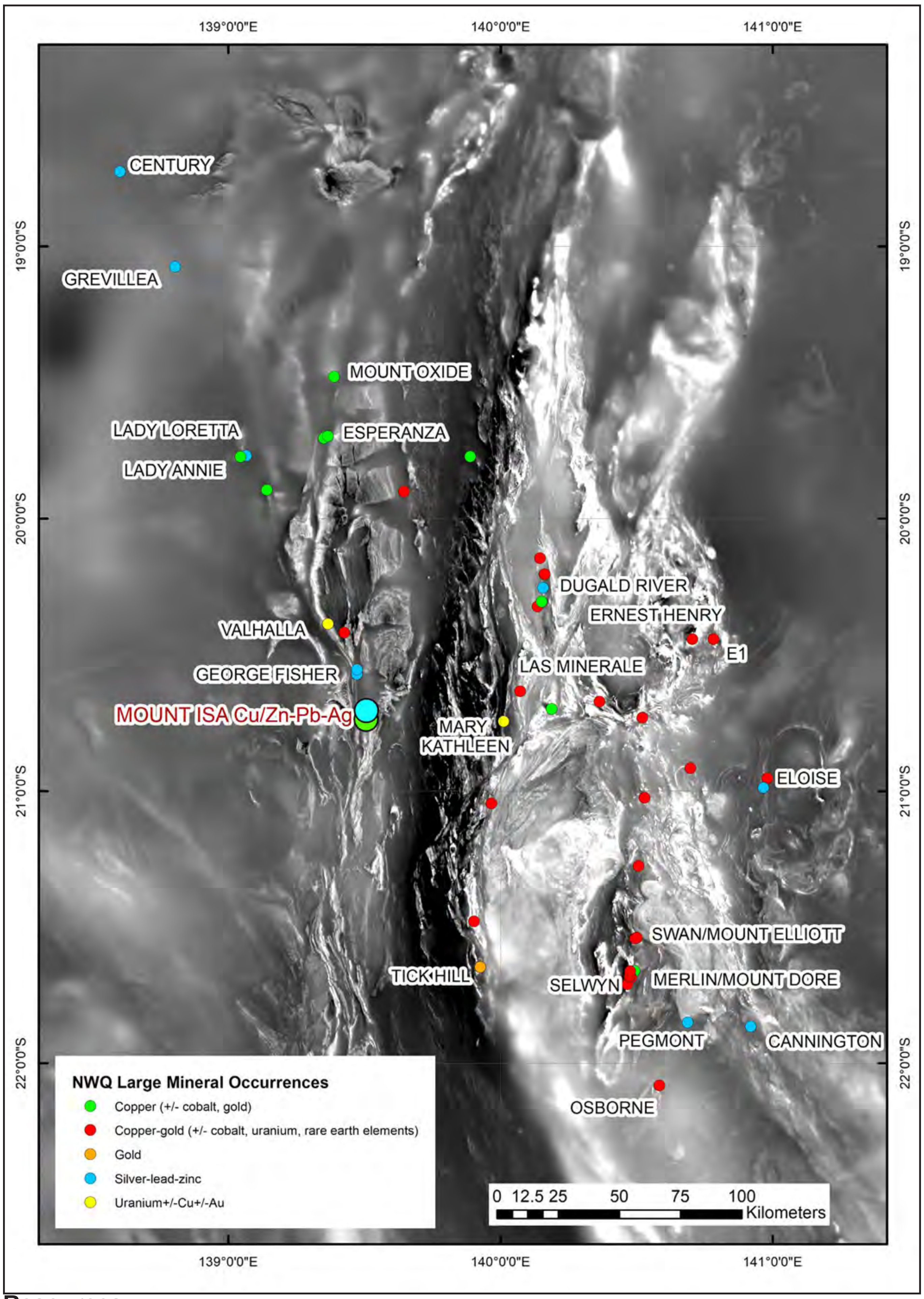

mine area include:

Structural History

The structural history of the rocks exposed in the Mount Isa mine can be summarised as follows:

- The Eastern Creek volcanics were deposited in a broadly N-S rift structure, and trends of sequence thickening suggest the existence of a main rift-bounding fault to the west of the Mount Isa mine (Betts and Lister, 2003)
- Post Leichhardt inversion
- Emplacement of the Sybella granite associated with EW extension
- Deposition of Mount Isa group associated with NNW-SSE extension
- N-S shortening, producing EW folds and cleavage
- EW shortening, producing NS folds and cleavage
- ENE-WSW shortening, producing NNW-trending folds and cleavage, including the Mount Isa fold
- NE-dextral, NW-sinistral, layer-parallel reverse and low angle reverse (eg Buck Quartz) faults

Major Structural Styles

Brittle-ductile deformation predominates in the mine, with common development of disharmonic folding within the Pb-Zn orebodies. Pb-Zn mineralisation is stratiform, but abundant evidence exists of hand specimen-scale transitions from ore layers to barren siltstones suggestive of wallrock replacement. Mineralisation in the copper orebodies occurs as a mixture of veins and wallrock replacement, Miller (2007) noted that Cu-hosting structures have a steep S-pitching intersection with bedding and are consistent with sinistral-reverse slip on bedding

WALLROCK ALTERATION

General Characteristics

Pb-Zn-Ag

There is relatively little wallrock alteration associated with Pb-Zn-Ag mineralisation, apart from the already-noted extensive pyrite halo and mineralogical variations within ore horizons

Cu

Cu mineralisation occurs in association with an extensive zone of “silica-dolomite” alteration. The high grade core of the copper deposit is hosted in brecciated and intensely silicified Urquhart Shale. The high grade siliceous zone is surrounded by a zone of dolomite

Resources

Resources reported by Lilly et al (2017) are as follows:

	Measured and Indicated				
	Tonnage (mT)	Cu (%)	Zn (%)	Pb (%)	Ag (%)
Mount Isa Copper (31/12/2016)	82.9	2.1			
Mount Isa Lead (30/06/2005)	11.2		6	7.2	191

	Inferred				
	Tonnage (mT)	Cu (%)	Zn (%)	Pb (%)	Ag (g/t)
Mount Isa Copper (31/12/2016)	7.9	1.8			
Mount Isa Lead (30/06/2005)	1.5		5.6	7.7	195

Total In-Situ Metal

	Metal Endowment			
	Cu (mT)	Zn (mT)	Pb (mT)	Ag (mOz)
Mount Isa Copper (31/12/2016)	1.9			
Mount Isa Lead (30/06/2005)		0.8	0.9	78.2

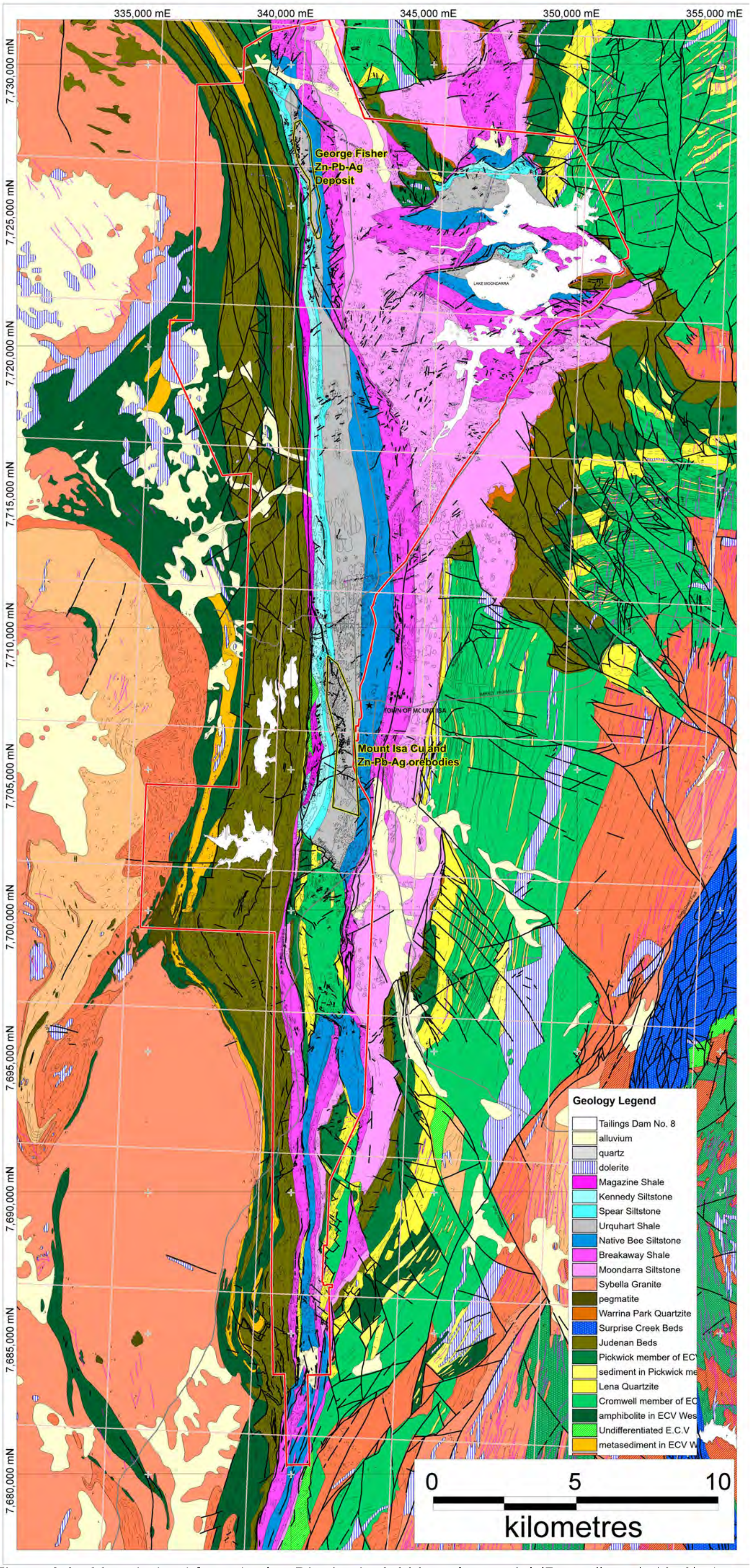

Figure 2.3. Map derived from the Isa District 1:50,000 scale special (Russell et al, 1973) showing the location of the Mount Isa mine, Map Projection GDA94/MGA54.

alteration, with varying texture types including irregularly recrystallised and brecciated shale, crystalline dolomite, and recrystallised shale. Chlorite, talc and stilpnomelane-bearing zones occur at the margins of the silica dolomite body, often where silica dolomite alteration is in contact with Pb-Zn mineralisation.

INNER HALO

Extent

The footprint of the combined Cu and Pb-Zn orebodies covers a zone of 5km in a N-S direction and approximately 1km across strike. Patchy high grade intercepts of Zn-rich mineralisation are present in drillholes at least 1km to the north of the economic mineralisation. Low grade copper intercepts continue at least 500m past the southern limit of the 1100 orebody.

Geophysical Expression

- Pb-Zn orebodies and associated pyritic stratigraphy are dense and produce significant gravity anomalies, offset in practice by the associated presence of low density surficial leaching (Leaman, 1991). Where pyrrhotite-bearing, the Pb-Zn orebodies also produce a weak magnetic signature
- Cu orebodies and associated silica-dolomite produce a 2.5 mGal gravity anomaly (Leaman, 1991b). Cu mineralisation has little magnetic expression
- Both Pb-Zn and Cu mineralisation would be expected to have a significant response in IP, MT and EM surveys, though the presence of infrastructure over the deposit has limited the application of modern surveys and resulted in a scarcity of publicly available data. The carbonaceous and conductive nature of host rocks such as the Urquhart Shale, the Breakaway Shale and the Magazine Shale present a major challenge to exploration with electrical geophysics.
- In a pristine environment, elevated K associated with the deposits may be detectable in radiometric surveys

Exploration Geochemistry

- A survey above the southern 1100 orebody showed a strong multi-element response in Cu, Au, As, Pb, Zn, Mo in soils with an Aqua Regia digest (Lilly 2014). Notable though more complex responses were also present in Co, U, Bi and Ce (Lilly 2014).
- Metal Soil Gas orientation data show elevated Cu, Ag, Ba, Ce, Co, Ga, Li, Pb, Zn and Tl above the 1100 Cu orebody (Lilly 2014).

Lithogeochemistry

- Elements which are not elevated in the outer halo of the Mount Isa system but do markedly increase within

Figure 2.4. Map derived from the 2017 GSQ Digital Geology of Queensland, with colour legend modified to match the Legend of Lilly et al (2017). The location of the section in Figure 2.5 is also shown. Map projection MGDA94/ MGA54

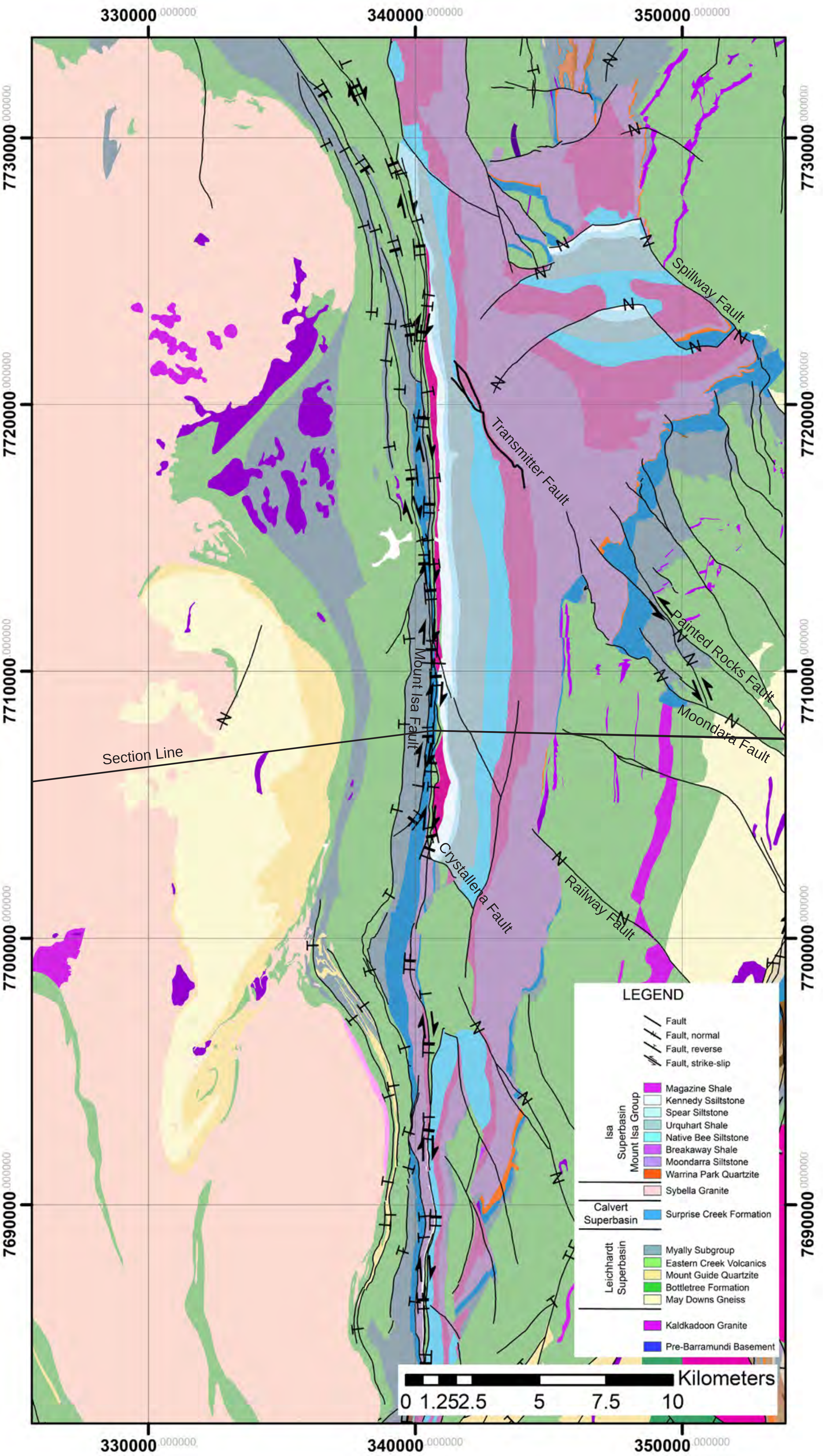

1-1.5km of economic mineralisation include Mn, Pb, Fe and Sb. In addition whole rock analyses of Urquhart Shale show a decrease in SiO2 in the inner halo.

- The Ba/Al ratio (Ba/(Ba + 10Al_2O_3) is also elevated within the inner halo but decreases to background beyond that point (Painter, 2003)

Mineralogy

- Dolomites in the Urquhart Shale within approximately 1km of economic Pb-Zn mineralisation are elevated in Fe compared to dolomites at greater distances (Painter, 2003)
- Painter (2003) also noted an increase in the occurrence of manganiferous dolomite cements associated with mineralisation.
- Pyrite content decreases systematically with distance from the Pb-Zn orebodies, though significant pyrite persists well beyond the inner halo (Painter 2003)

A comparison of PIMA spectra from within the orebodies and a hole from the inner halo (F968) noted a higher incidence of phengite, dolomite, intermediate chlorite, ankerite, talc and calcium and potassium sulphates associated with economic ore (Duckworth, 2008)

Figure 2.5. Geological cross section through the Mount Isa Mine (see Figure 2.4 for location). Information sources for the section include an AusIMM presentation for the mine area; Eastern Creek Volcanics geometry to the east of the Mount Isa Fault based on Leaman (1991) and Betts and Lister (2003); structure to the west of the Mount Isa Fault based on a section from Gordon (2004).

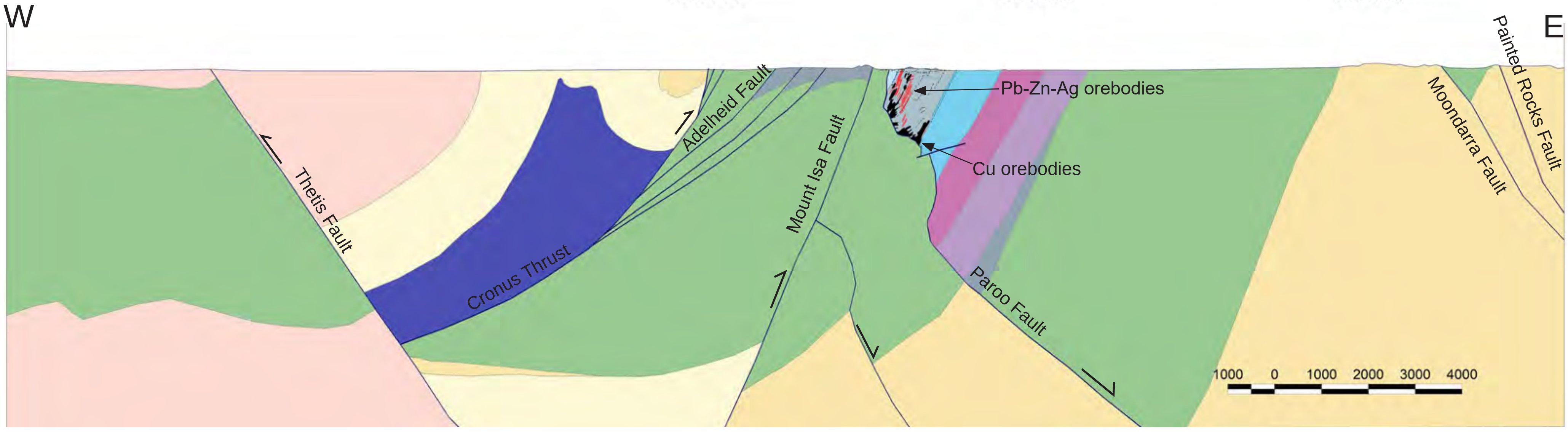

Figure 2.6. Aeromagnetic image over Mount Isa - Colour Reduced to Pole overlain on Vertical Derivative Reduced to Pole. Map Projection GDA94/MGA54

OUTER HALO

Extent

- Evidence of the Mount Isa system extends more than 10km to the north of the mine within the Urquhart shale, and anomalous copper extends southward all the way to the Crystallena block

Geophysical Expression

- Regional interpretation and modelling of the Eastern Creek volcanics has defined a zone of demagnetisation in the Eastern Creek Volcanics where they occur in contact with the Cu orebodies (Leaman, 1991a)
- Pyritic stratigraphy extends up to 10km to the north of the limit of economic mineralisation and would be expected to have an electrical response as well as potentially a weak gravity response.

Exploration Geochemistry

- Anomalous Cu, Pb and Zn extend up to 10km away from the Mount Isa deposit in stream sediments
- Anomalous Pb and Zn in near-surface samples extends more than 5km to the north of economic mineralisation
- Anomalous Cu in RAB drilling extends southward to the Crystallena block

Lithogeochemistry

- From Painter's 2003 study of the northern halo of the Mount Isa orebodies, it can be seen that S, Tl, Zn, Ge, Cd and Se all show a systematic increase with increasing proximity to mineralisation, starting in most cases from nearly 10km away from economic mineralisation.
- In addition, Painter (2003) confirmed the effectiveness of a number of indices including:
    - o the SEDEX4 of Large et al (2000) (100FeO + 10MnO)/(FeO + 10MnO + MgO + (SiO2/10);
    - o the Metal Index of Large and McGoldrick (1998) (Zn + l00Pb + l00Tl)
    - o a new "Isa Vector" (Tl/Ge(FeO_{dol}+10MnO_d)) where FeO_{dol} is calculated from FeO and S analyses assuming that all FeO not in pyrite is in dolomite and MnO_d is calculated on the basis of (MnO x 30.41)/CaO (Large and McGoldrick 1998)

Mineralogy

- The dominant mineralogical indicator of the outer halo is the extensive envelope of fine-grained pyrite, which extends as much as 10km from the

Figure 2.7. Aeromagnetic image over Mount Isa - Colour Reduced to Pole overlain on Vertical Derivative Reduced to Pole. Overlain lines are boundaries from the Mount Isa District 1:50000 geological map. The footprint of the Cu and Lead-Zinc orebodies are shown in orange and red respectively. Map Projection GDA94/MGA54

deposit.

- Cudahy et al (2008) noted an 18km strike length zone of elevated AlOH clay, Kaolinite and White Mica content mapped from airborne hyperspectral data centred around the Mount Isa deposit in quartzites outcropping to the west of the Mount Isa Fault
- Jakob et al (2016) were able to use airborne hyperspectral data to map gossanous ridges associated with the Mount Isa deposit

Figure 2.8. Map derived from the Isa District 1:50,000 scale special (Russell et al, 1973) shown for reference for Figure 2.7, Map Projection GDA94/MGA54.

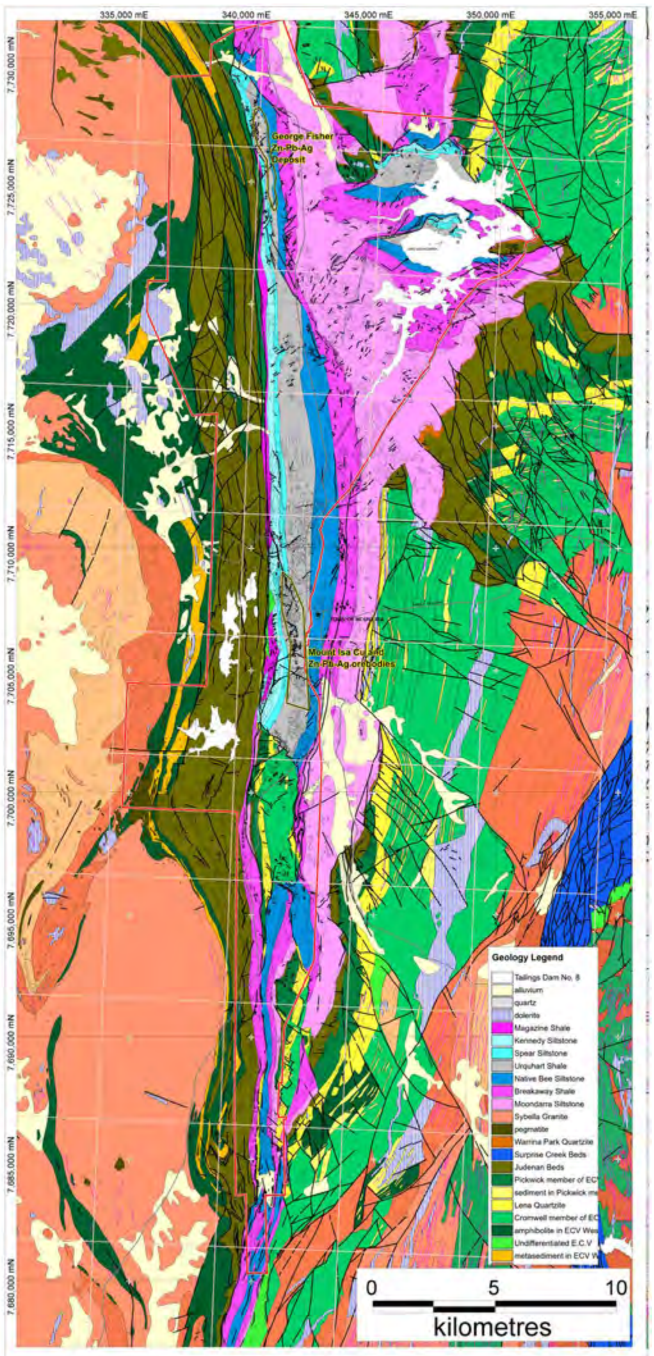

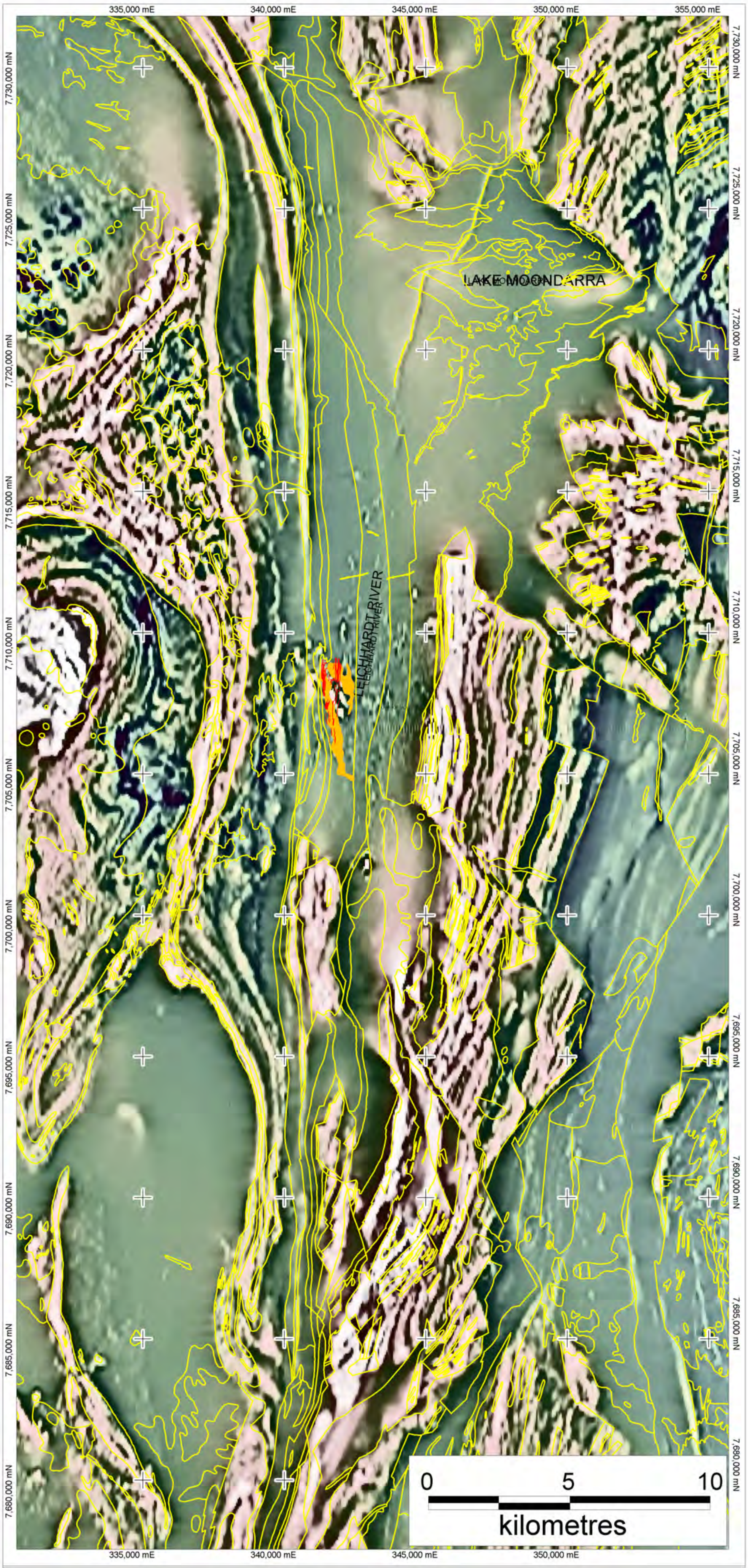

Figure 2.9. Aeromagnetic image over Mount Isa with tilt processing applied (Tarlowski and Scott, 1999). The effect of tilt processing in this region is to highlight the subsurface distribution of blocks of Eastern Creek Volcanics. Map Projection GDA94/MGA54

Figure 2.10. Greyscale tilt algorithm magnetics, with a colour overlay of magnetic susceptibility of the Eastern Creek Volcanics as modelled by Leaman (1991a), showing the lower magnetic susceptibility in the Eastern Creek Volcanics underlying the Mount Isa mine, interpreted to be related to mineralisation-related hydrothermal alteration. Hannan et al (1993) noted a lack of magnetite in the altered Chlorite schists of the Eastern Creek Volcanics under the copper orebodies and silica dolomite

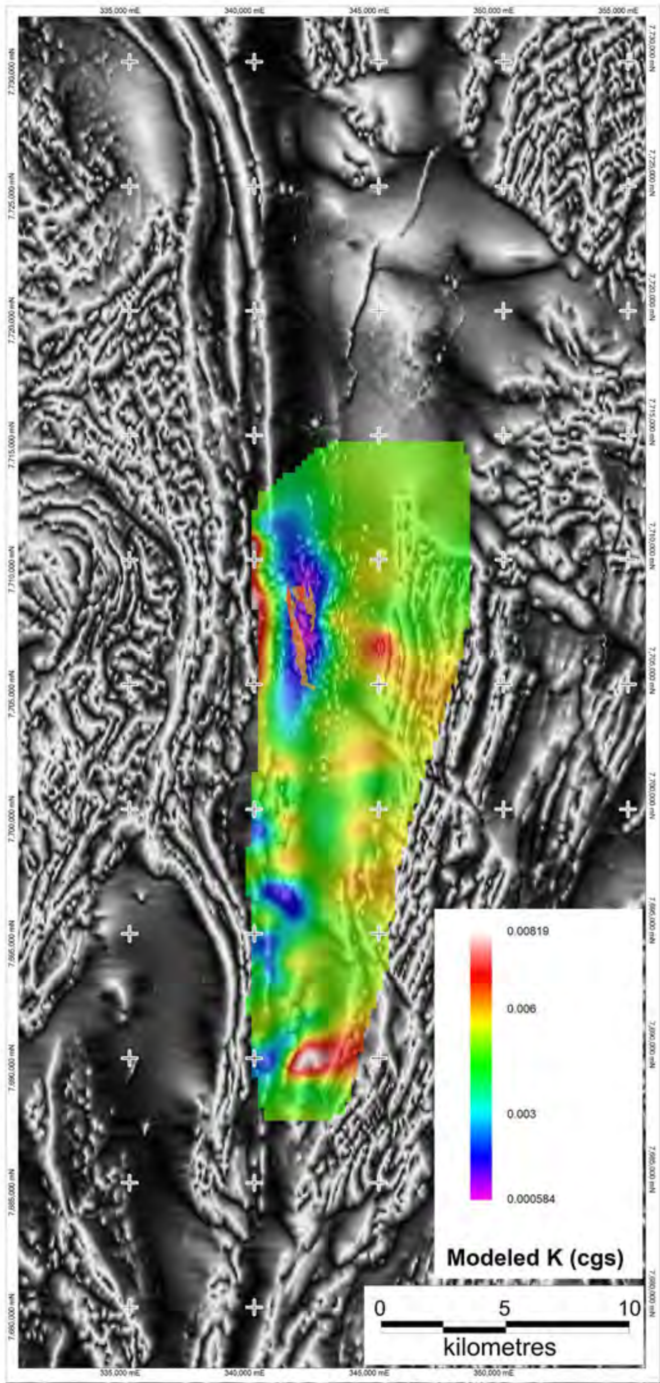

Figure 2.11. Aeromagnetic image over Mount Isa with tilt processing applied (Tarlowski and Scott, 1999). Overlain lines are boundaries from the Mount Isa District 1:50000 geological map. The footprint of the Cu and Lead-Zinc orebodies are shown in orange and red respectively. The effect of tilt processing in this region is to highlight the subsurface distribution of blocks of Eastern Creek Volcanics. Map Projection GDA94/MGA54

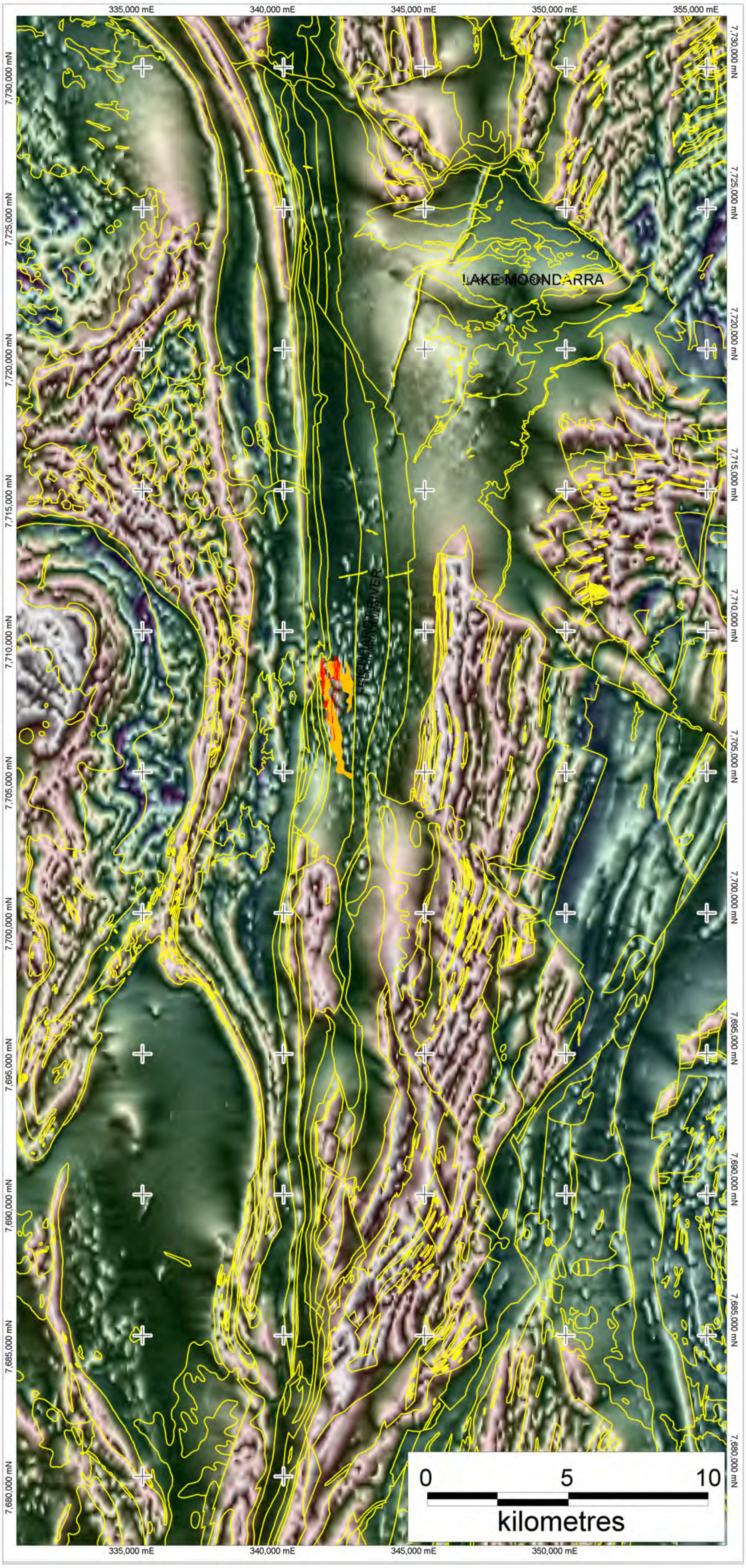

Figure 2.12. Map derived from the Isa District 1:50,000 scale special (Russell et al, 1973) shown for reference for Figure 2.11, Map Projection GDA94/MGA54.

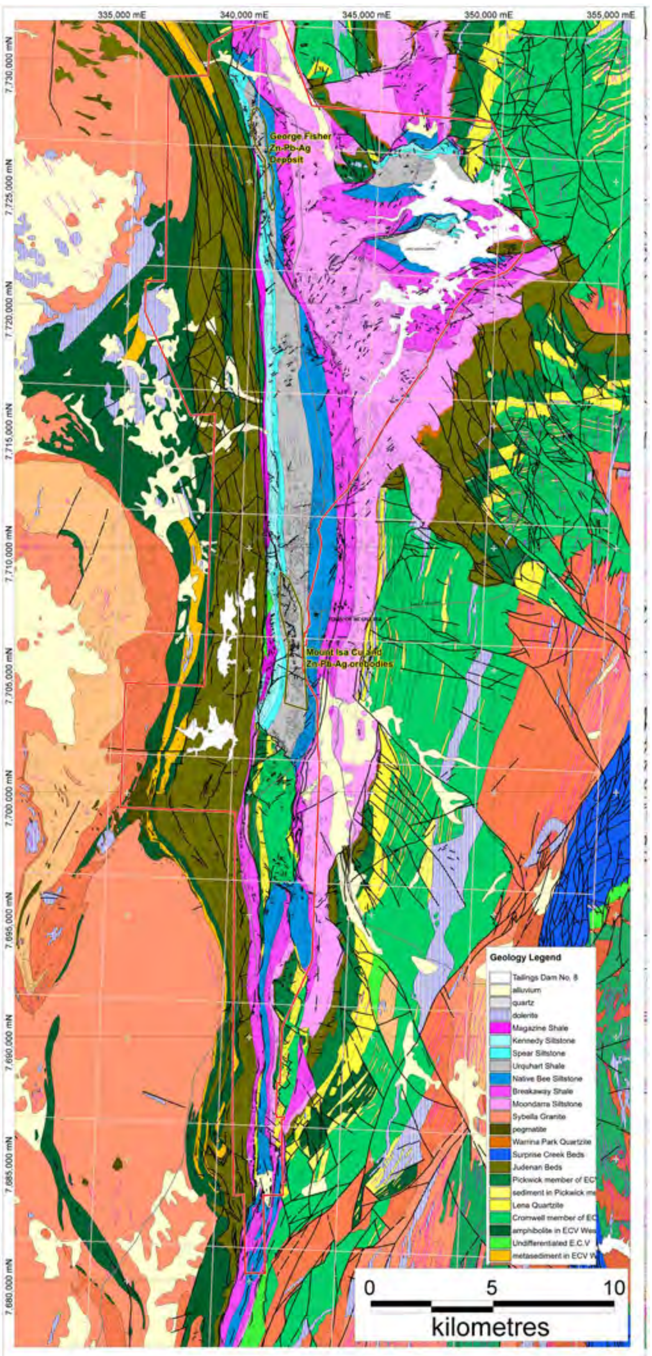

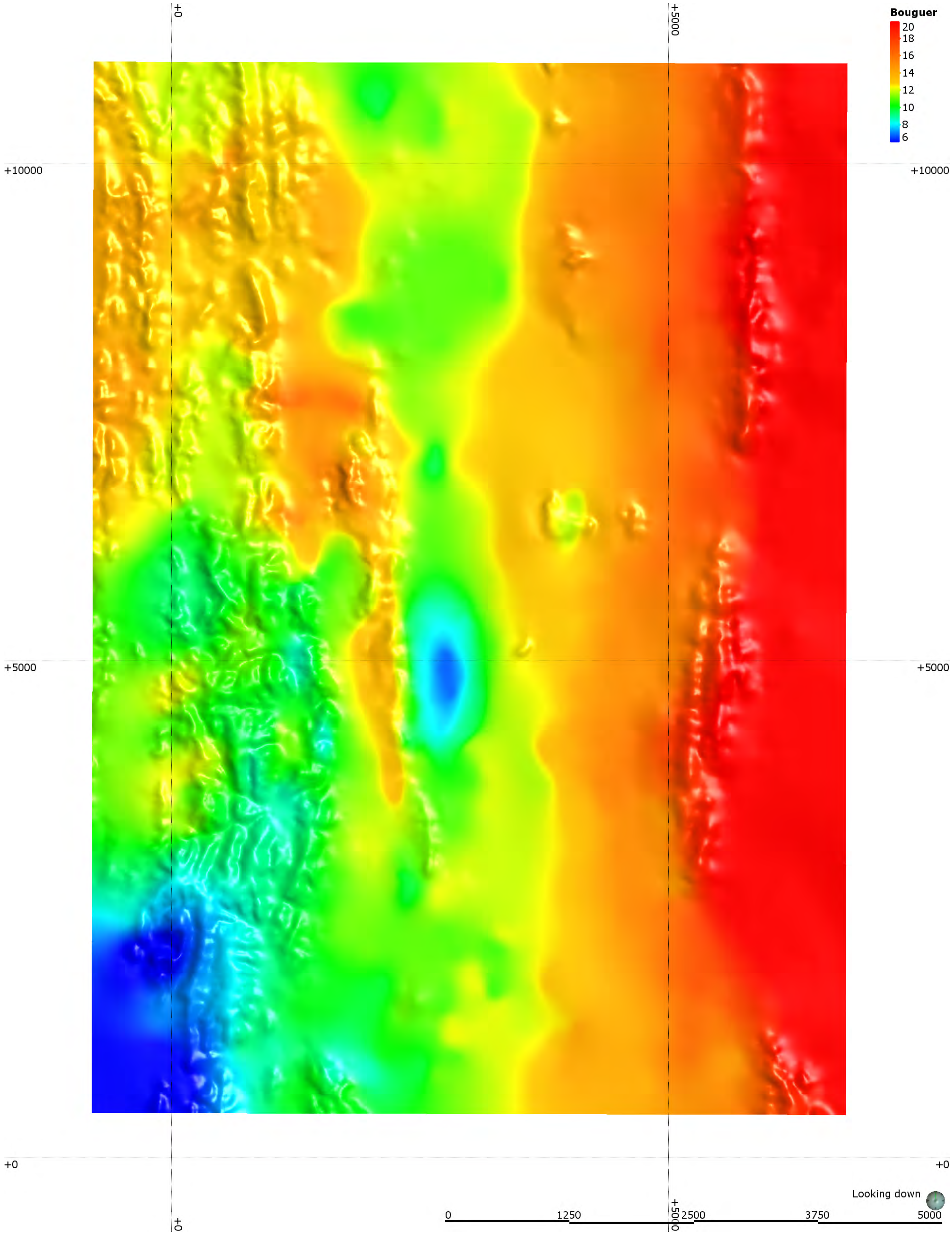

Figure 2.13. Bouguer gravity (mGal) digitised from Leaman (1991b) contours. Isa mine grid.

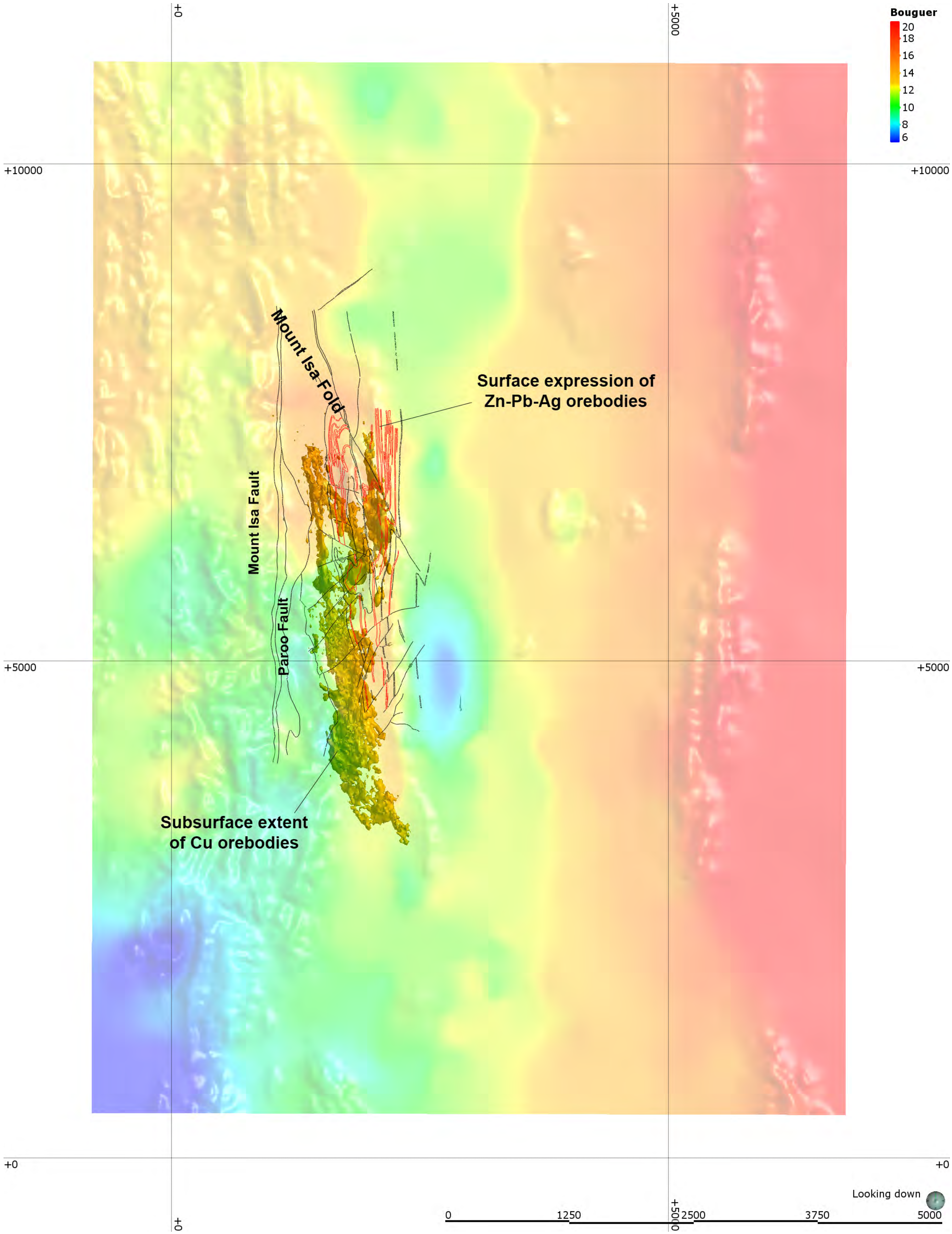

Figure 2.14. Companion to Figure 2.13 (facing page), showing the position of Pb-Zn-Ag and Cu orebodies relative to gravity data, showing the coincidence of a gravity high with mineral-isation, as well as gravity lows related to low density leached rocks (Leaman, 1991b).

Figure 2.15. Image of airborne radiometrics over Mount Isa, Red - K; Green - Th; Blue - U in colour with greyscale underlay of NW-shaded Digital Terrain Model. Map Projection GDA94/MGA54

TIMING OF MINERALIZATION

Relative Timing

The timing of the Mount Isa Orebodies with respect to sedimentation and deformation has been the subject of long term study, with timing interpretations mainly falling into four main groups when considering Pb-Zn-Ag/Cu and Synsedimentary (S) Diagenetic (D) and Epigenetic (E) relative timings. In the paragraphs below the two letters refer to timing of Pb-Zn-Ag and Cu respectively, separated by the slash.

S/S Timing: (Stanton, 1963; Finlow-Bates & Stumpfl). In this interpretation, Cu-Pb-Zn-Ag mineralisation was synchronous with sedimentation and exhalative on the sea floor, with the silica-dolomite alteration representing a stockwork associated with the Paroo Fault as a synsedimentary feeder system. Subsequent deformation and metamorphism modified the textures of the ores and rendered their interpretation ambiguous.

D/D Timing: (McGoldrick, 1986; McGoldrick & Keays 1990). In this interpretation, Cu-Pb-Zn-Ag mineralisation was interpreted to have formed as a diagenetic replacement, with the silica-dolomite alteration representing a stockwork associated with the Paroo Fault as a synsedimentary feeder system. Subsequent deformation and metamorphism modified the textures of the ores and rendered their interpretation ambiguous.

D/E Timing: (Neudert and Russell, 1981; Perkins, 1984; Swager, 1985; Bell et al, 1988; Painter, 2003; Miller 2006). In this interpretation, Pb-Zn-Ag mineralisation is interpreted to be replacive but overprinted by deformation of the Isa Orogeny, whereas Cu mineralisation is interpreted to have formed synchronously with the Isan Orogeny, though a range of timings with respect to deformation have been proposed. Subsequent deformation and metamorphism modified the textures and metal distribution of the Pb-Zn-Ag ores and rendered their interpretation ambiguous.

E/E Timing: (Grondijs & Schouten, 1937; Myers et al, 1996; Perkins, 1997; Davis, 2004). In this interpretation, both Cu and Pb-Zn-Ag mineralisation were introduced as a single system during deformation, consistent with the presently observed textures, spatial association and metal zoning in the orebody. Strongly folded sulphides are interpreted to be a replacement of pre-existing folding of a material which must have had similar rheological characteristics to galena and sphalerite.

The arguments for each of these have been well summarised in the NWQMEP 2010 data

Figure 2.16. Image of airborne radiometrics over Mount Isa, Red - K; Green - Th; Blue - U in colour with greyscale underlay of NW-shaded Digital Terrain Model. Overlain lines are boundaries from the Mount Isa District 1:50000 geological map. The footprint of the Cu and Lead-Zinc orebodies are shown in orange and red respectively. Map Projection GDA94/MGA54

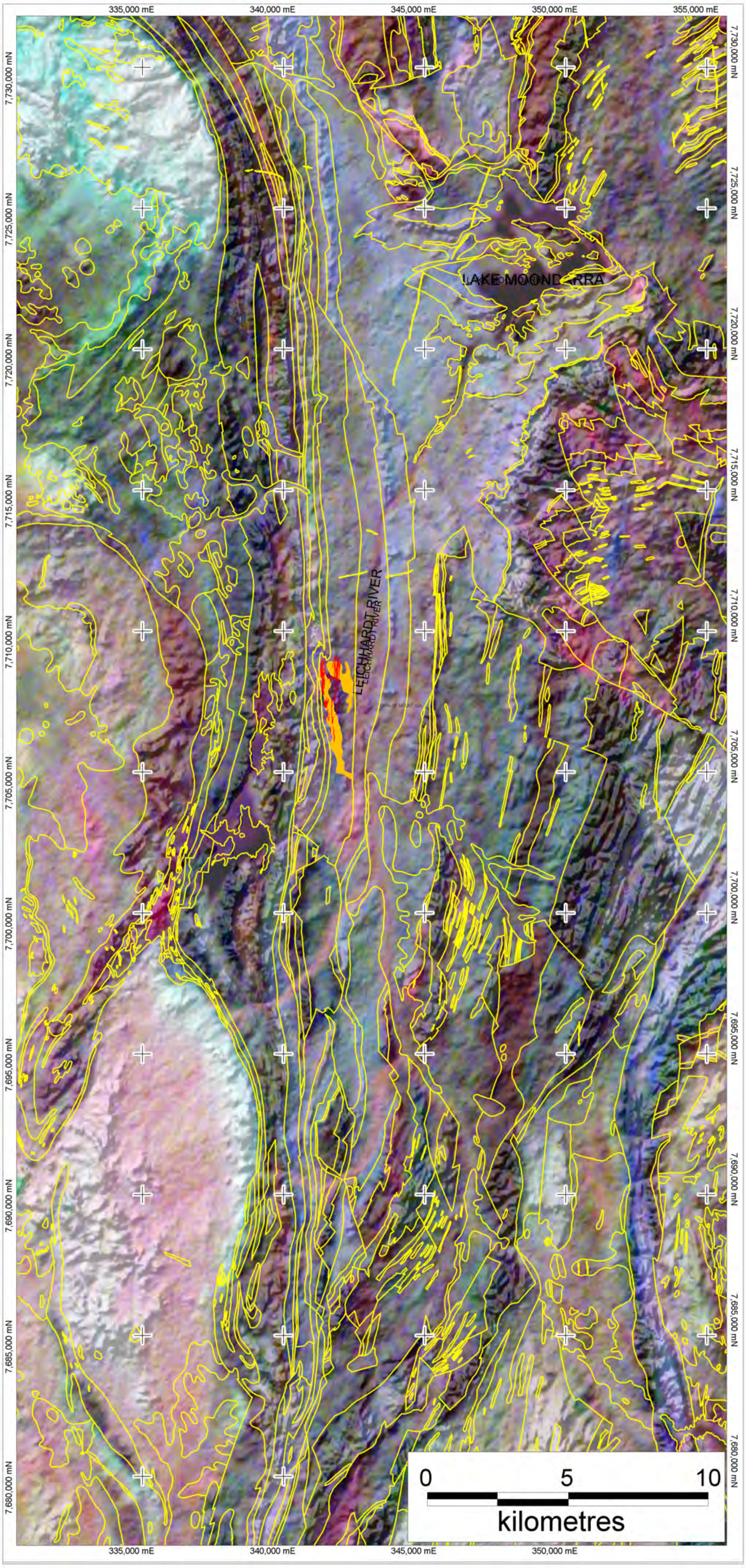

Figure 2.17. Map derived from the Isa District 1:50,000 scale special (Russell et al, 1973) shown for reference for Figure 2.16, Map Projection GDA94/MGA54.

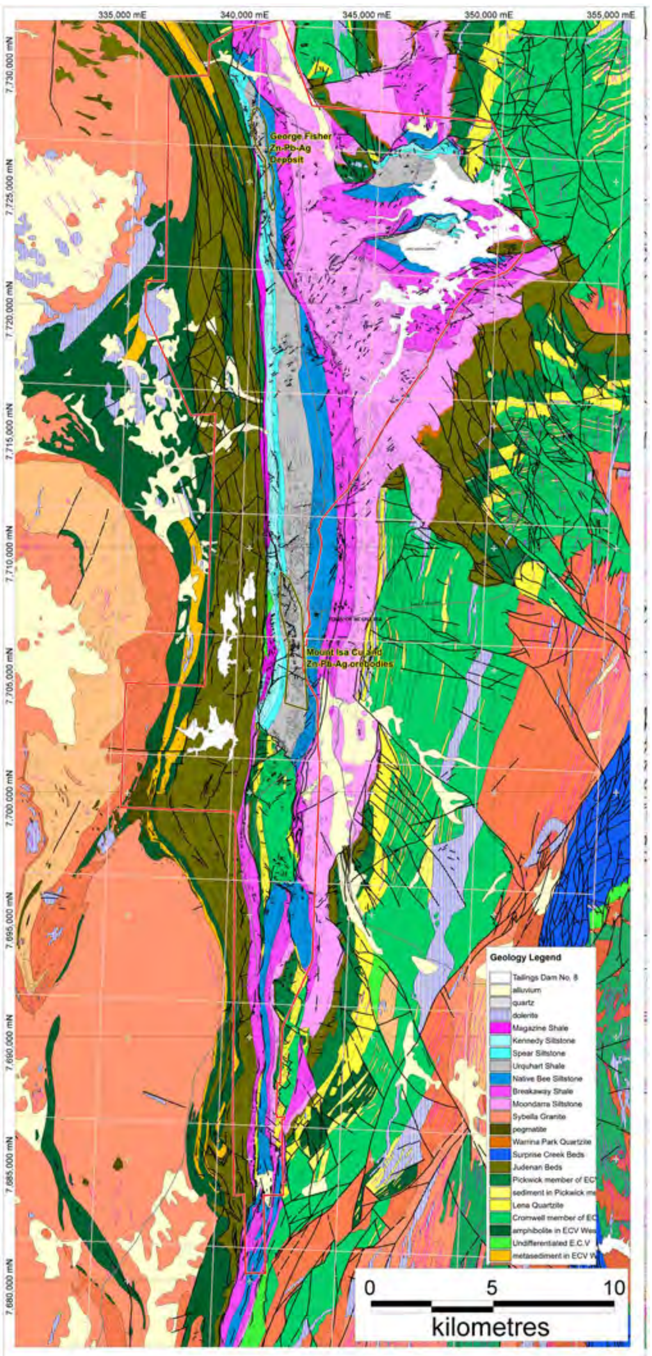

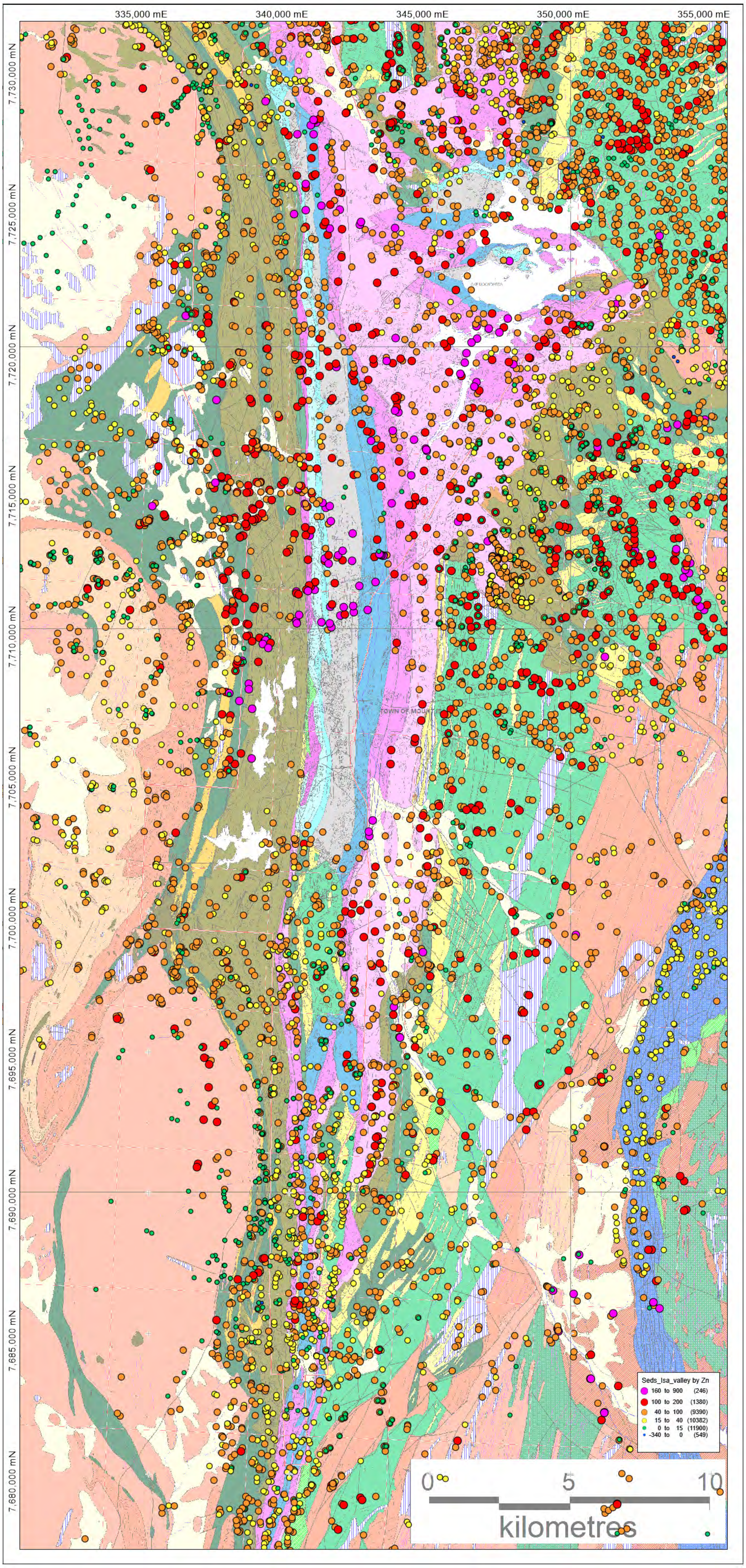

Figure 2.18. Thematic plot of stream sediment Zn values from the 2006 Mount Isa West Block Exploration Geochemistry and Drill Hole Database (QDEX 2006). Map Projection GDA94/MGA54

package and they will not be repeated here.

Absolute age

Cu orebodies:

- Ar/Ar dating of phlogopite associated with Cu mineralisation yielded an age of 1523±3Ma (Perkins et al, 1999)
- Re-Os dating of a whole rock sample of chalcopyrite, pyrrhotite and pyrite yielded an age of 1371±41Ma (Gregory et al, 2008)

Pb-Zn-Ag orebodies

- Pb/Pb model age of 1653 (Carr et al., 1996, 2003)

GENETIC MODEL

Despite disagreements over timing and co-genesis, there is more recently general agreement that the Pb-Zn-Ag and Cu orebodies formed by hydrothermal replacement and dilation of the Urquhart Shale. The process model aspects of the genetic model for Mount Isa have been well summarised in the NWQMEP 2010 data package and they will not be repeated here.

POST-FORMATION MODIFICATION

- Faulting
- Surface weathering

EXPLORATION

Discovery Method

The Mount Isa Pb-Zn-Ag deposit was discovered in 1923 by prospecting. Copper mineralisation was discovered by drilling in the late 1920s.

Figure 2.19. Thematic plot of stream sediment Pb values from the 2006 Mount Isa West Block Exploration Geochemistry and Drill Hole Database (QDEX 2006). Map Projection GDA94/MGA54

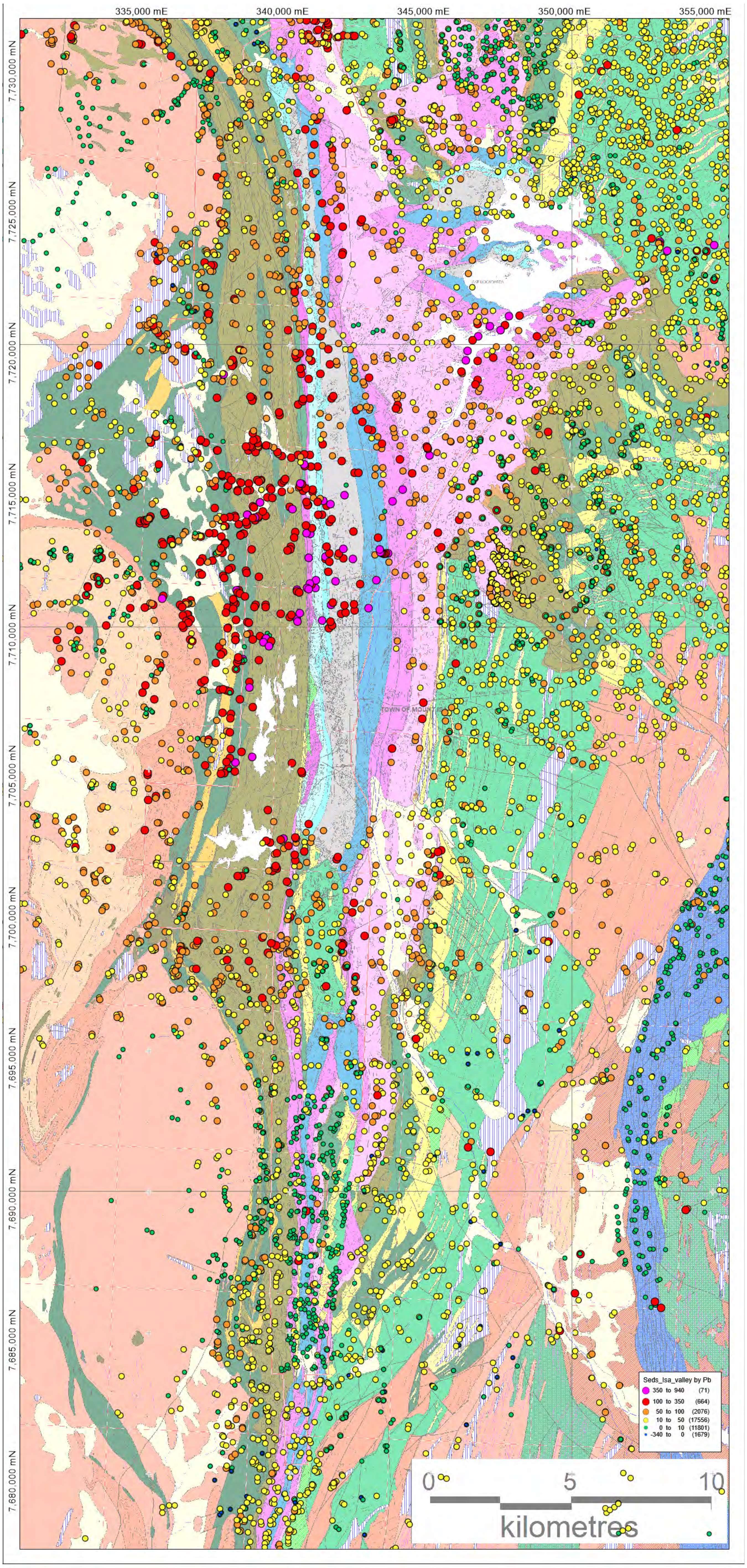

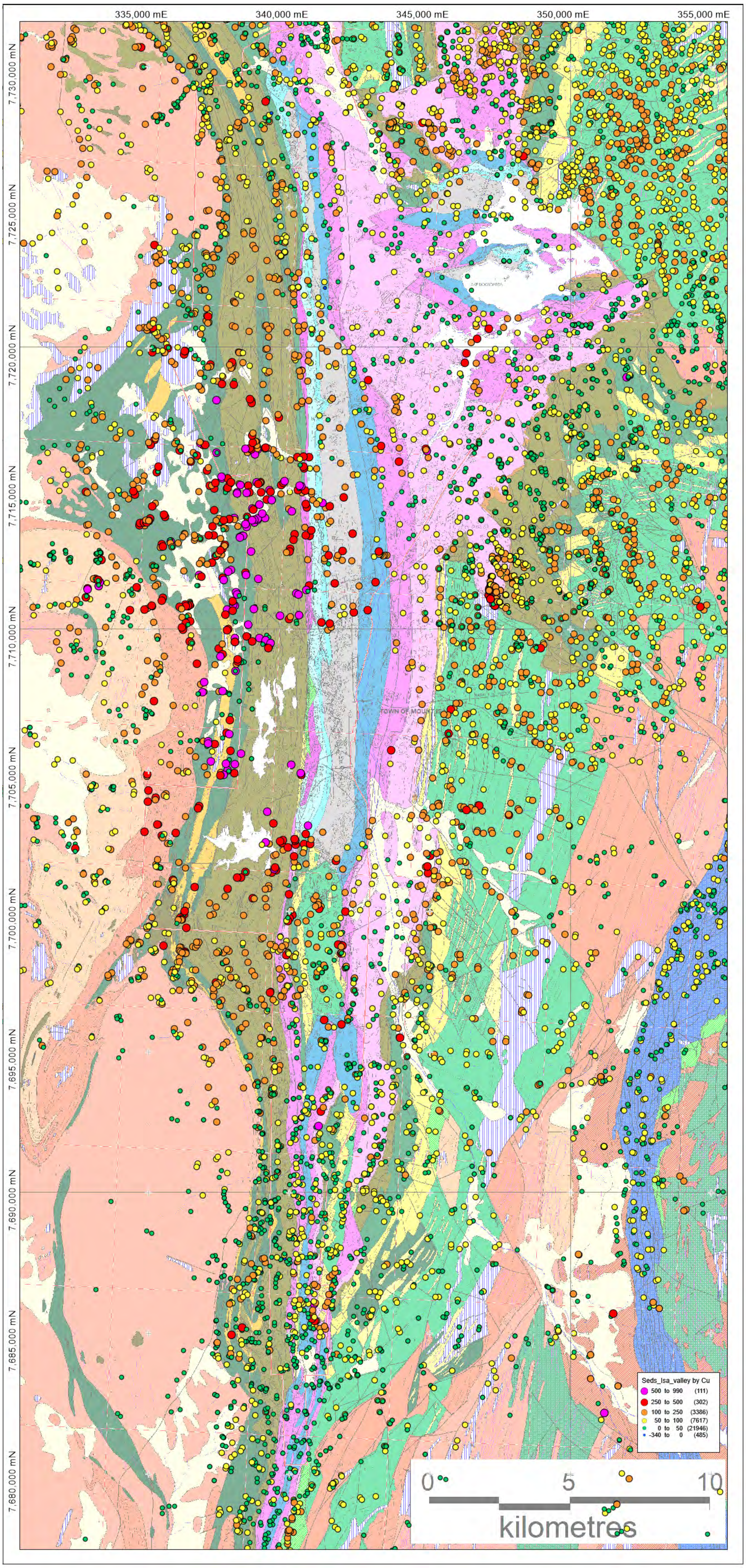

Figure 2.20. Thematic plot of stream sediment Cu values from the 2006 Mount Isa West Block Exploration Geochemistry and Drill Hole Database (QDEX 2006). Map Projection GDA94/MGA54

Figure 2.21 (facing page). Maps showing distributions of Cu, Pb and Zn in RAB and diamond drill holes (Conaghan et al 2003). The surface projection of the Cu orebodies is also shown. Strong base metal anomalism extend more than 5km to the north of the limit of mineralisation, and copper anomalism extends south as far as the Crystallena block.

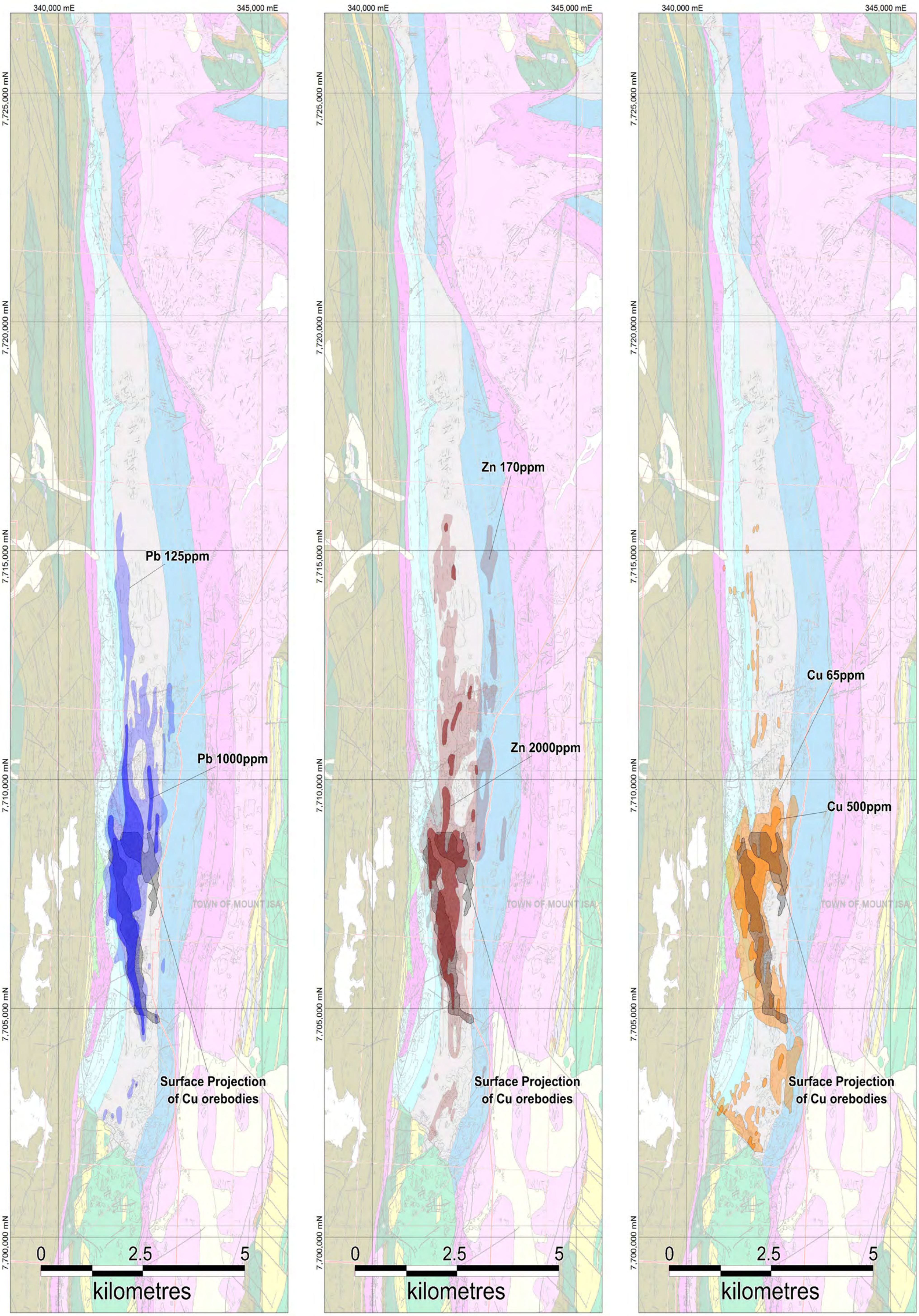
340,000 mE
345,000 mE
7,725,000 mN
7,720,000 mN
7,715,000 mN
7,710,000 mN
7,705,000 mN
7,700,000 mN
Pb 125ppm
Pb 1000ppm
TOWN OF MOUNT ISA
Surface Projection
of Cu orebodies
0
2.5
5
kilometres
340,000 mE
345,000 mE
7,725,000 mN
7,720,000 mN
7,715,000 mN
7,710,000 mN
7,705,000 mN
7,700,000 mN
Zn 170ppm
Zn 2000ppm
TOWN OF MOUNT ISA
Surface Projection
of Cu orebodies
0
2.5
5
kilometres
340,000 mE
345,000 mE
7,725,000 mN
7,720,000 mN
7,715,000 mN
7,710,000 mN
7,705,000 mN
7,700,000 mN
Cu 65ppm
Cu 500ppm
TOWN OF MOUNT ISA
Surface Projection
of Cu orebodies
0
2.5
5
kilometres

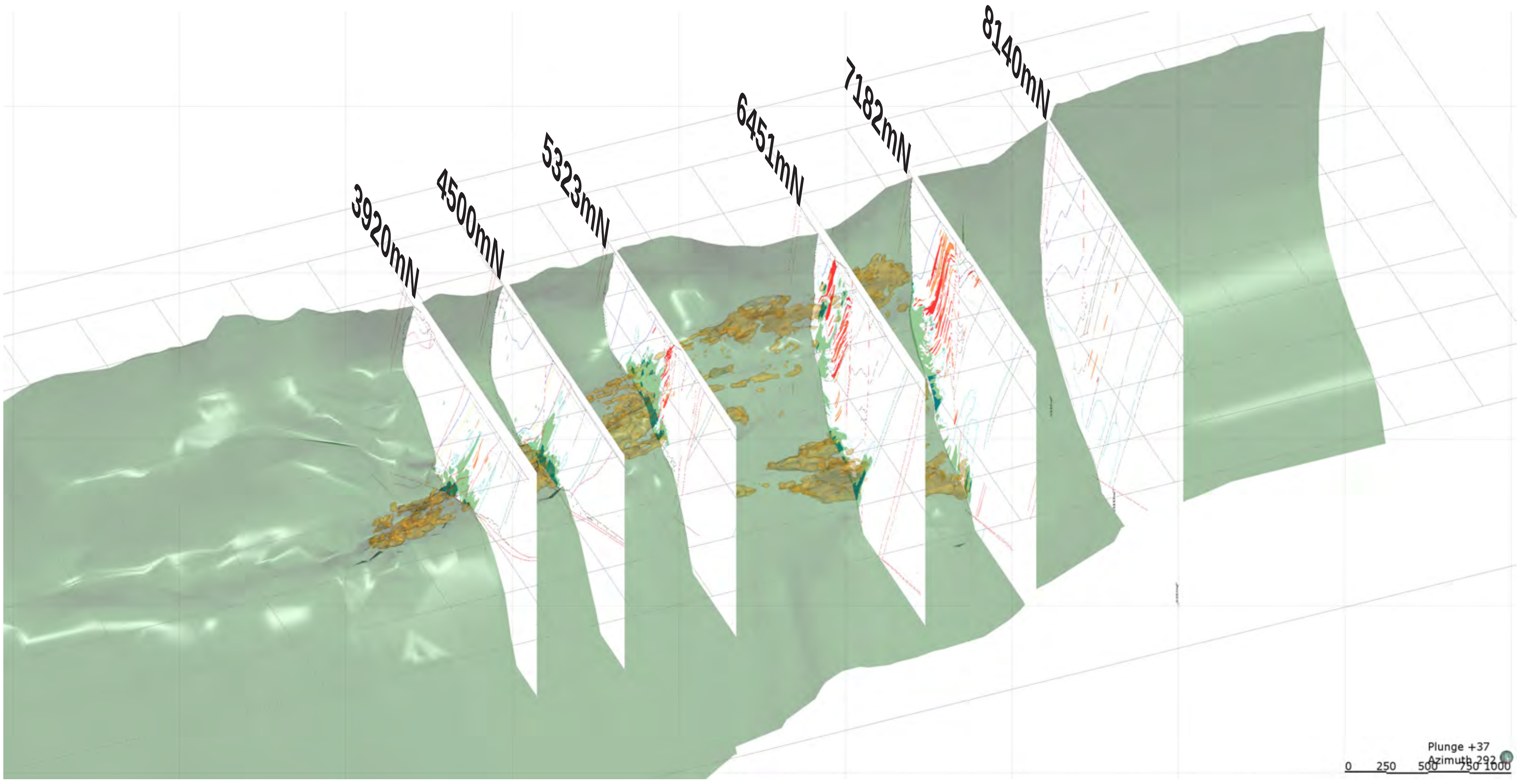

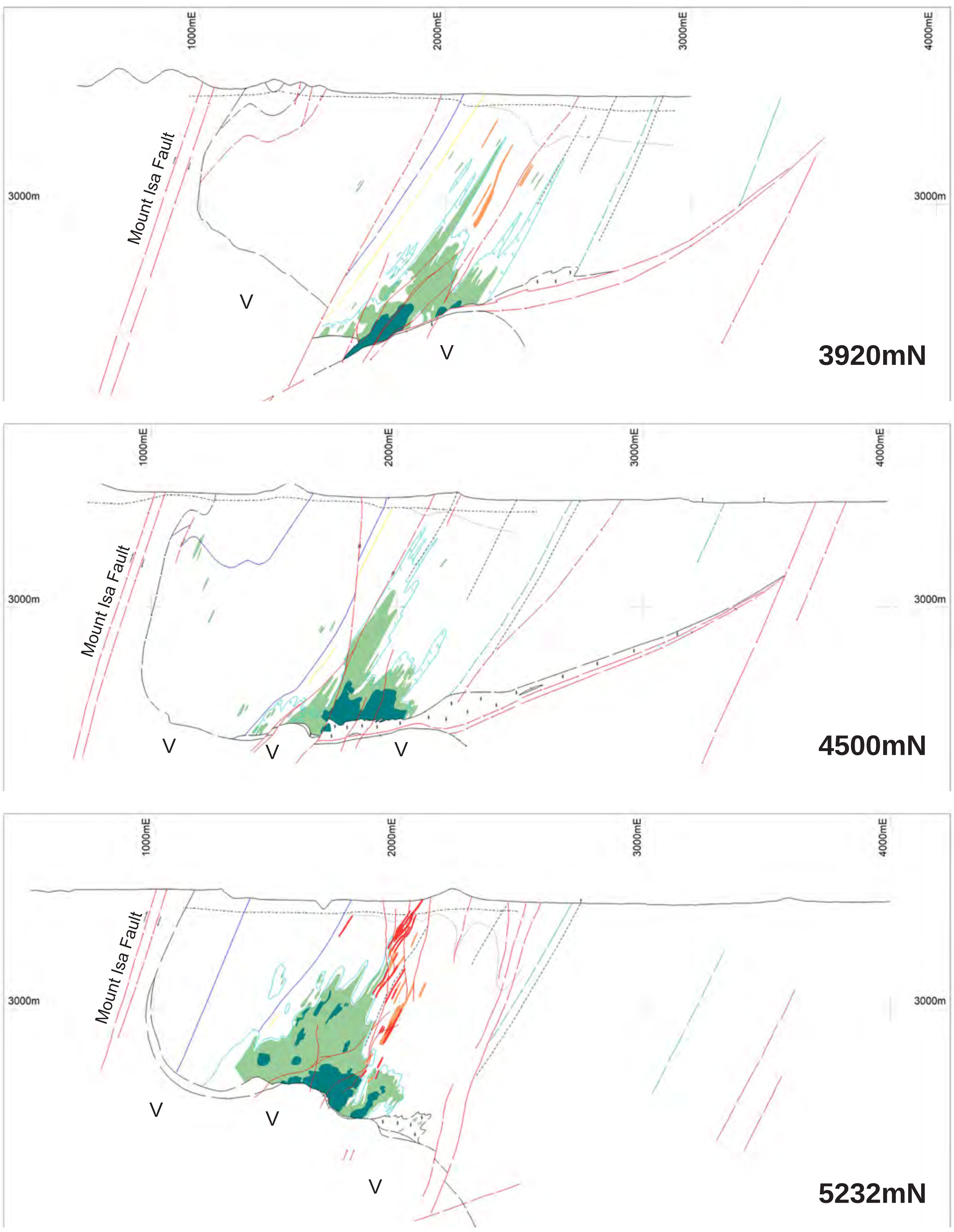

LEGEND

- Surface
- Base of complete oxidation
- Base of moderate leaching
- Spear-Urquhart boundary
- Pyrite rib
- Tuff Marker Bed
- Urquhart - Native Bee boundary
- Silica dolomite alteration boundary
- Fault / Shear Zone
- 8% Pb equivalent
- 12.5% Pb equivalent
- 0.5% Cu
- 2-2.5% Cu

Figure 2.22. (this page and facing page). Set of sections depicting N-S variation in the geometry of Cu mineralisation, silica-dolomite alteration and lead-zinc mineralisation, and its relationship to bedding and faults. From the 1992 Mine Exploration review.

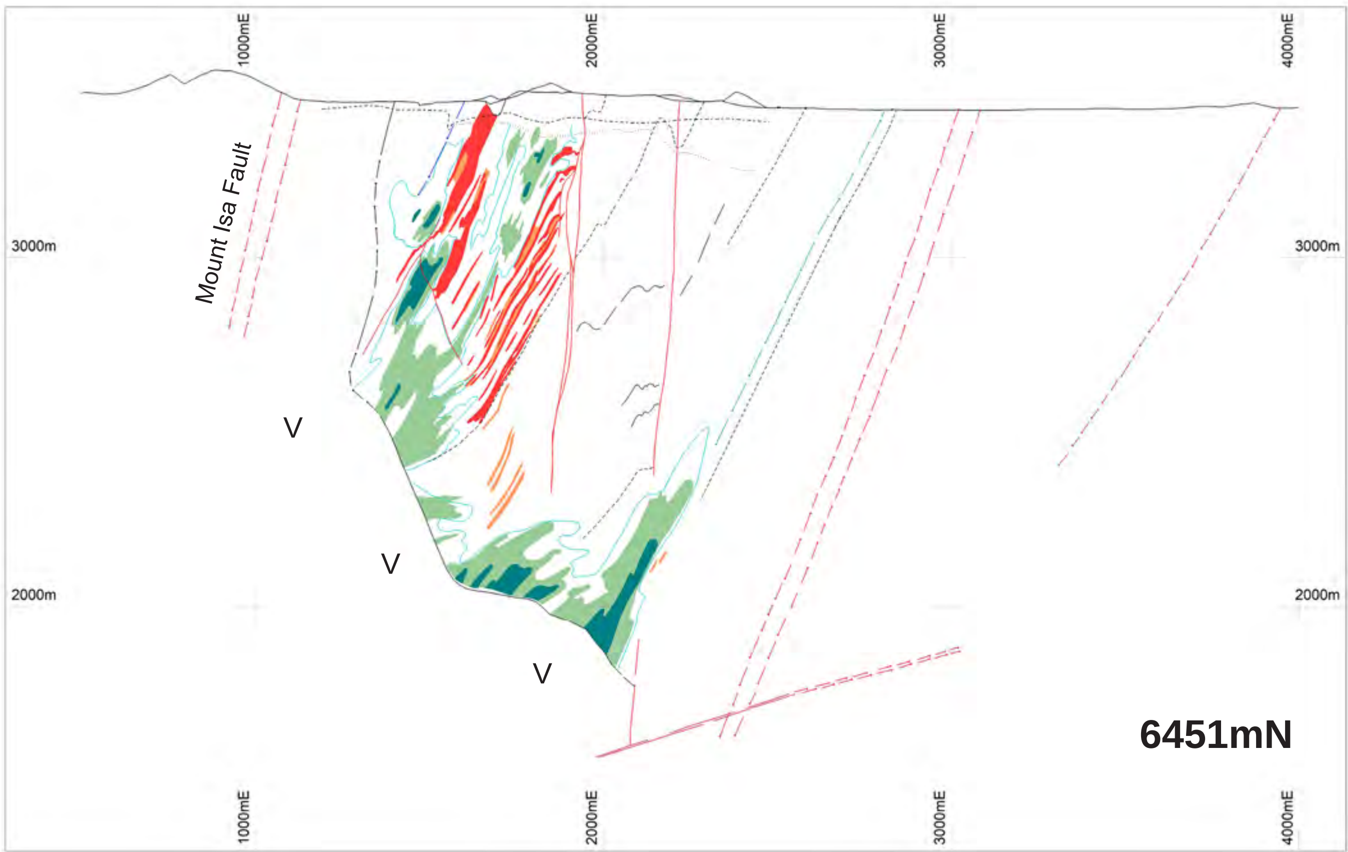

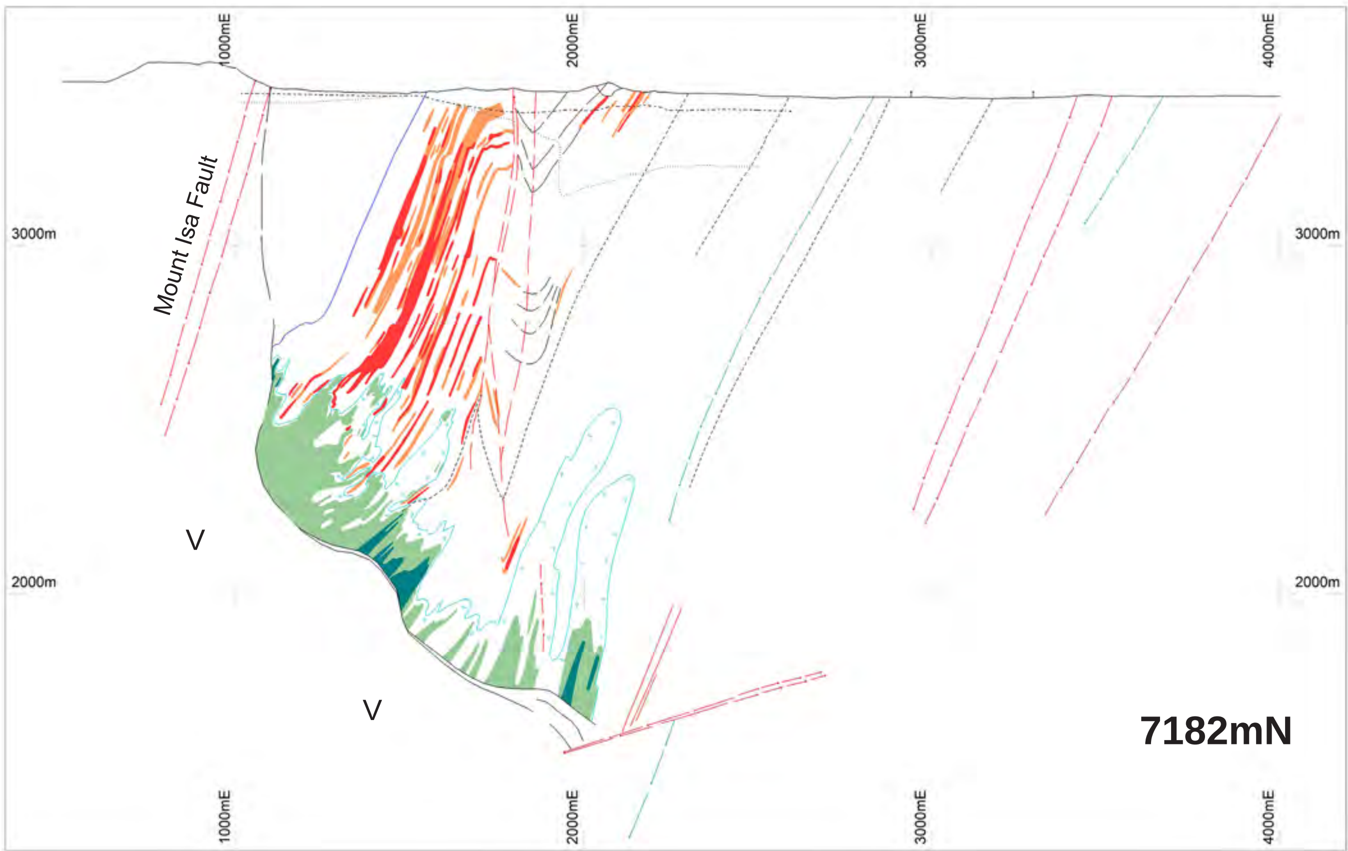

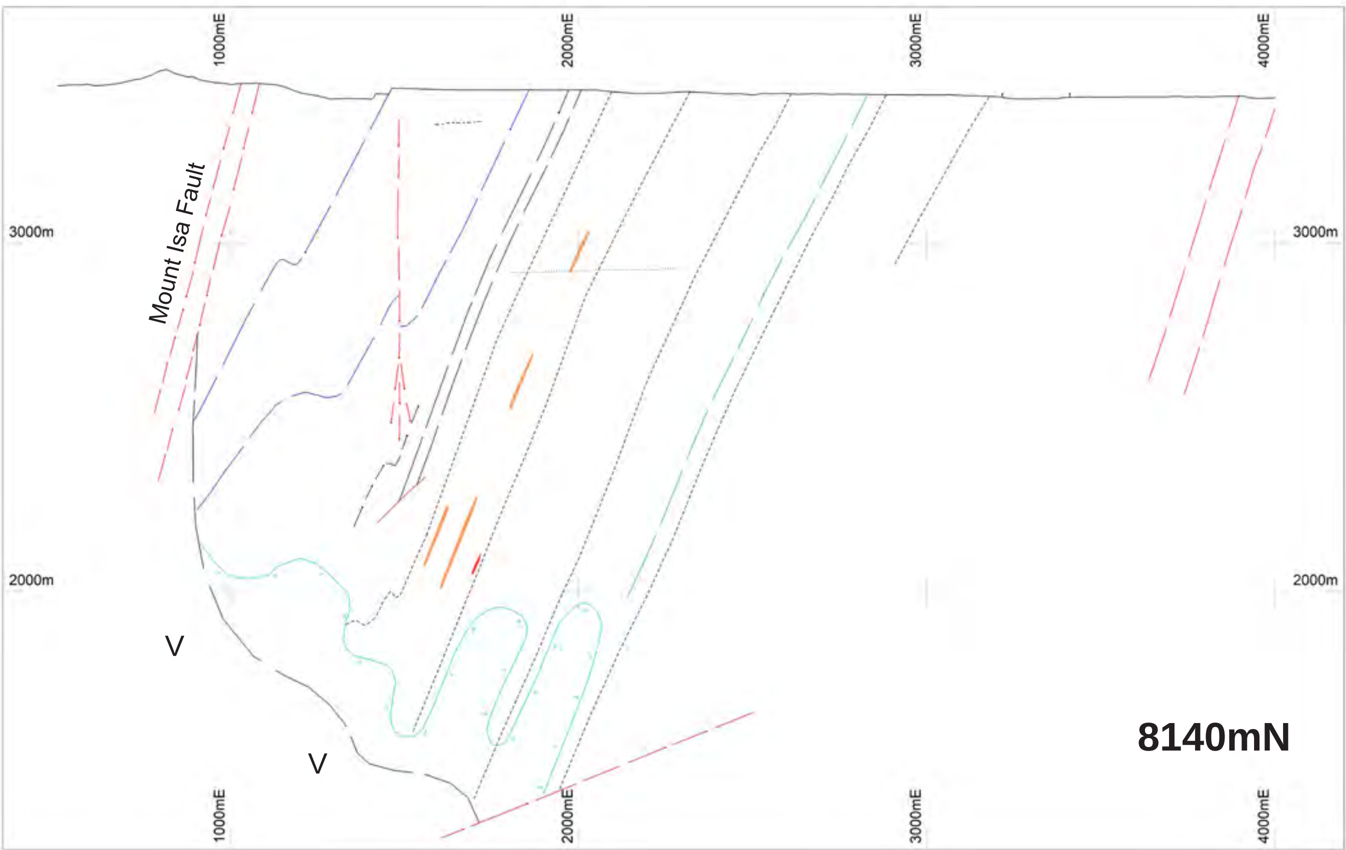

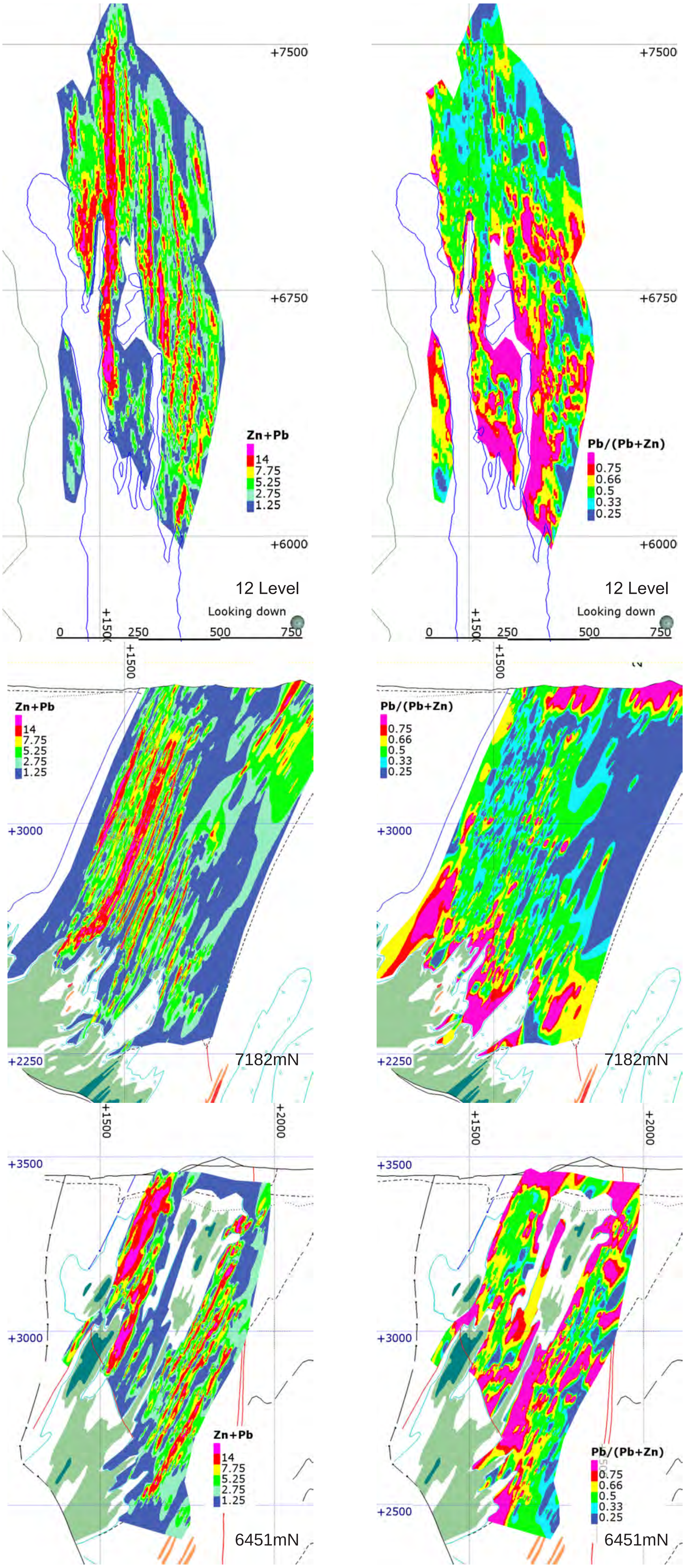

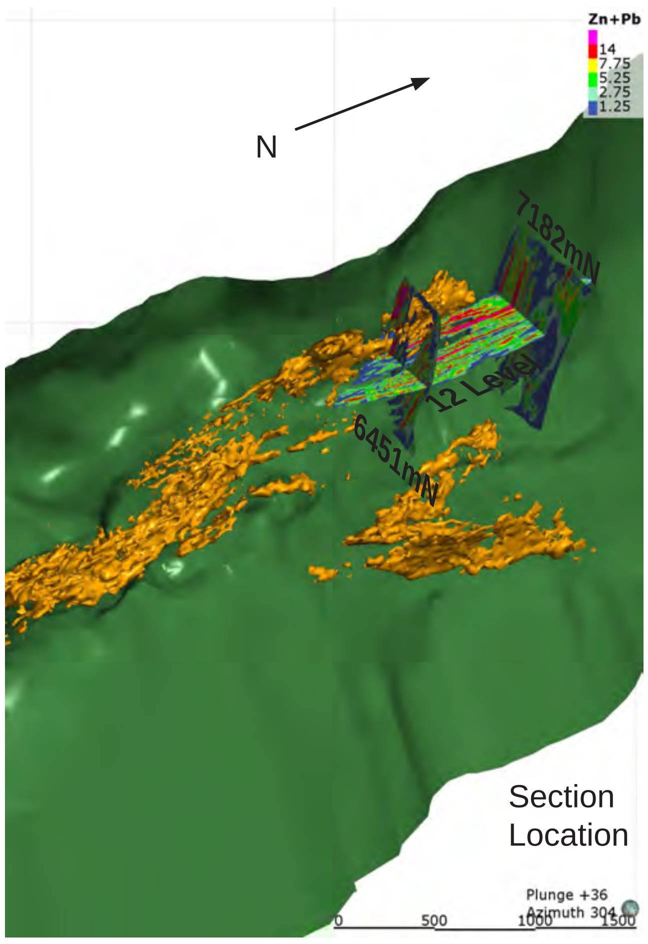

Figure 2.23. Metal zoning diagrams for the Blackstar and Racecourse orebodies based on Davis (2004). See index diagram below for locations of plans and sections. Diagrams show the distinctive pattern in which Pb+Zn are persistent and broadly stratabound, but with a strong grade boundary which is spatially coincident with the position of the Mount Isa fold. Pb/(Pb+Zn) ratios show pronounced zonation relative to the silica dolomite alteration system, with Pb contents highest near the silica dolomite and progressively transitioning away to more Zn-rich mineralisation.

Figure 2.24. (Facing page). Some representative photographs of Pb-Zn-Ag mineralisation

Alternating sphalerite-rich, pyrite-rich and shale layers. Unknown photographer.

Galena-rich mineralisation enveloping intensely folded and boudinaged shale layers. Unknown photographer.

Carbonate-veined tuff marker bed (not in place). Unknown photographer.

Small-scale disharmonic folds in Pb-Zn ore from the hinge of the Mount Isa fold. Unknown photographer.

Galena-rich mineralisation enveloping intensely folded and boudinaged shale layers. Unknown photographer.

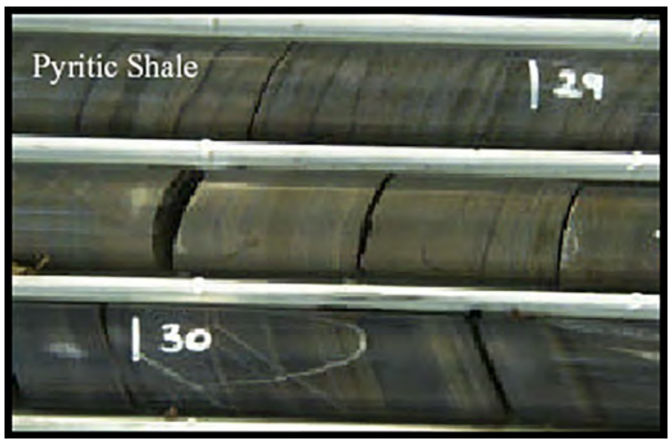

Pyritic shale. MIM AusIMM presentation.

Alternating sphalerite-rich, pyrite-rich, galena-rich and shale layers. Unknown photographer.

Galena-rich detachment surface. Unknown photographer.

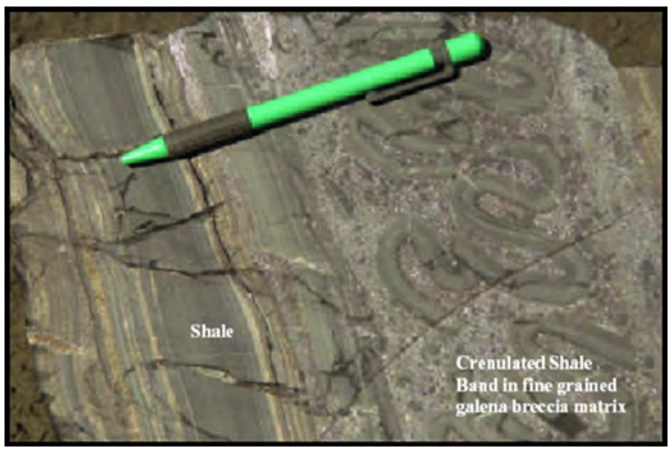

Galena-rich mineralisation enveloping intensely folded and boudinaged shale layers. MIM AusIMM presentation.

Hand specimen photograph showing a lateral transition from barren shale and siltstone to bedded sphalerite-pyrite mineralisation across a vein, strongly indicating a replacive origin for the mineralisation. Photo from Perkins (2011).

Sphalerite and galena rich bands enveloping a zone of disharmonic folding in pyritic shale. MIM AusIMM presentation

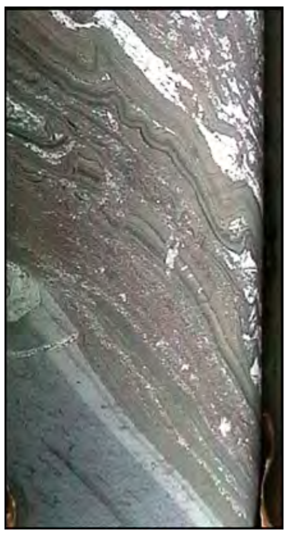

Sphalerite-rich layers occurring between folded and boudinaged pyritic shale layers, associated with coarse grained carbonate. MIM AusIMM presentation

Galena-rich mineralisation associated with weakly folded and boudinaged shale layers. Unknown photographer.

Copper system rocktypes

From MIM rocktypes poster - Figure 2.25

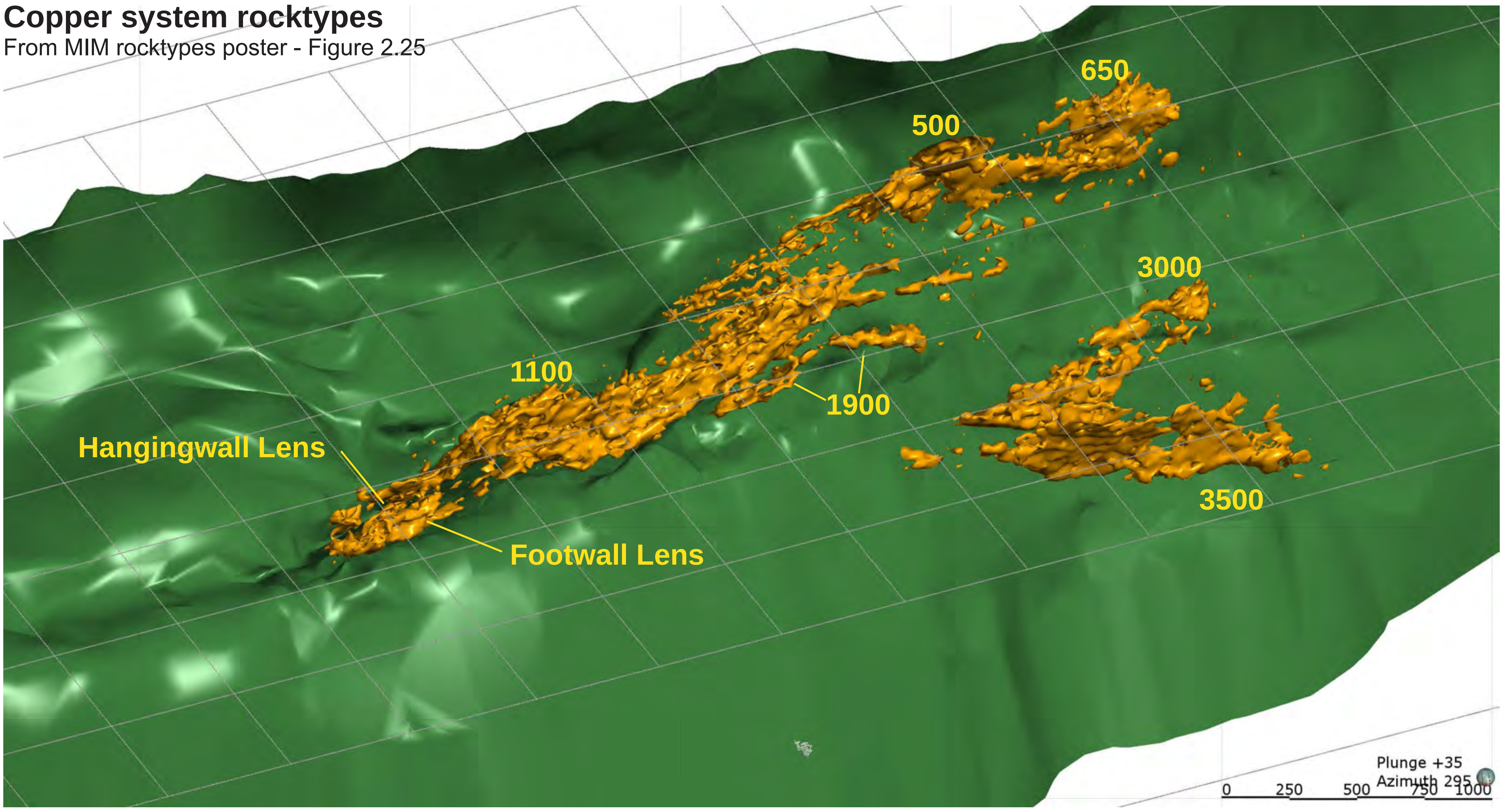

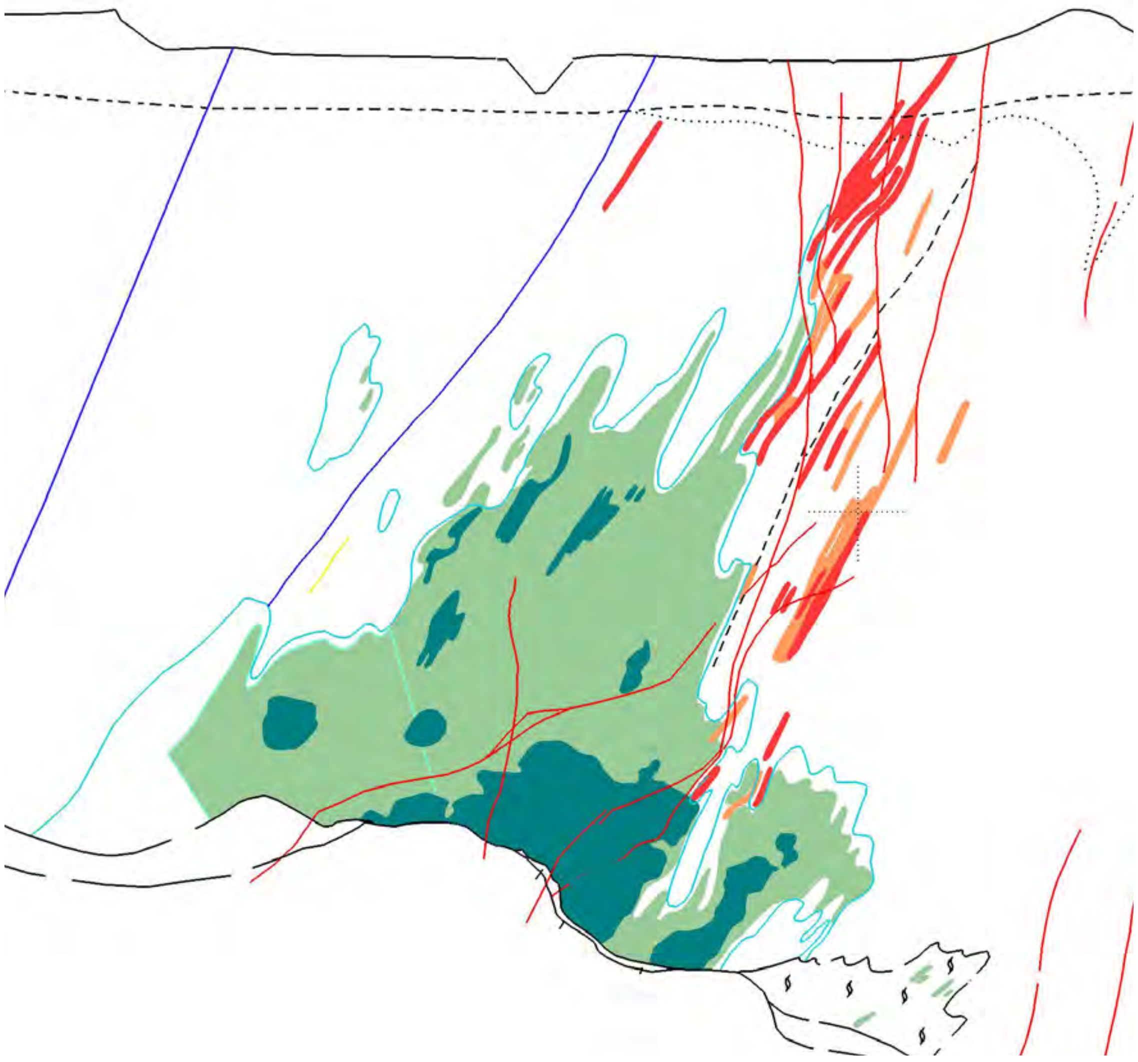

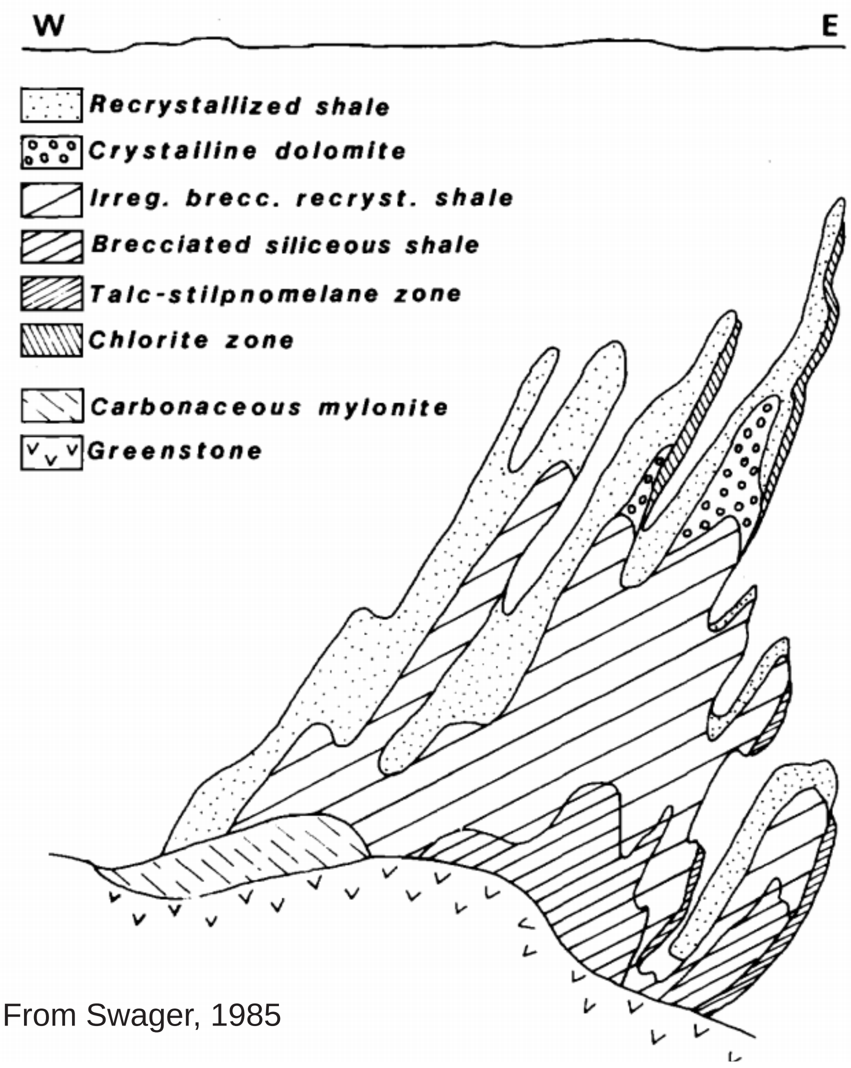

From Swager, 1985

Sheared Eastern Creek Volcanics (Basement)
Dark green to grey, fine grained foliated chlorite with occasional Quartz veining.

Mylonite
Black strongly foliated rock, with graphite and quartz. Found predominantly along the basement contact.

Recrystallised shale (Recryst)
Well bedded rock with alternating bands of black to grey shale and crystalline dolomite. May also occur with bands of fine grained pyrite.

Irregularly brecciated and recrystallised Shale (Irreg)
Pale grey breccia of dolomitic and/or siliceous fragments in crystalline dolomite matrix

Fractured Siliceous Shale (FSS)
Black to grey brecciated carbonaceous chert. Main ore bearing rock with chalcopyrite being deposited through veins in the rock.

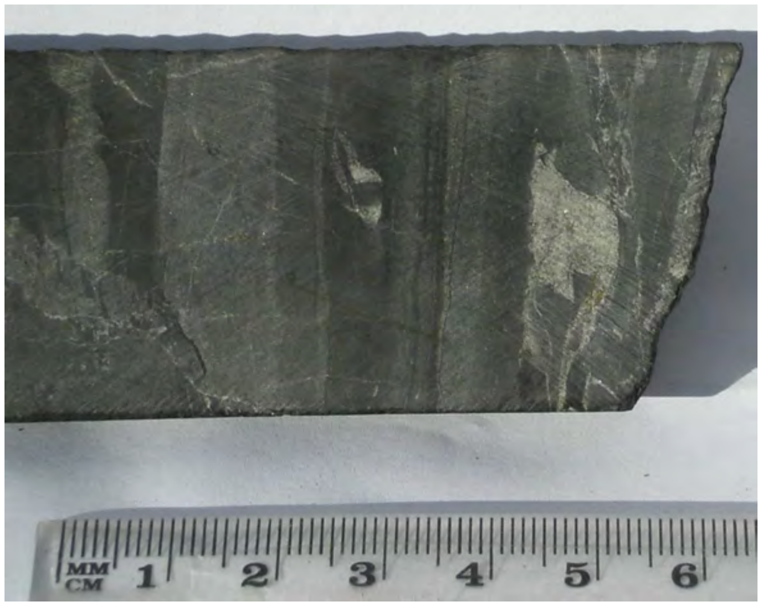

Siliceous Shale
Very dark grey to black carbonaceous chert with bedding textures. Hard to scratch due to siliceous nature

Slatey Shale
Dark grey to black shale with well preserved penetrative cleavage. Little to no original bedding textures. Highly sheared.

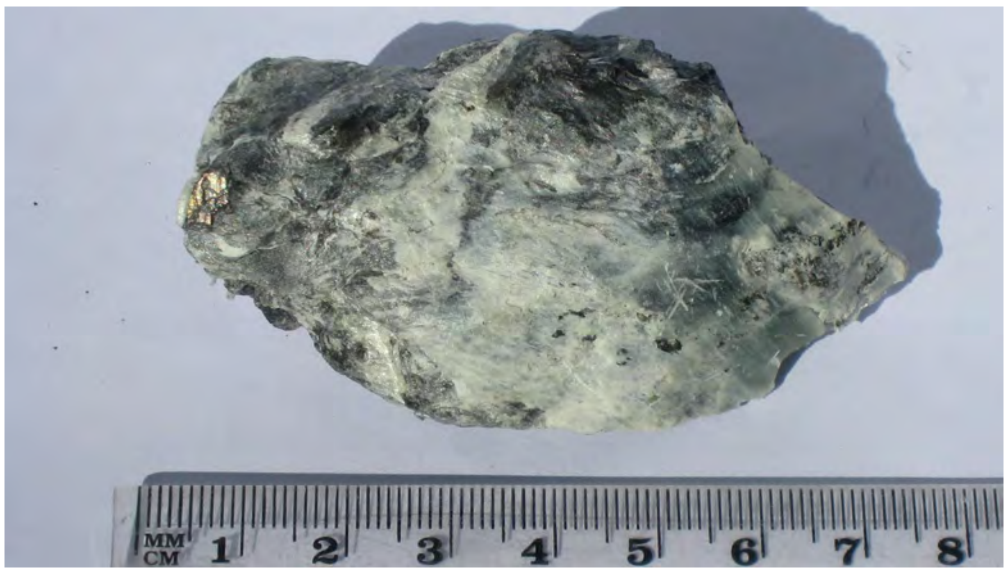

Talc
Part of the group of talc-chlorite-stilpnomelane rocks occurring

Urquhart Facies diagrams and photographs from Painter (2003) PhD Thesis

Figure 2.26

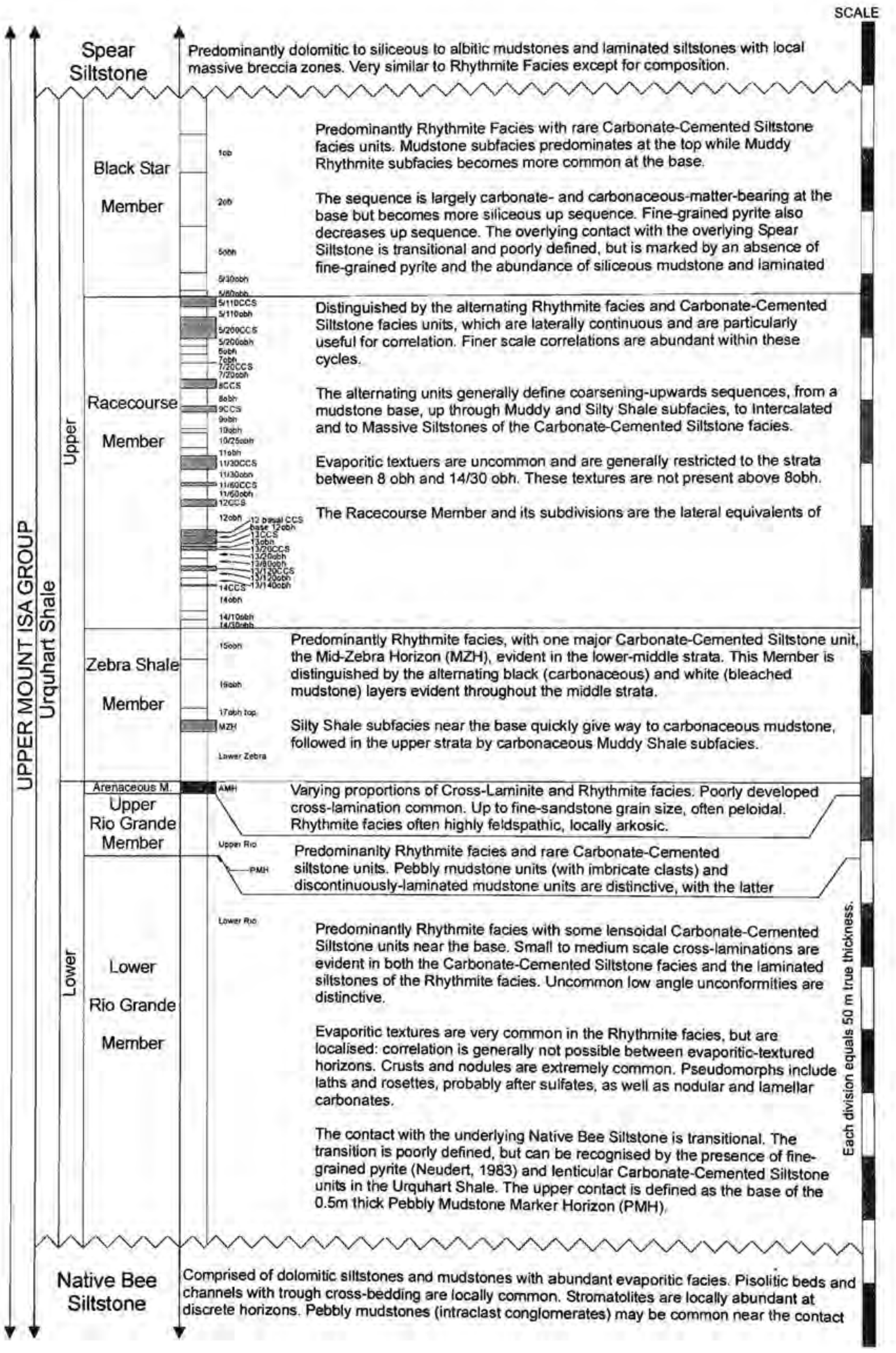

Figure 4.10 - The Thinly-bedded shale subfacies of the Rhythmite facies, Racecourse Member, Urquhart Shale. Sedimentary way-up is to the top of each column. Alternating mudstone (light grey) and laminated siltstone (dark grey) are commonly interbanded on a scale of less than 1 cm. Each couplet represents a bed Coarse-grained pyrite is common as blebs or bands, but fine-grained pyrite is absent (Qz010, tray 179, 987.3-993.5m).

Figure 4.13 - Large displacive carbonate nodules in the Rhythmite facies, Racecourse Member. Deflection of bedding, which is either a result of displacive growth, differential compaction or a combination of both, is present around large nodules. Both nodules have grown in the laminated siltstone portion of the bed, which in both cases is fine-grained pyritic.(Qz010, 1064.3 and 1067.5m).

Figure 4.19 - Molar tooth structure, Zebra Shale Member. **a)** Large structure displaying local differential compaction around intact, subvertical portions and little or no evidence of compaction around fractured portions (Qz010, 1216 m). **b)** Closer view of a molar tooth structure. The material in the vein is micritic calcite and dolomite. The concentration of carbonaceous matter is variable. In the upper right and lower right, carbonaceous matter is significantly more concentrated in the to the right of that vein than in the left (Qz010, 1294.5m)

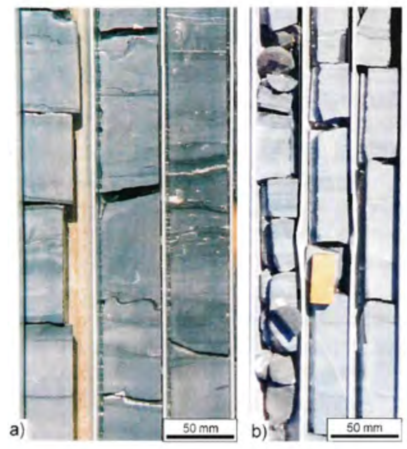

Figure 4.21 - Coarse siltstone subfacies, Carbonate-Cemented Siltstone facies, Racecourse Member, Urquhart Shale. The precompactional cement imparts a lighter colour to the rock than that of the Rhythmite facies. **a)** Carbonaceous stylolites are present in columns 1 and 2, and swaley lamination is present at the base of column 2 and 3. The top of column 3 contains coarse-grained pyrite and contain intercalated mudstone beds (Qz010, tray 206, 1149.0-1156.0m) **b)** Lighter coloured, intense cementation. Stylolites are present at the tops of columns 2 and 3, and swaley lamination is present at the base of these columns. Poorly-defined concretions are present in the middle of column 2. Column 1 represent the Intercalated siltstones subfacies (Zw295, tray 24, 744.9-753.2m)

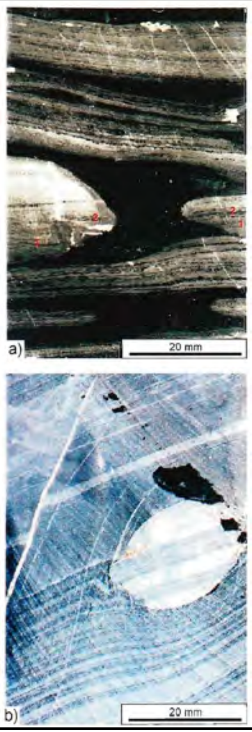

Figure 4.25 - Carbonate-Cemented Siltstone type concretions. a) Numerous concretions in the Intercalated Siltstones subfacies, Qz010, 1132.0m. Each of the laminae marked (1, 2) can be traced from one concretion, through the carbonaceous siltstone and into the other concretion b) Solitary CCS-type concretion in Rhythmite facies rocks, Qz011, 1059.7m. Laminated siltstone portions of beds can be traced through the precompactional concretion, indicating compaction in excess of 50%. The millimetre thick units of mudstone and laminated siltstone, which comprise the couplets beneath those beds in the concretion, also represents beds. Dark patches are small pits in the sample.

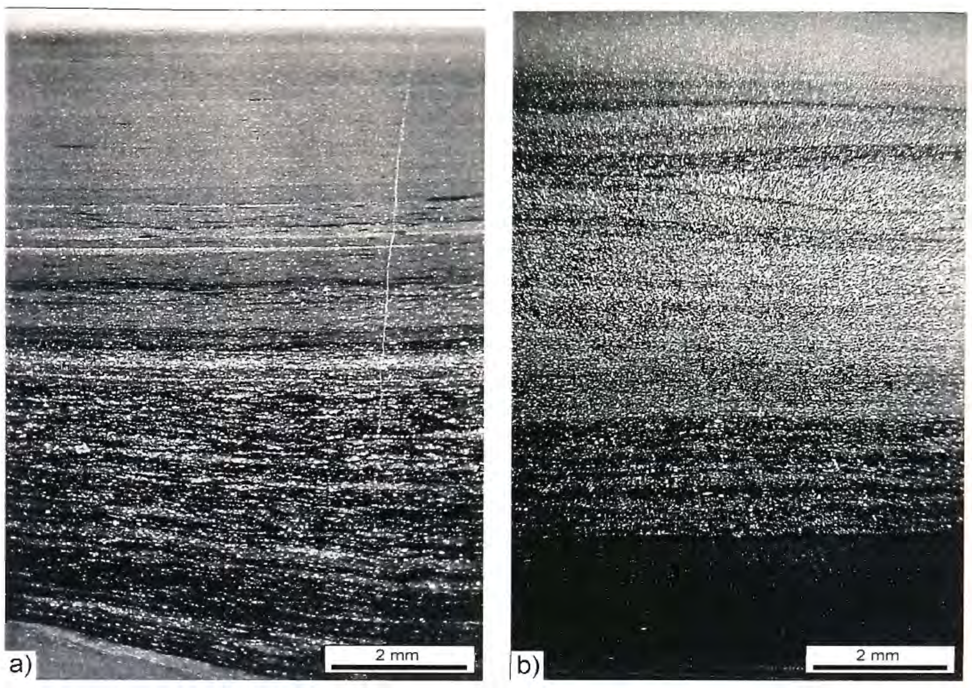

Figure 4.06 - Rhythmite facies. a) Graded bed of the Rhythmite facies. Carbonaceous laminae of the laminated siltstone at the base of the specimen grade up to discontinuous laminae in a fine siltstone to laminated mudstone towards the top. The white layer at the top is an evaporitic crust (note the diffuse lower margin). The mudstone in the lower left corner is the underlying mudstone top of the previous graded bed (O865, 1091.1 m). b) Carbonaceous laminated siltstone with a sharper gradation to the overlying discontinuously laminated fine siltstone. The fine siltstone exhibits a poorly developed cross lamination before grading up to the massive mudstone at the top of the picture. The dark band at the base of the picture is the uppermost carbonaceous mudstone of the underlying depositional cycle (Qz010, 1253.0 m).

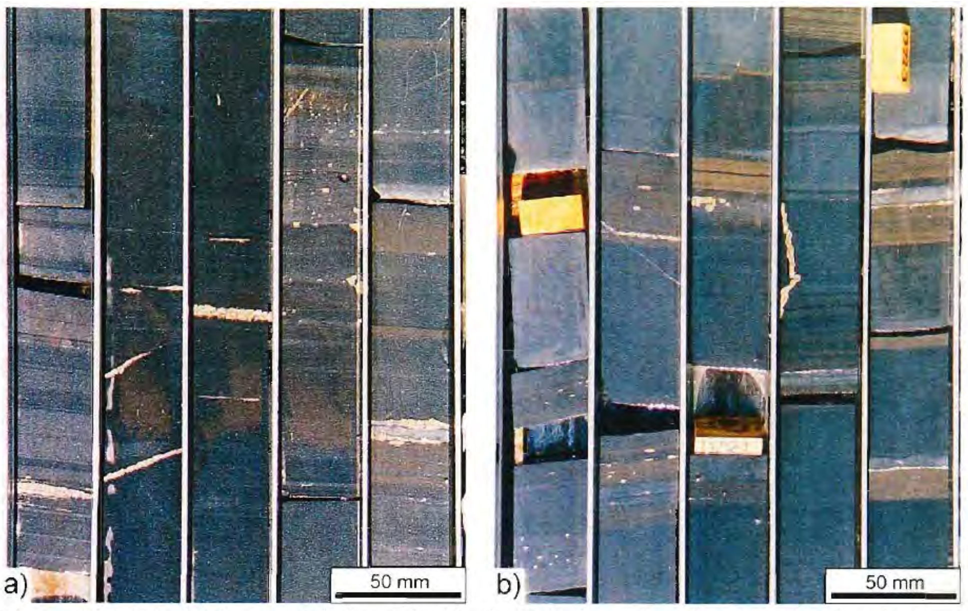

Figure 4.07 - The Mudstone subfacies of the Rhythmite facies, Zebra Shale Member, Urquhart Shale. Younging is to the top of each column. **a)** Mudstone subfacies showing banded light grey and dark grey mudstone in column 1, carbonaceous mudstone in columns 2 , 3, and 4. Column 4 also contains a coarser-grained, light grey laminated siltstone. (Brown colouring on columns 2, 3 and 4 is surface dust.) Column 5 contains pyritic laminated siltstone interbanded with mudstone (Muddy Shale subfacies). The light coloured bands and blebs are coarse-grained pyrite (Qz010, tray 231, 1310.0-1316.0m). **b)** Mudstone subfacies containing minor laminated mudstone and siltstone that contains fine-grained pyrite (columns 1-4). The top of column 4 and all of column 5 contains a high porportion of laminated siltstone (fine-grained pyritic) relative to mudstone, indicative of the Muddy Shale subfacies (Qz010, tray 240, 1367.0-1374.0m).

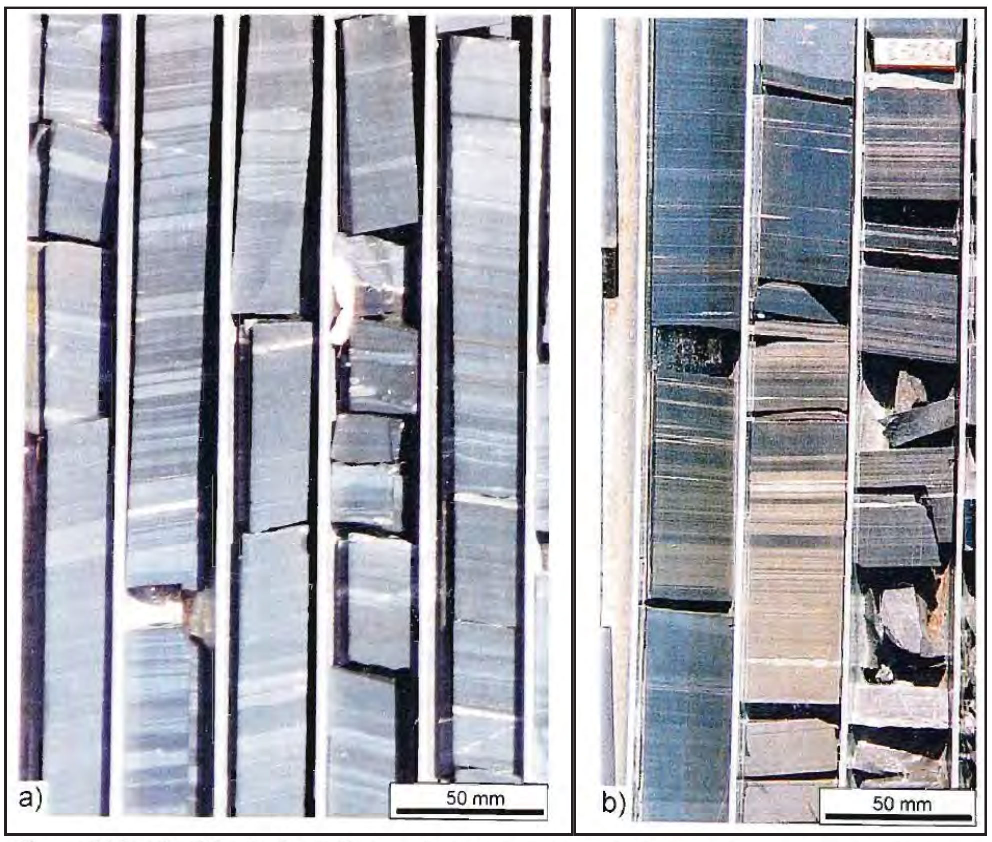

Figure 4.09 - The Silty Shale subfacies of the Rhythmite facies. Sedimentary way-up is to the top of each column. **a)** Racecourse Member, Urquhart Shale. Carbonaceous laminated siltstone with subordinate light to medium grey mudstone. Couplets define bedding, which is of variable thickness. Parts of column 2 are Thinly-bedded Shale subfacies (beds < 10mm). Minor fine-grained pyrite is present in thin laminated siltstone bands in column 5 (bronze colour). The light coloured bands and blebs are coarse-grained pyrite (Zw295, tray 28, 802.8-812.5m). **b)** Zebra Shale Member, Urquhart Shale. Silty Shale subfacies dominated by thickly bedded carbonaceous laminated siltstone and fine-grained pyritic laminated siltstone. Intense fine-grained pyrite mineralisation in column 2 has not destroyed the fine lamination. The light coloured bands and blebs are coarse-grained pyrite (Qz010, tray 242, 1386.0-1391.8m).

Figure 4.08 - The Muddy Shale subfacies of the Rhythmite facies . Sedimentary way-up is to the top of each column. **a)** Zebra Shale Member, Uruquhart Shale. Most thin dark bands are laminated siltstone, whereas mudstone varies from light to dark grey. Couplets of these bands define bedding. The light coloured bands and blebs are coarse-grained pyrite (Qz010, tray 230, 1303.4-1310.0m). **b)** Racecourse Member, Urquhart Shale. Fine-grained pyritic laminated siltstone interbanded with massive to laminated mudstone. White carbonate layers are probably crusts. (Qz010, tray 191, 1054.5-1059.7m)

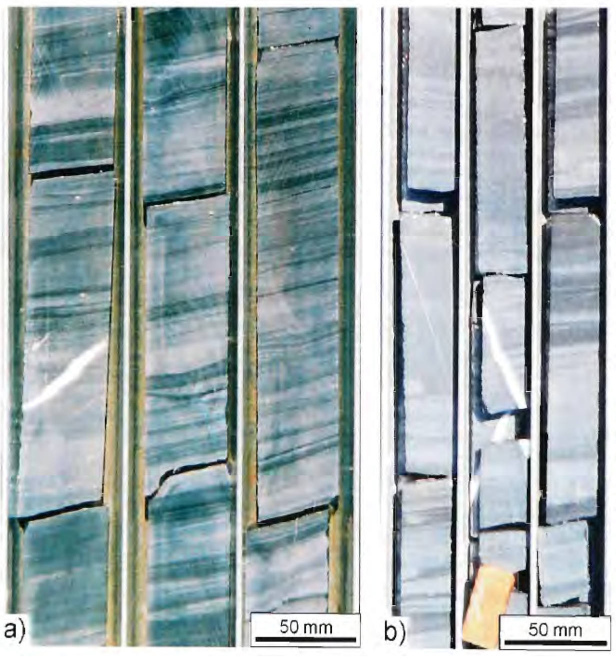

Figure 4.22 - Intercalated siltstones subfacies, Carbonate-Cemented Siltstone facies, Racecourse Member, Urquhart Shale. The precompactional cement imparts a lighter colour to the rock than that of the Rhythmite facies. **a)** Alternating bands of carbonate-cemented coarse siltstone, mudstone and laminated siltstone, similar to that of the Rhythmite facies (Qz010, tray 189, 1043.0-1048.6m) **b)** Similar to a), but with variable intensity precompactional cementation. In column 1, a concretion containing intense cementation is hosted by less strongly cemented coarse siltstone. Irregular bedding, accentuation of flutes by cementation and load structures is present at the base of column 1. Columns 2 and 3 show variably cemented units interbanded with one another, locally showing swaley lamination and irregular bedding (Zw295, tray 25, 753.2-762.0m)

Figure 4.12 - Numerous crusts in Muddy Shale subfacies of the Rhythmite Facies, Lower Rio Grande Member. Bedding structure is well-defined, from laminated siltstone (carbonaceous or fine-grained pyritic) through medium to light grey massive mudstone, to light grey to white calcitic micrite crust at the top. The top of each crust is sharp, but the bases vary between sharp and diffuse (Qz010, tray 247, 1410.5-1417.0m).

Figure 4.27 - The Cross Laminite facies, Arenaceous Member, Urquhart Shale (O865, tray 120, 767.4-773.7m). The Cross Laminite facies is predominant in columns 1, 3 and 4. Column 2 contain an intervening package of fine-grained pyritic Rhythmite facies rocks. The Cross Laminite facies is distinguished by the coarse parallel to wavy to crossed laminae and coarse grain size. The light coloured bands and blebs are coarse-grained pyrite.

Mineralogical and chemical summary zoning from Painter (2003) PhD Thesis - Figure 2.27

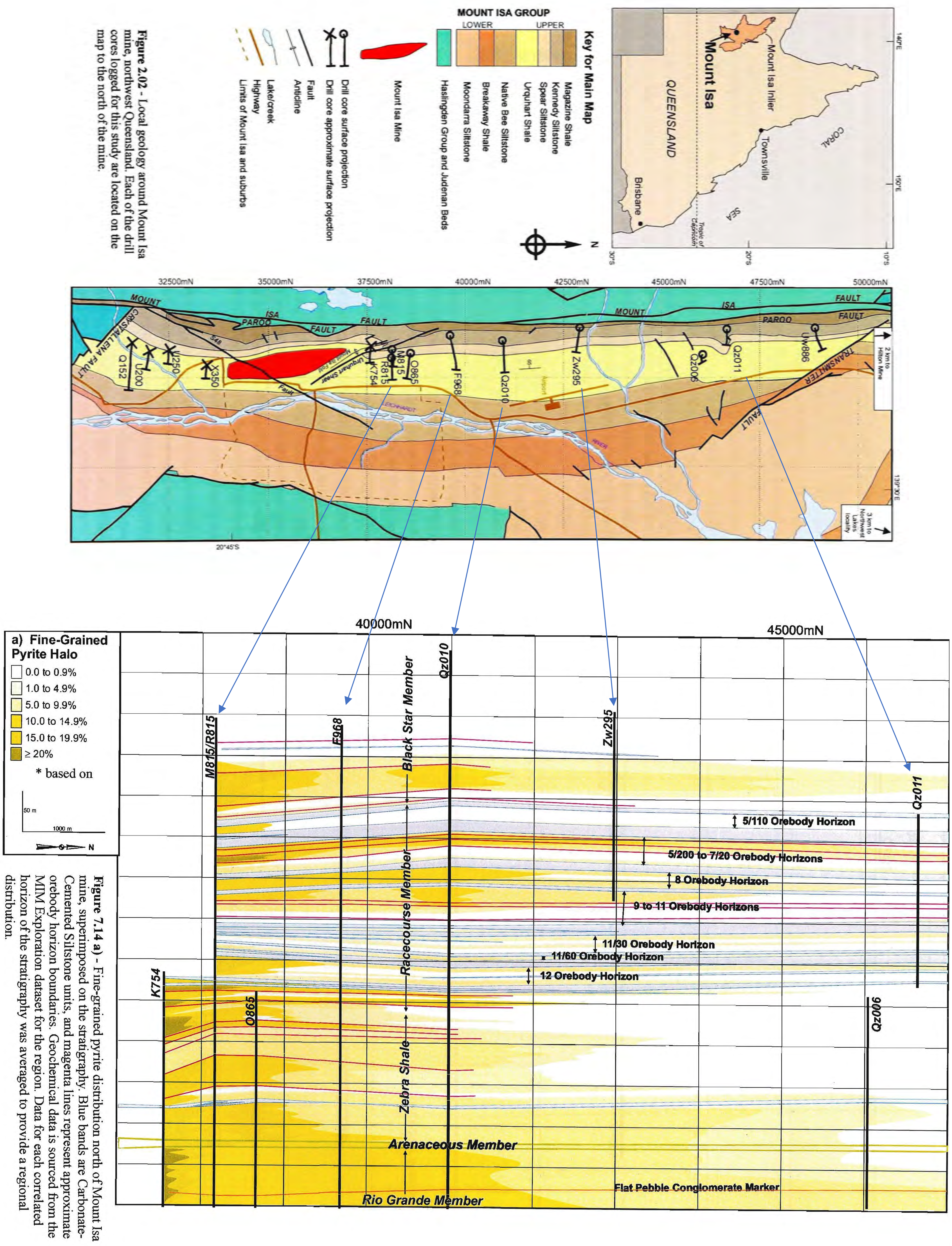

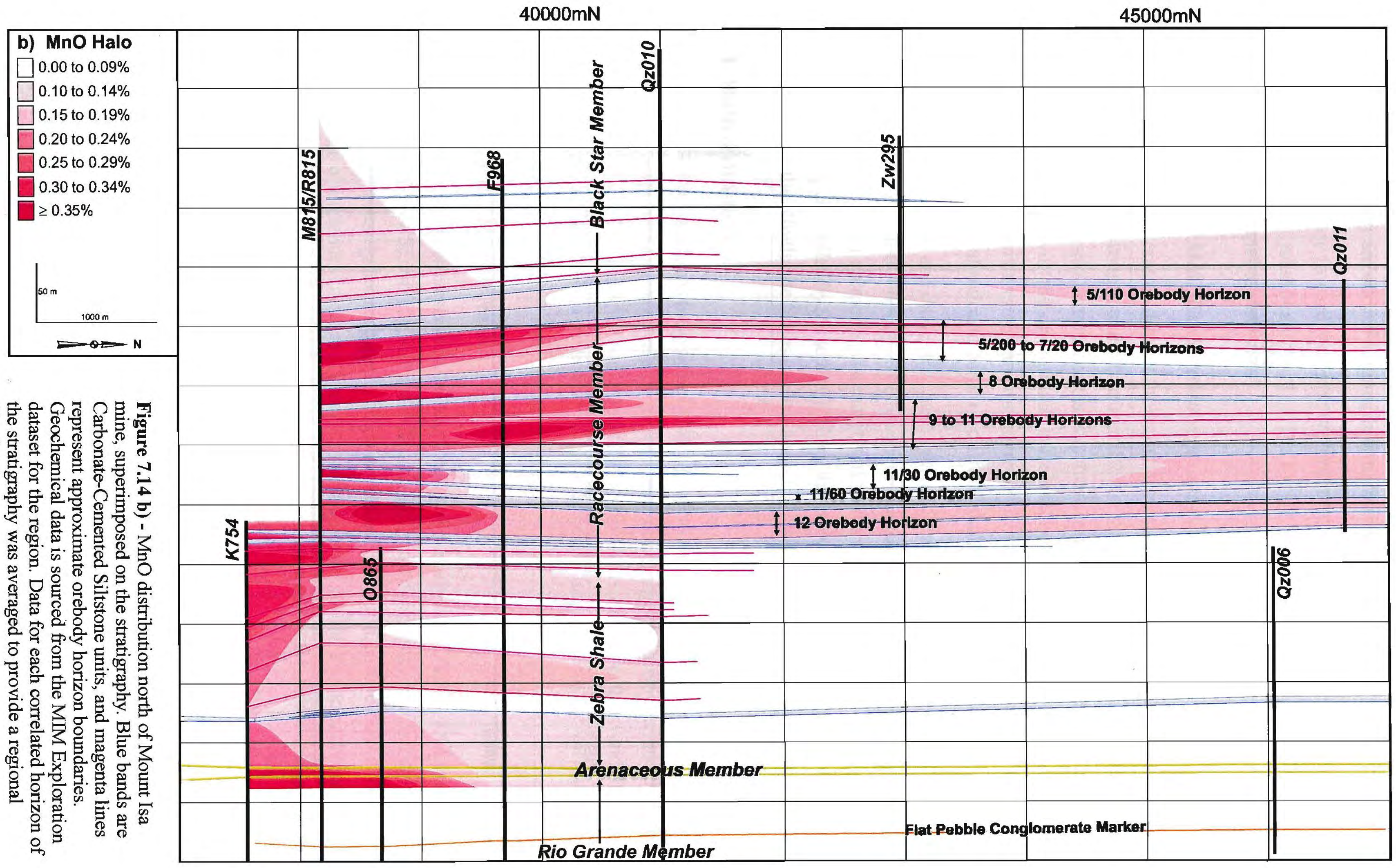

Figure 7.14 b) - MnO distribution north of Mount Isa mine, superimposed on the stratigraphy. Blue bands are Carbonate-Cemented Siltstone units, and magenta lines represent approximate orebody horizon boundaries. Geochemical data is sourced from the MIM Exploration dataset for the region. Data for each correlated horizon of the stratigraphy was averaged to provide a regional distribution.

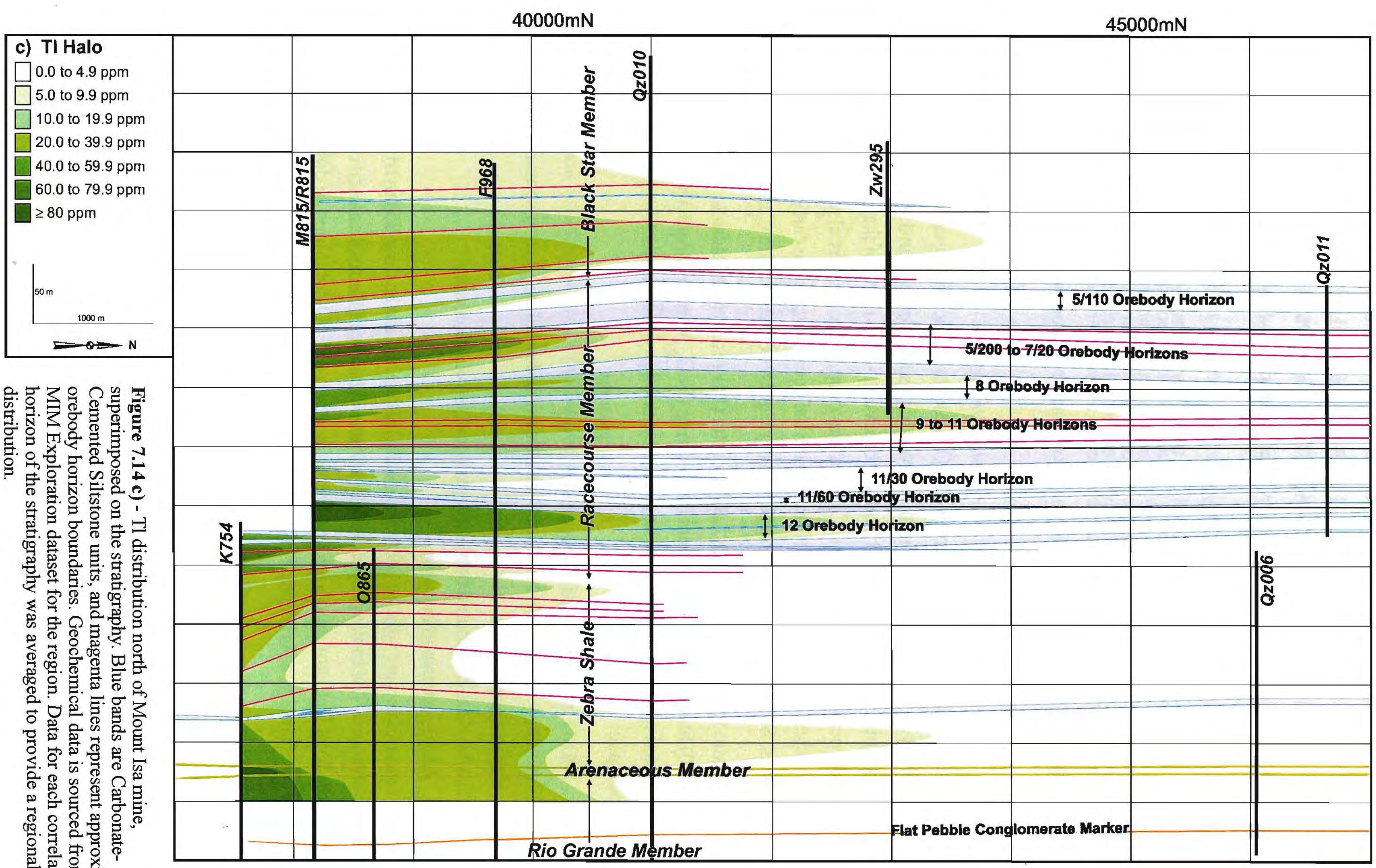

Figure 7.14 c) - Tl distribution north of Mount Isa mine, superimposed on the stratigraphy. Blue bands are Carbonate-Cemented Siltstone units, and magenta lines represent approximate orebody horizon boundaries. Geochemical data is sourced from the MIM Exploration dataset for the region. Data for each correlated horizon of the stratigraphy was averaged to provide a regional distribution.

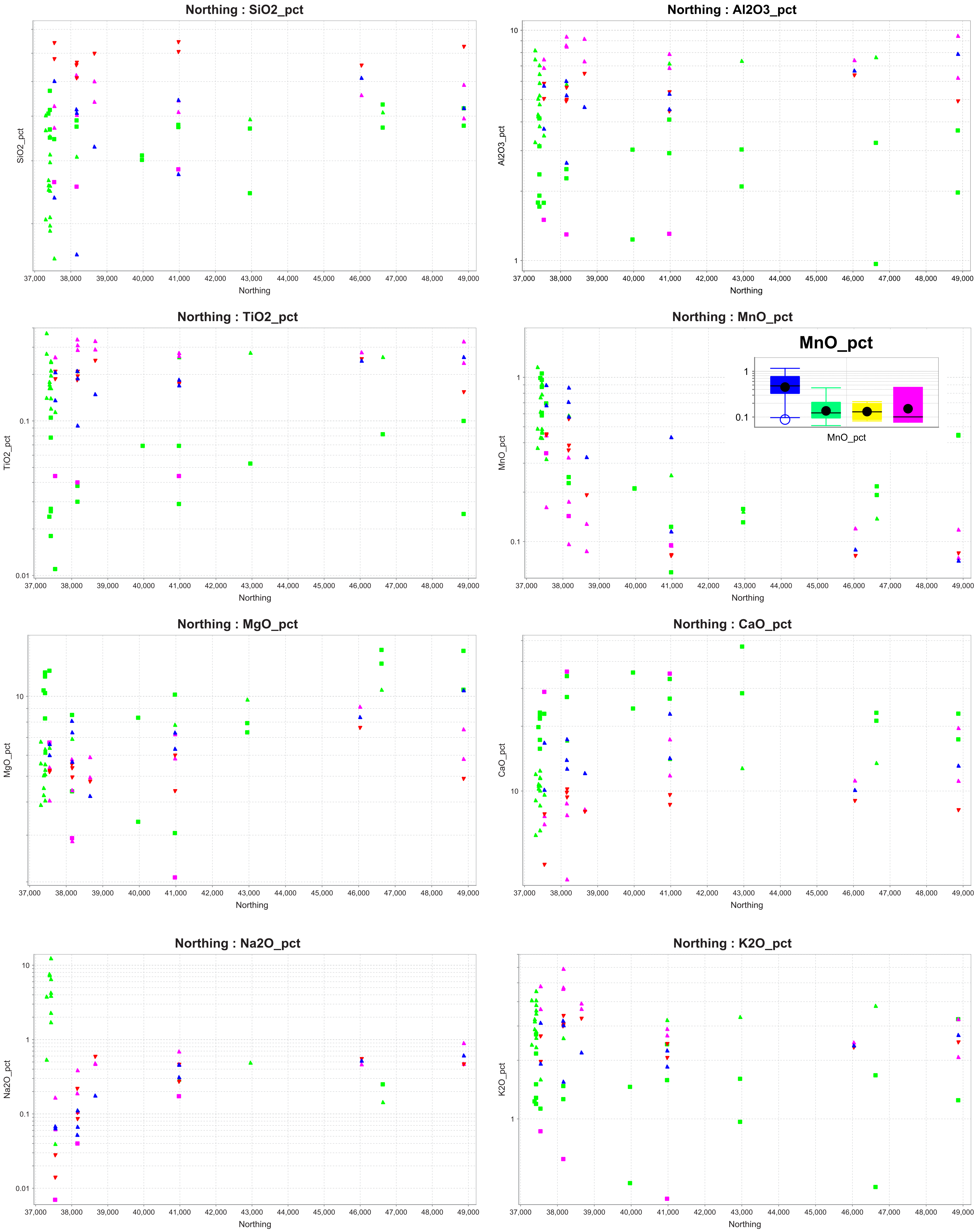

Figure 2.28 (this page, facing page and subsequent 2 pages). Elemental plots of analyses reported by Painter (2003), showing the variation in chemistry within the Urquhart Shale as a function of northing (Isa lease regional grid). The left hand side of each plot represents the northern end of the Isa mine Pb-Zn-Ag orebodies, and plotted results cover a distance of approximately 11km to the north of economic mineralisation within the same stratigraphic interval. Inset maps show box and whisker plots of data sorted into distance categories as shown in the legend. Individual elements and indices are discussed further in the halo section of the text.

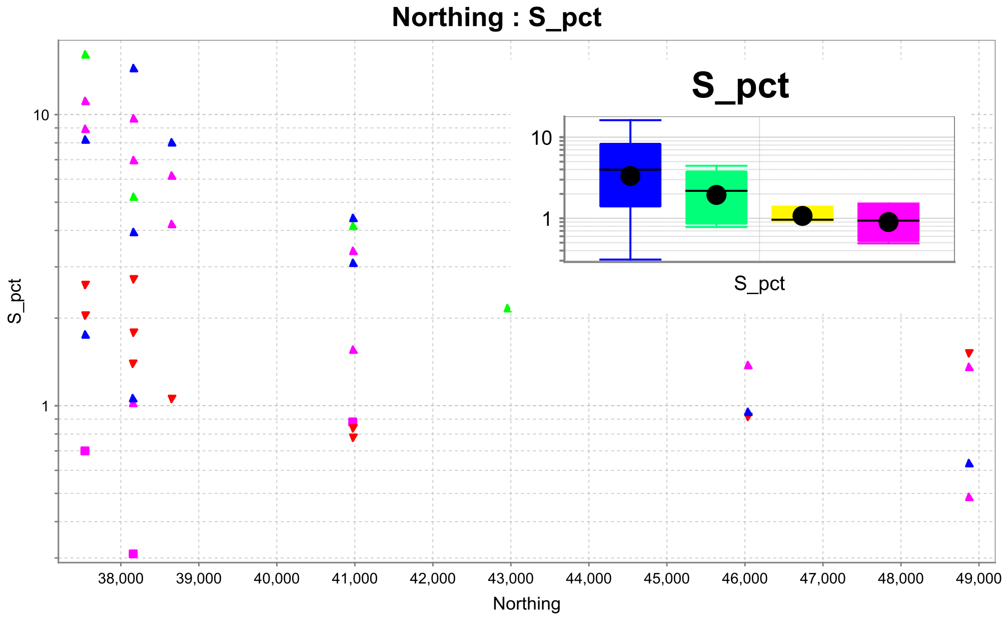
Northing : S_pct
S_pct
S_pct
Northing

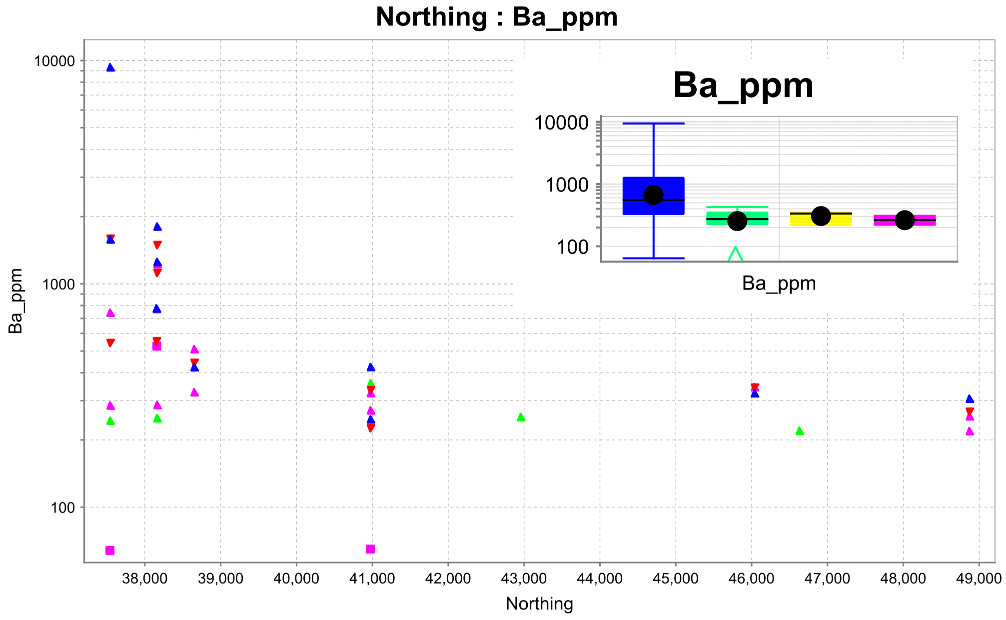
Northing : Ba_ppm
Ba_ppm
Ba_ppm
Northing

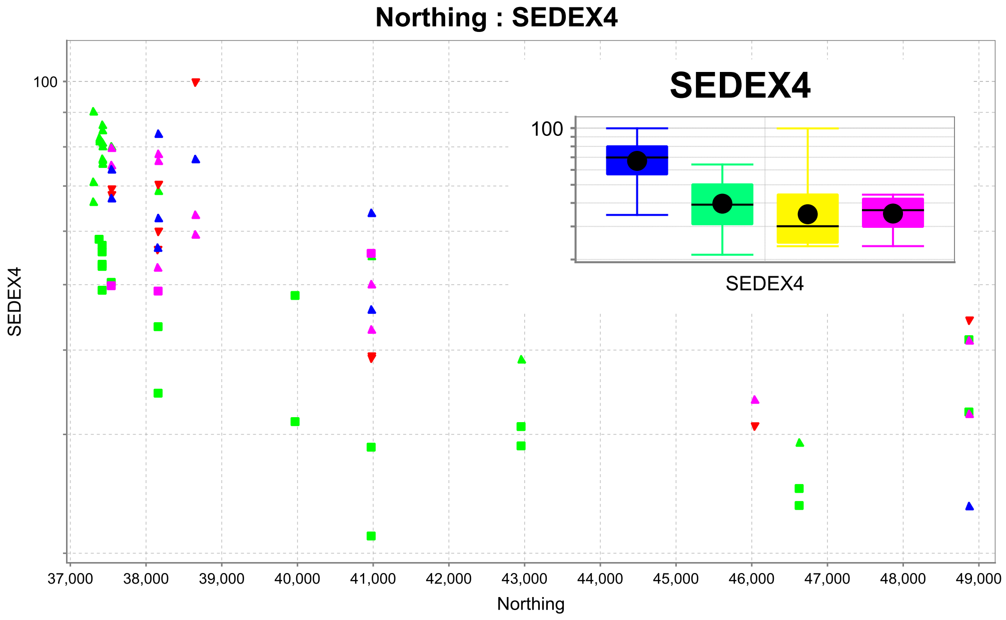
Northing : SEDEX4
SEDEX4
SEDEX4
Northing

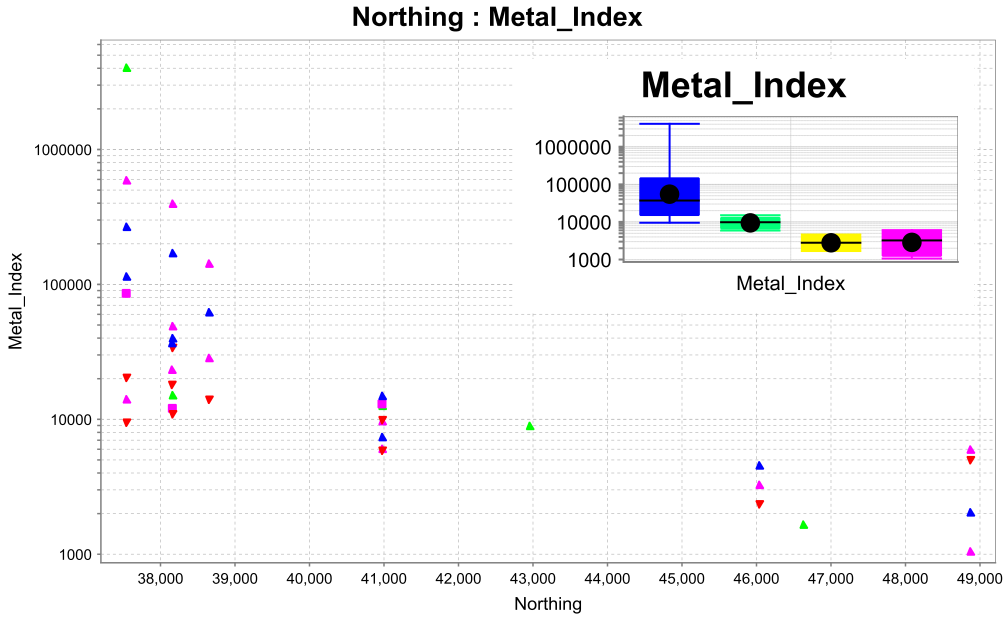
Northing : Metal_Index
Metal_Index
Metal_Index
Northing

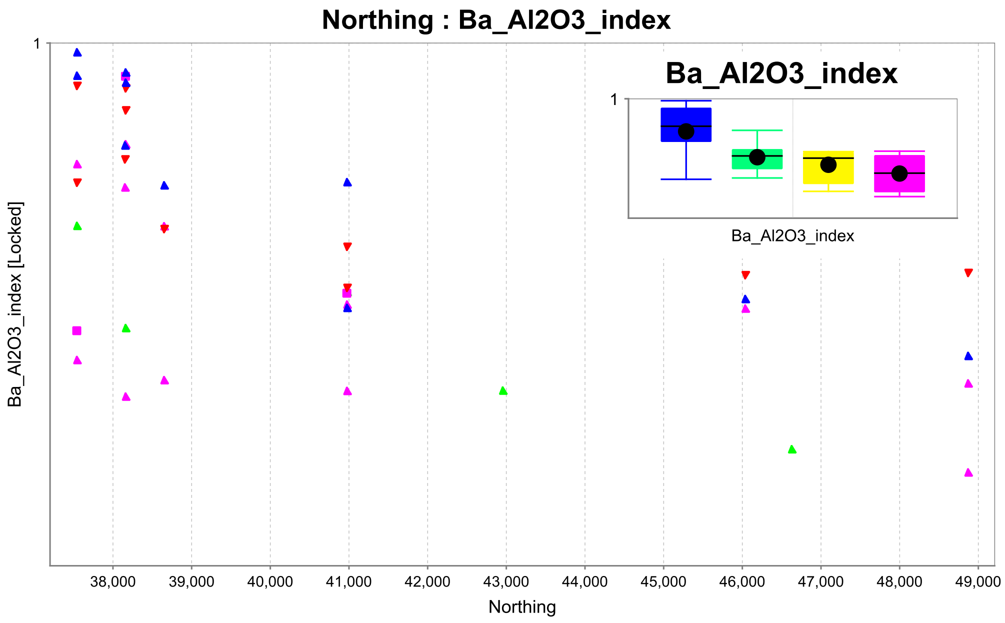
Northing : Ba_Al2O3_index
Ba_Al2O3_index
Ba_Al2O3_index [Locked]
Northing

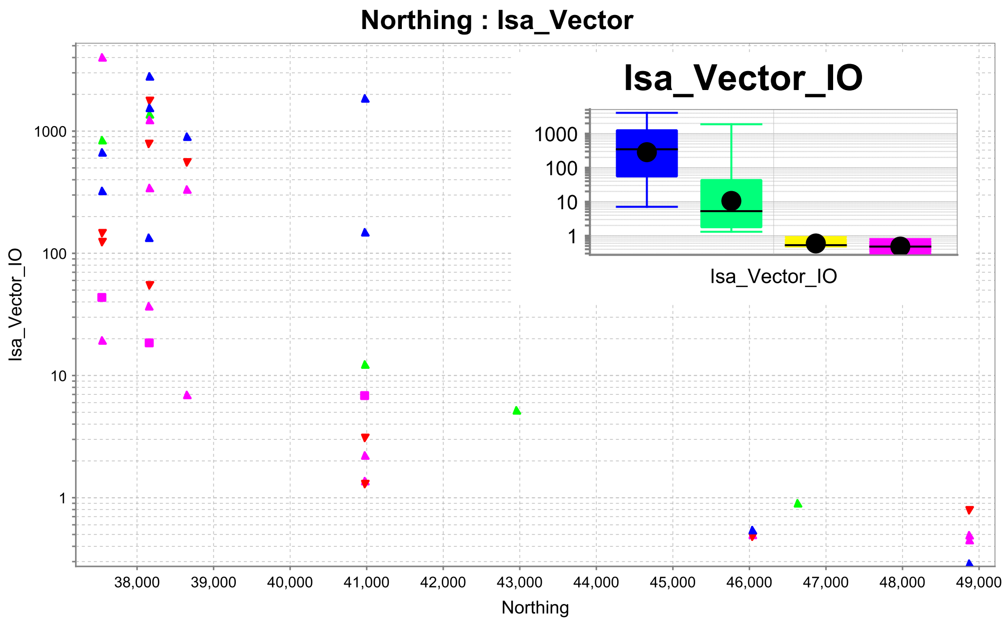
Northing : Isa_Vector
Isa_Vector_IO
Isa_Vector_IO
Northing


Colour
Member
Arenaceous
Racecourse
Rio Grande
Zebra Shale
Shape
Facies
CCS
Cross-Laminite
Rhythmite
Size
Default Size

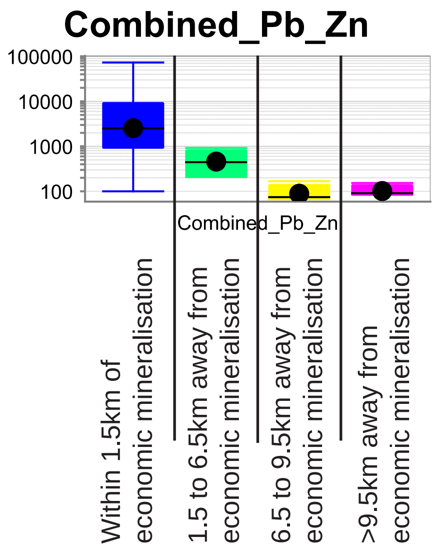
Combined_Pb_Zn
Combined_Pb_Zn
Within 1.5km of economic mineralisation
1.5 to 6.5km away from economic mineralisation
6.5 to 9.5km away from economic mineralisation
>9.5km away from economic mineralisation

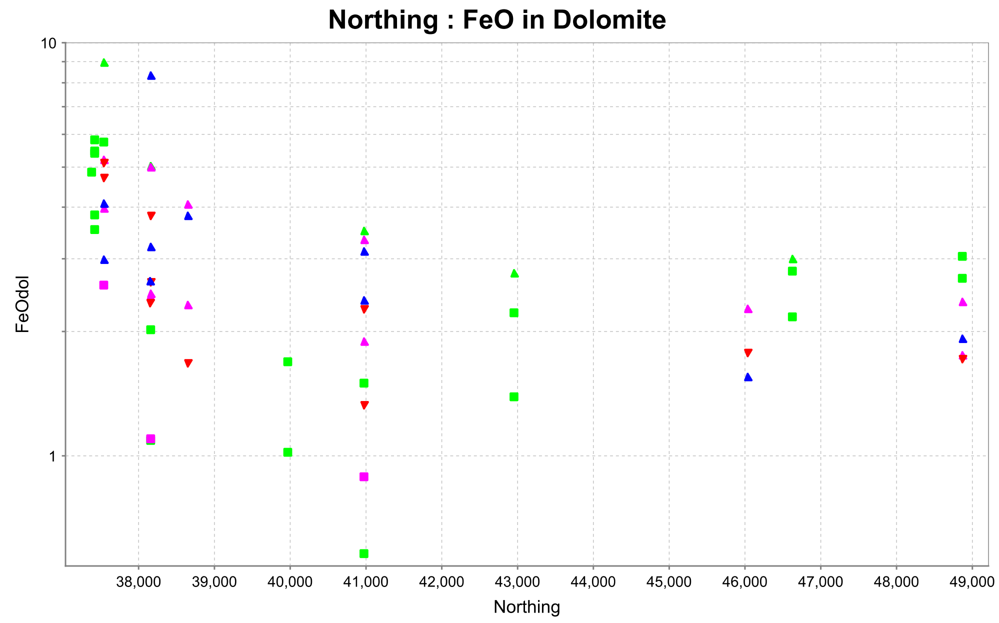
Northing : FeO in Dolomite
FeOdol
Northing

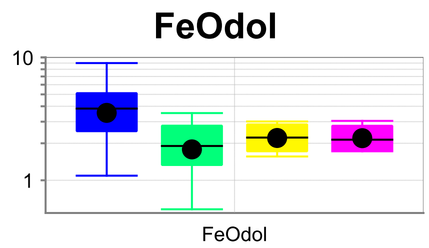
FeOdol
FeOdol

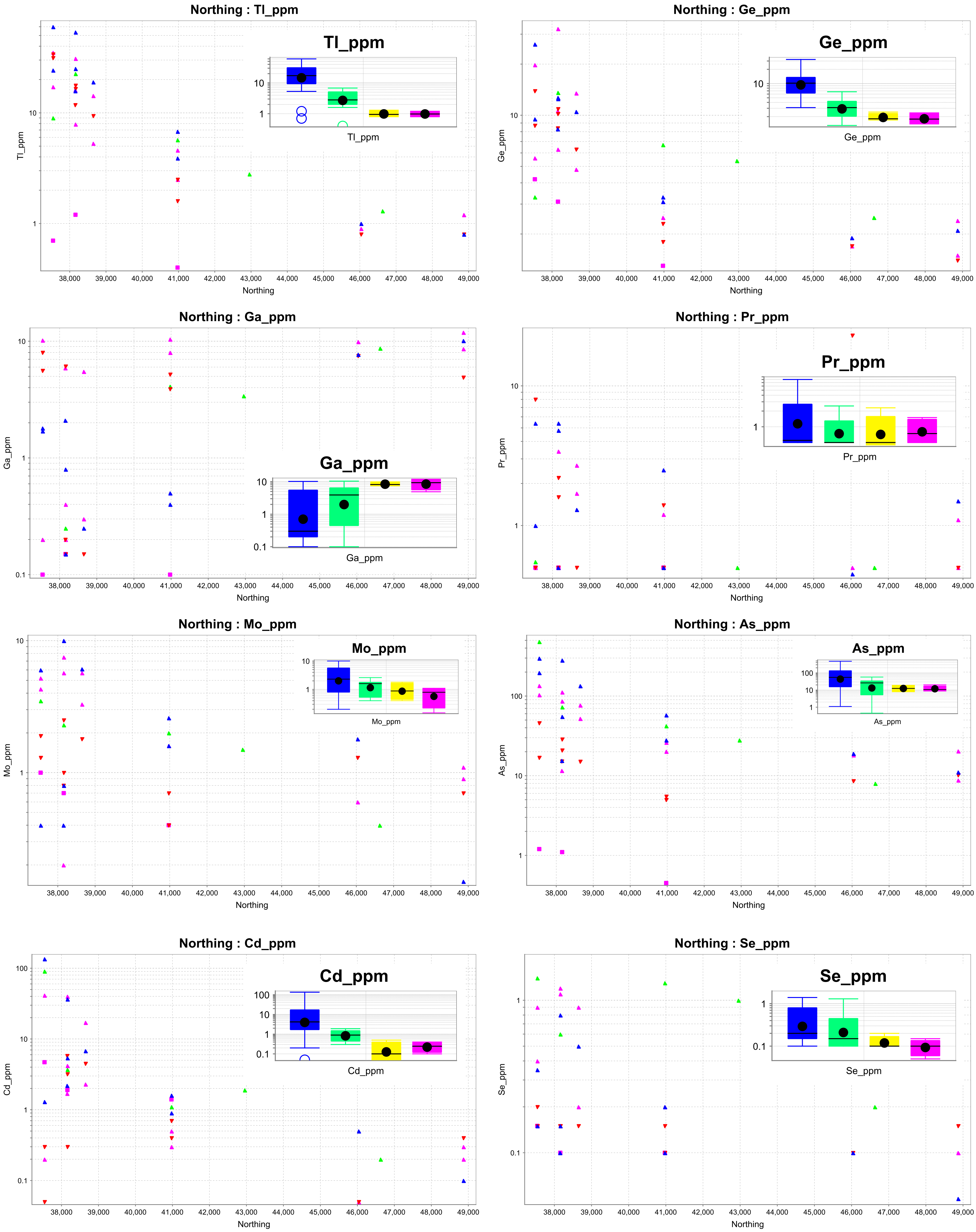

Figure 2.28 (cont'd) (this page, facing page and previous2 pages). Elemental plots of analyses reported by Painter (2003), showing the variation in chemistry within the Urquhart Shale as a function of northing (Isa lease regional grid). The left hand side of each plot represents the northern end of the Isa mine Pb-Zn-Ag orebodies, and plotted results cover a distance of approximately 11km to the north of economic mineralisation within the same stratigraphic interval. Inset maps show box and whisker plots of data sorted into distance categories as shown in the legend. Individual elements and indices are discussed further in the halo section of the text.

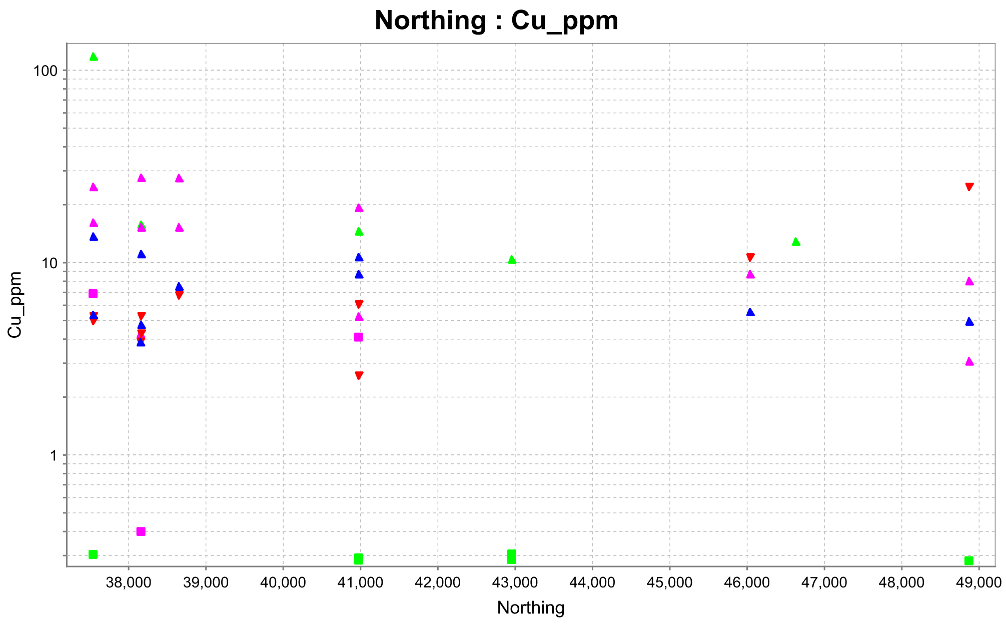
Northing : Cu_ppm
Cu_ppm
Northing

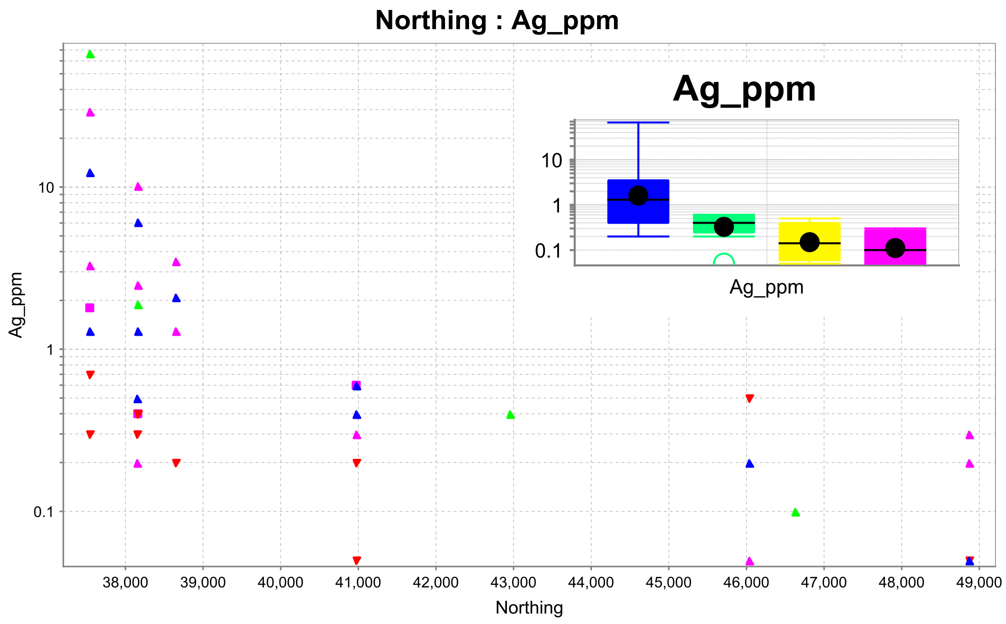
Northing : Ag_ppm
Ag_ppm
Northing
Ag_ppm

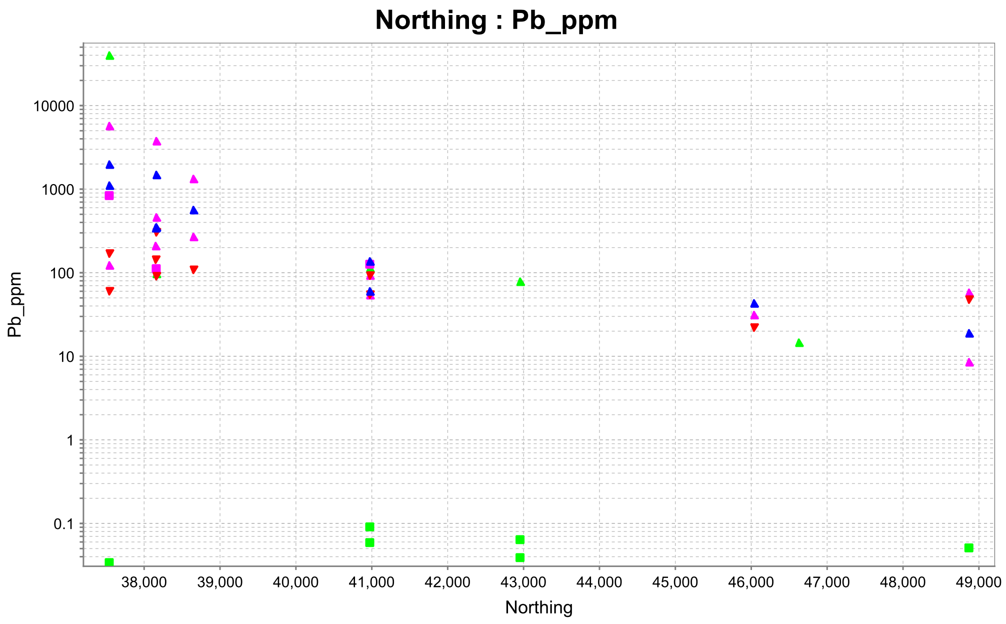
Northing : Pb_ppm
Pb_ppm
Northing

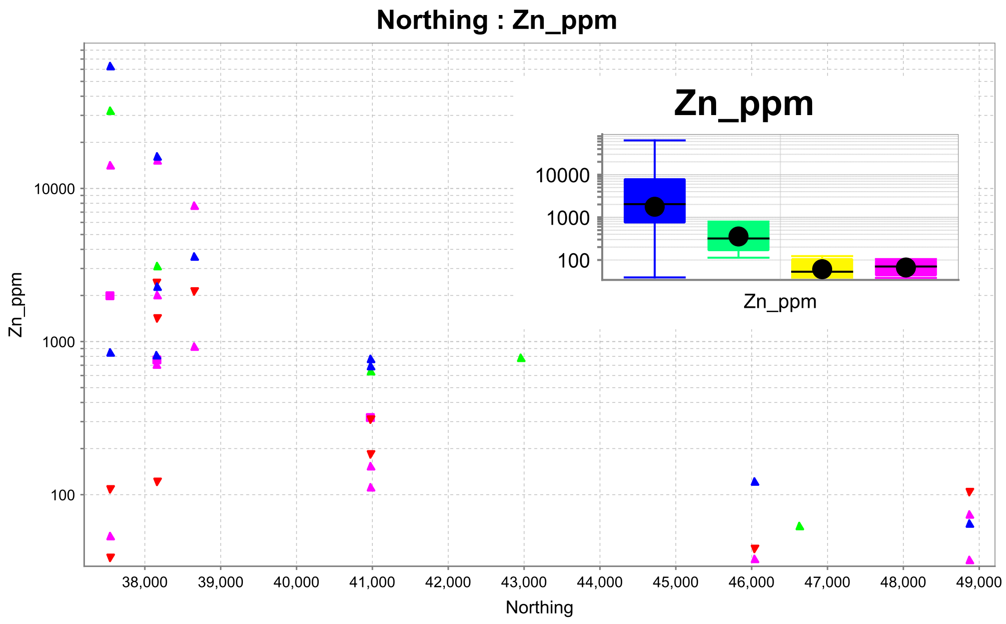
Northing : Zn_ppm
Zn_ppm
Northing
Zn_ppm

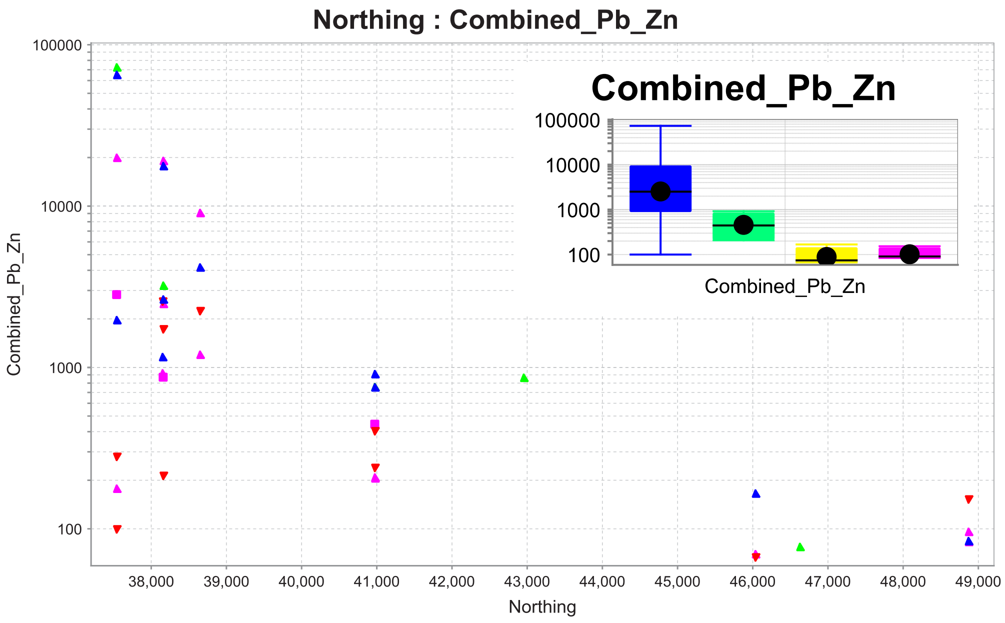
Northing : Combined_Pb_Zn
Combined_Pb_Zn
Northing
Combined_Pb_Zn

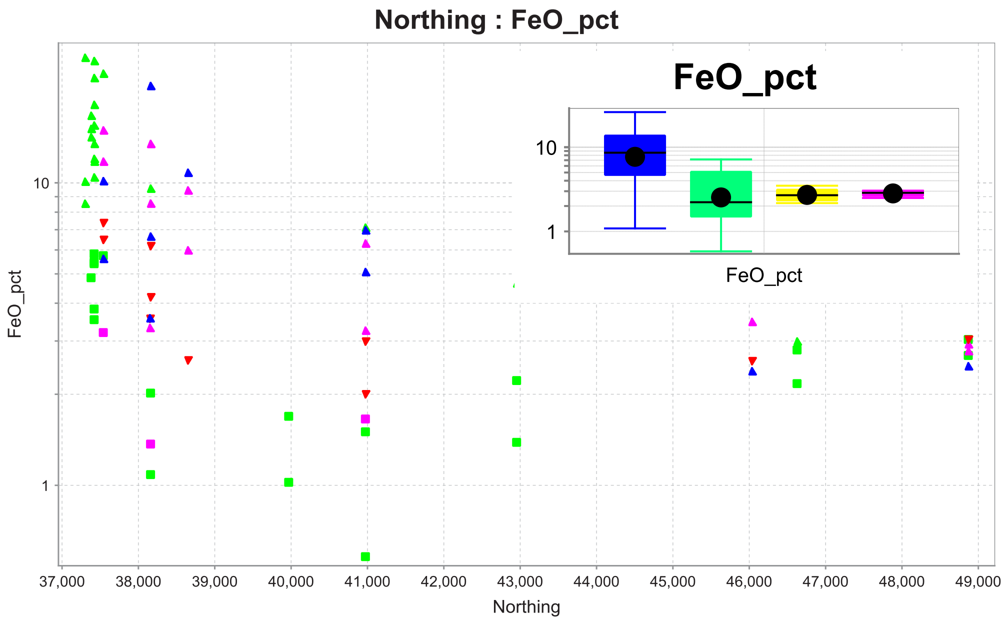
Northing : FeO_pct
FeO_pct
Northing
FeO_pct


Colour
Member
Arenaceous
Racecourse
Rio Grande
Zebra Shale
Shape
Facies
CCS
Cross-Laminite
Rhythmite
Size
Default Size

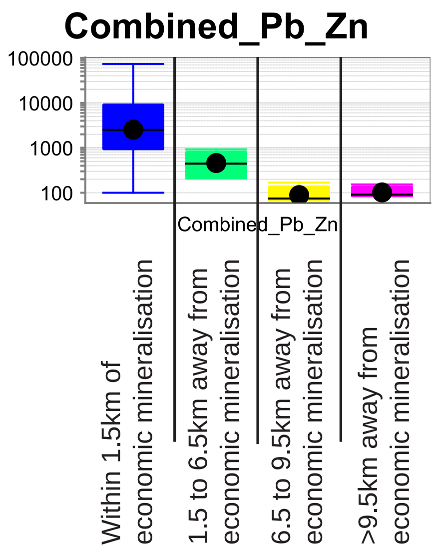
Combined_Pb_Zn
Combined_Pb_Zn
Within 1.5km of economic mineralisation
1.5 to 6.5km away from economic mineralisation
6.5 to 9.5km away from economic mineralisation
>9.5km away from economic mineralisation

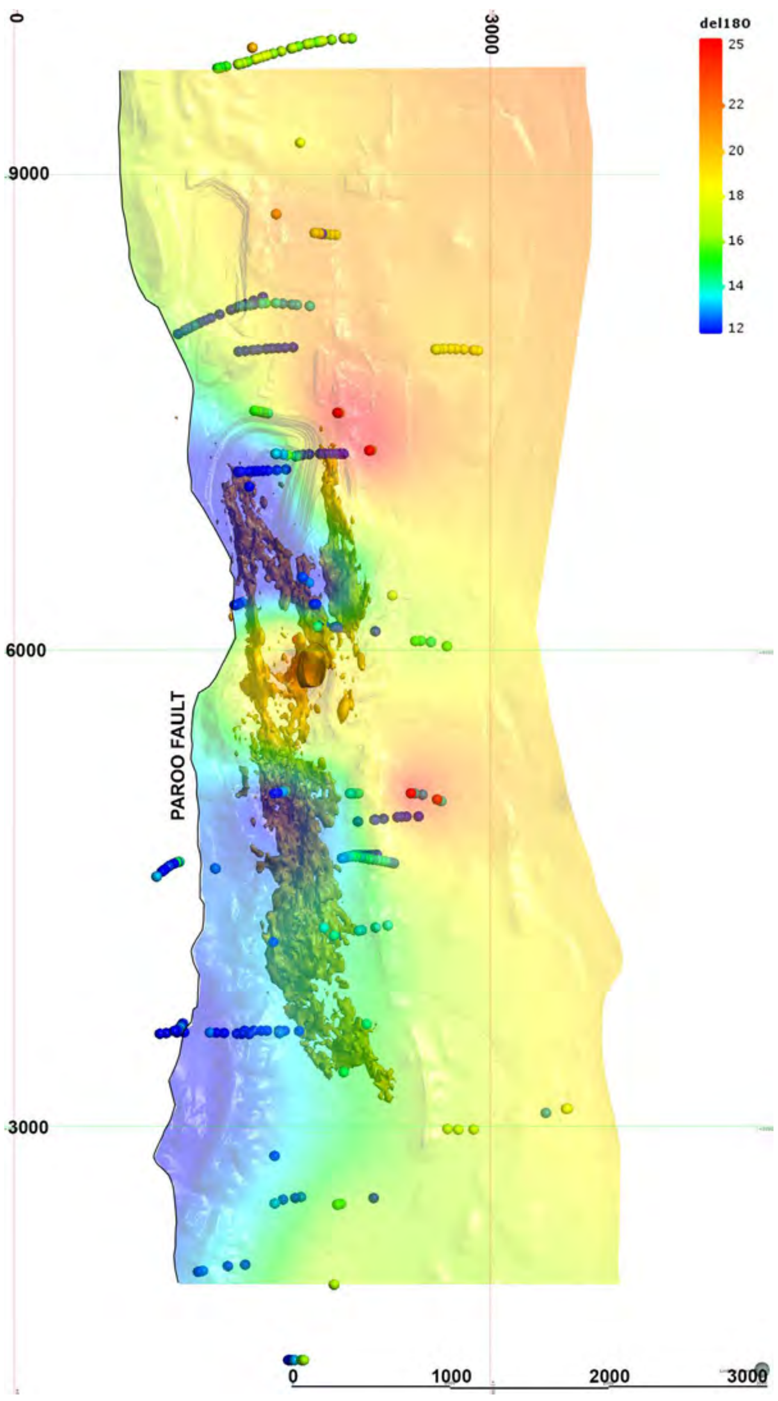

Figure 2.29. Colour gradation of $\delta^{18}O$ evaluated on the local DTM surface, showing an approximation of the expected pattern of $\delta^{18}O$ from shallow drilling. Data from the pmd*CRC I4 project compilation based on Waring (1990) stable isotope data..

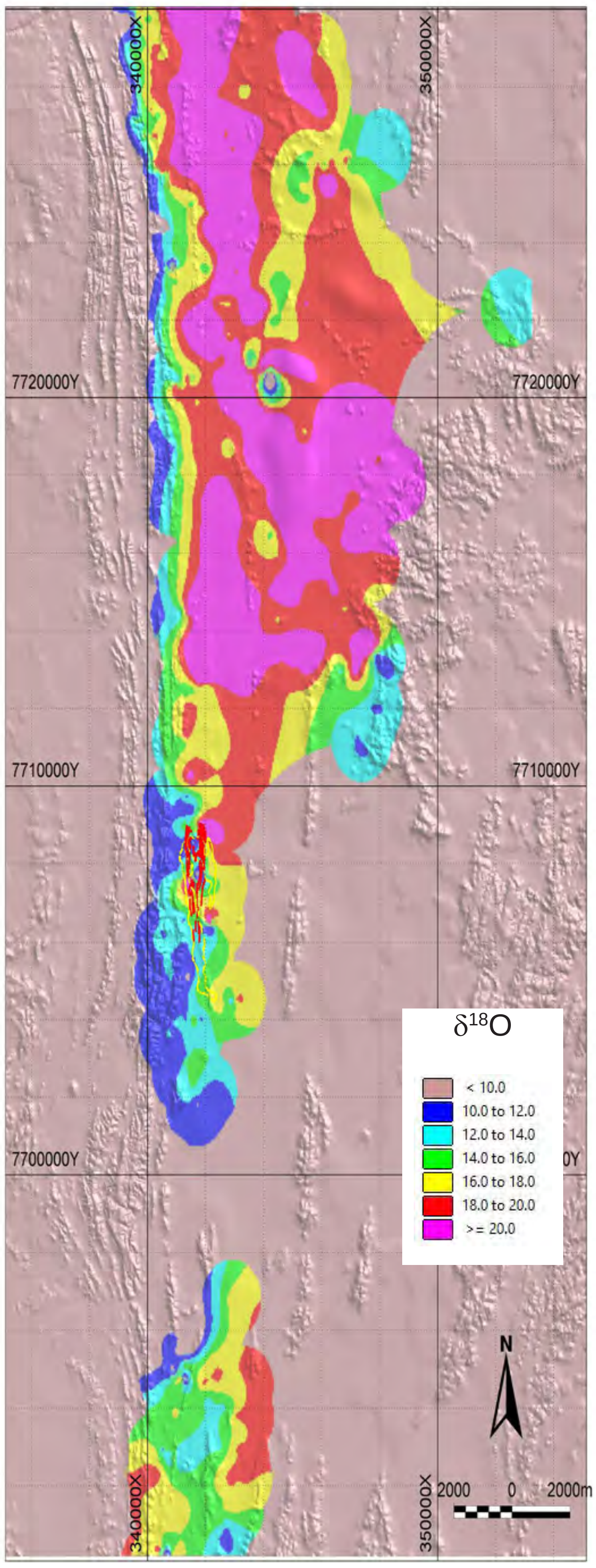

Figure 2.30. Regional pattern of $\delta^{18}O$ with all values projected to surface, showing a complex pattern but also showing a $\delta^{18}O$ depletion around and to the south of the mine. Data from the pmd*CRC I4 project compilation based on Waring (1990) stable isotope data.. .

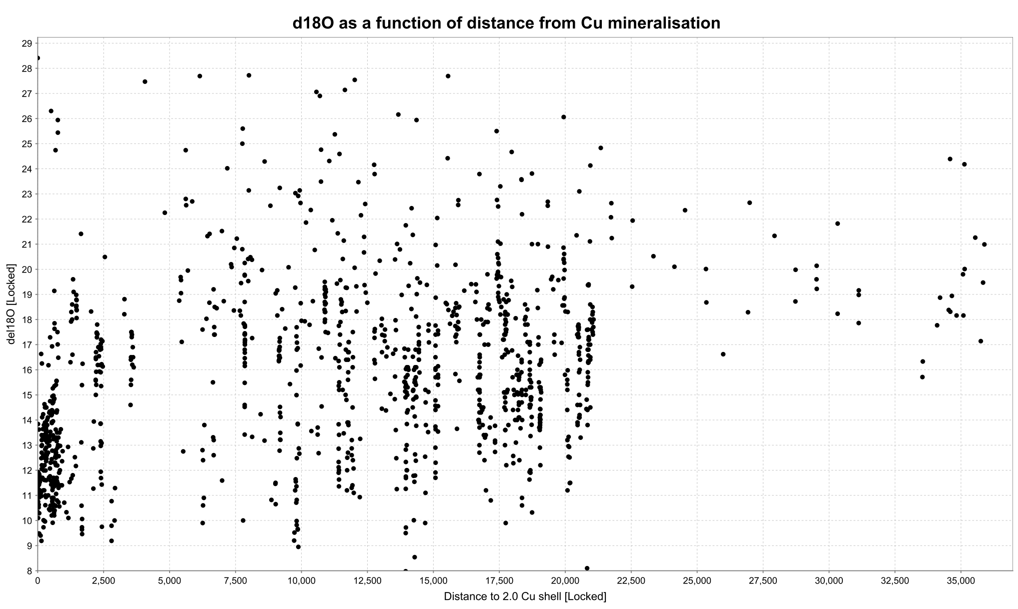

Figure 2.31. X-Y plot of $\delta^{18}O$ plotted against distance from the 2% copper shell, showing a depleted zone near the copper orebodies but also highlighting the existence of low $\delta^{18}O$ values in samples at a significant distance from copper mineralization. Data from the pmd*CRC I4 project compilation based on Waring (1990) stable isotope data.. .

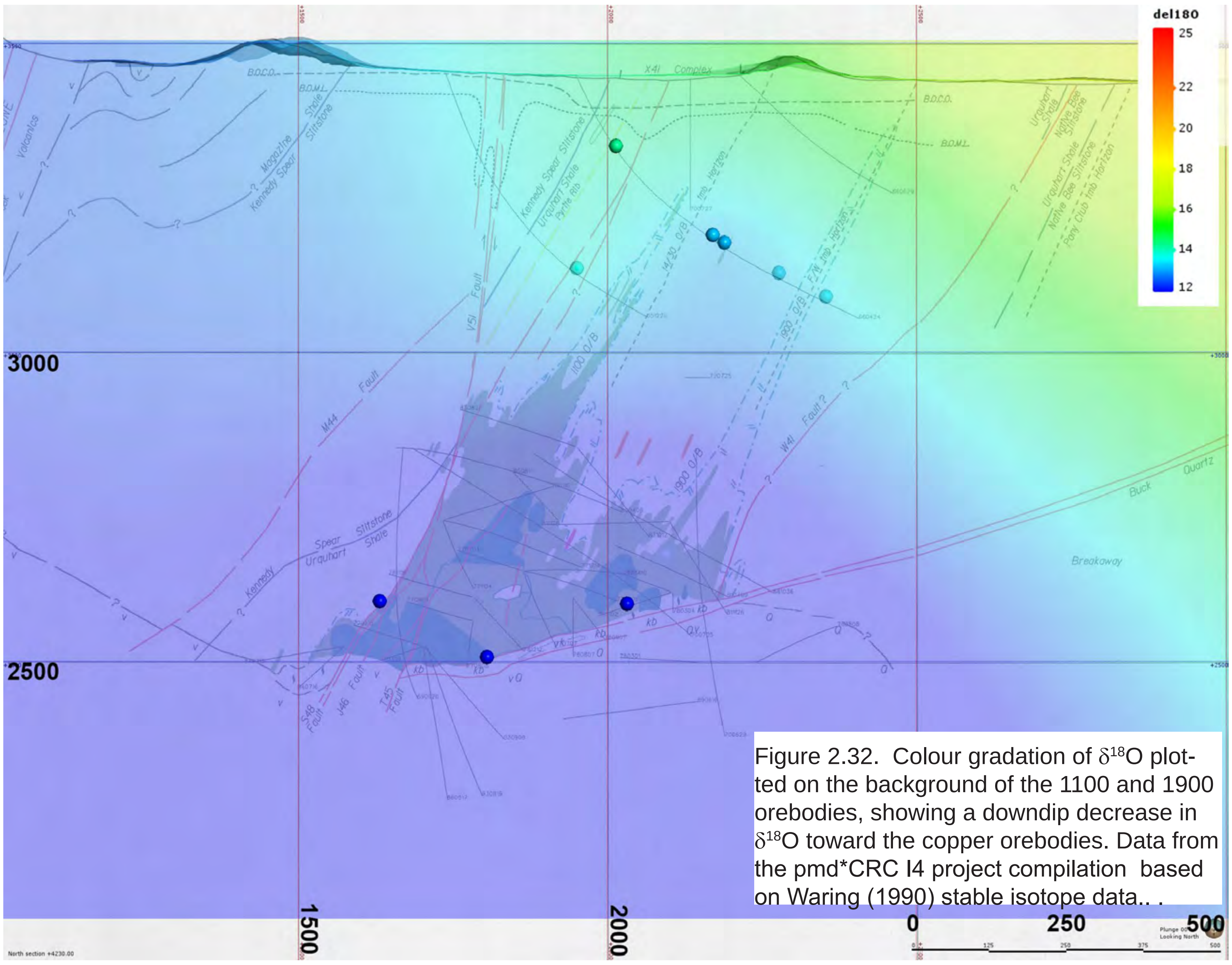

Figure 2.32. Colour gradation of $\delta^{18}O$ plotted on the background of the 1100 and 1900 orebodies, showing a downdip decrease in $\delta^{18}O$ toward the copper orebodies. Data from the pmd*CRC I4 project compilation based on Waring (1990) stable isotope data.. .

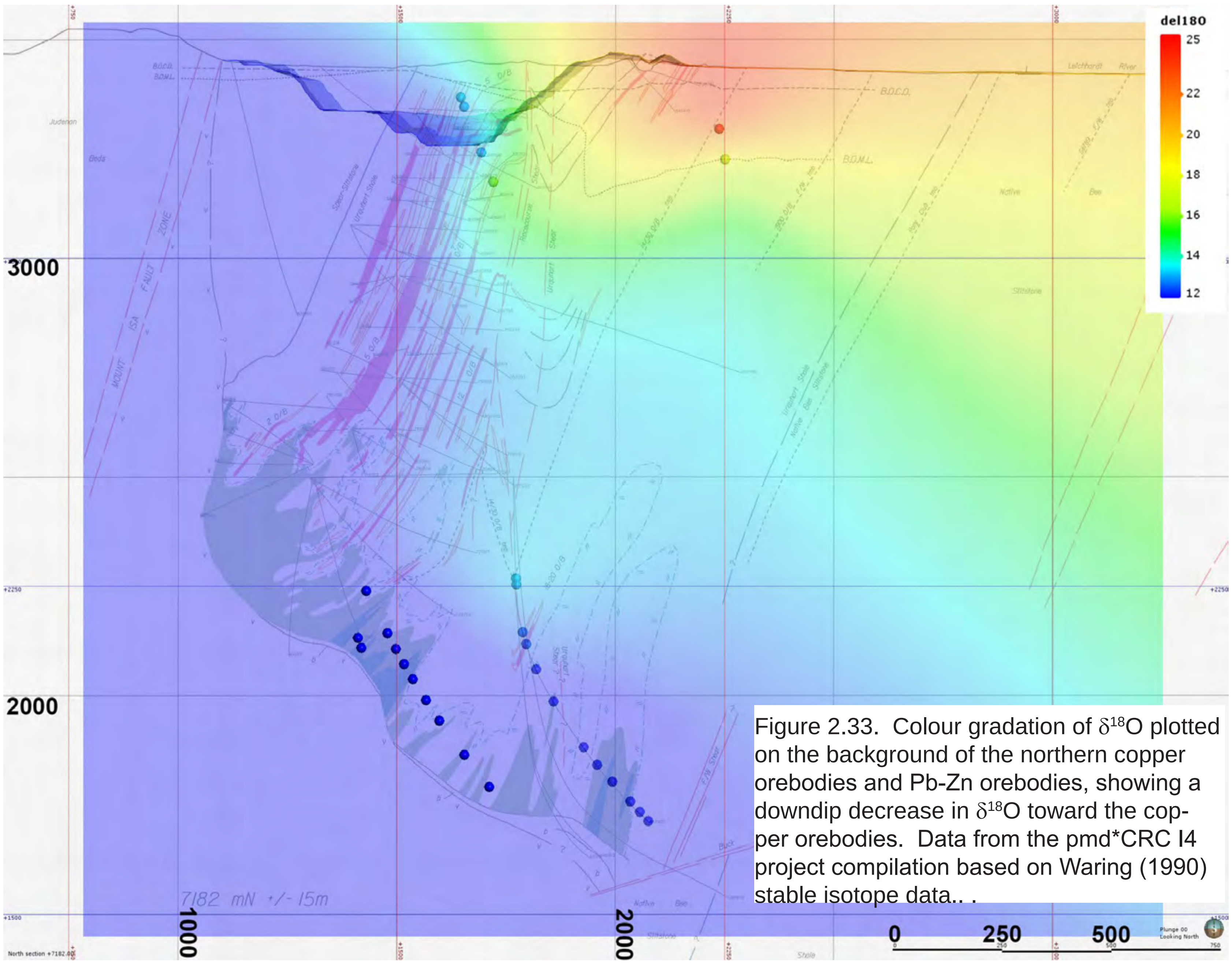

Figure 2.33. Colour gradation of $\delta^{18}O$ plotted on the background of the northern copper orebodies and Pb-Zn orebodies, showing a downdip decrease in $\delta^{18}O$ toward the copper orebodies. Data from the pmd*CRC I4 project compilation based on Waring (1990) stable isotope data.. .

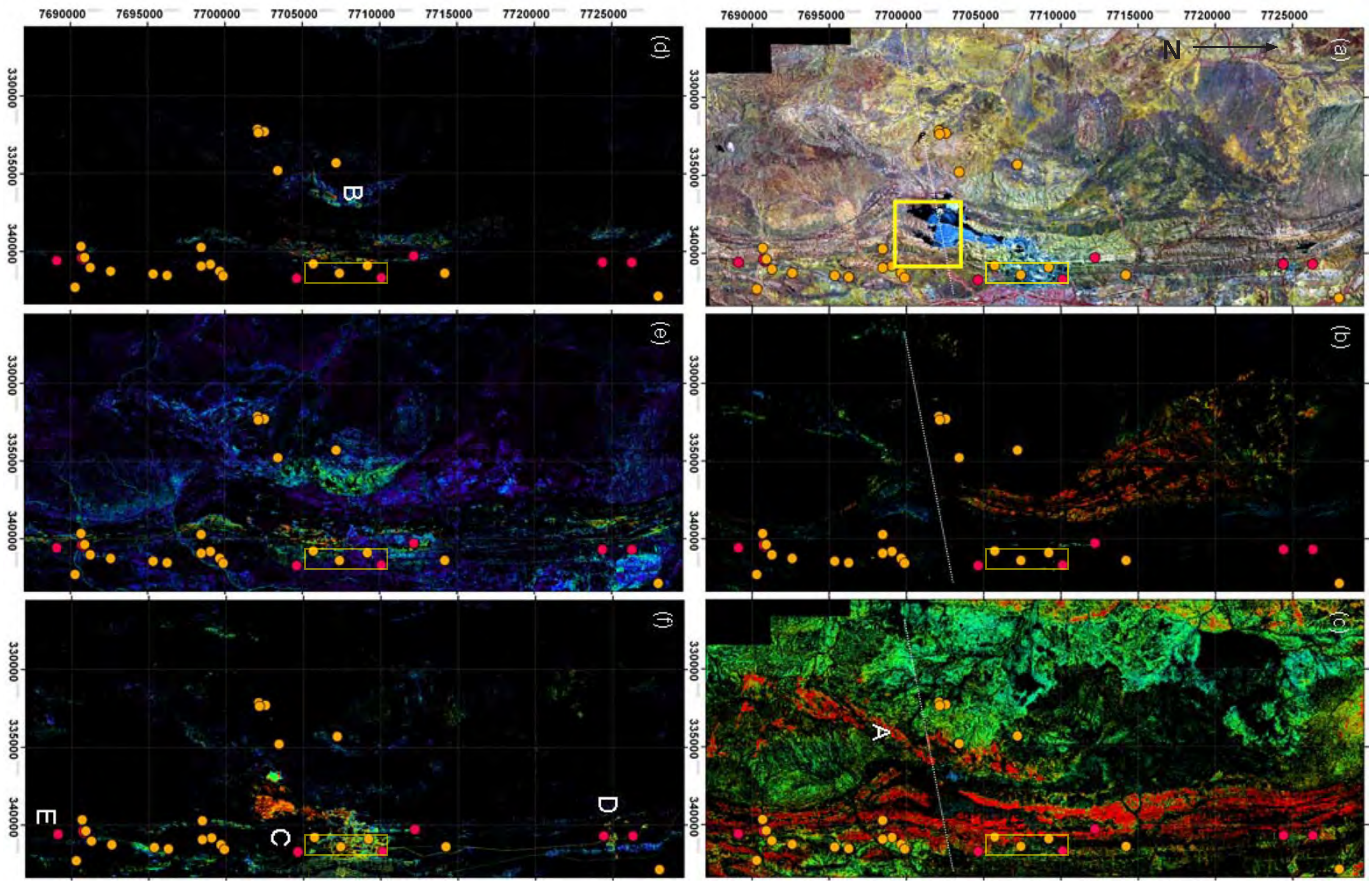

Figure 2.34. Images from Cudahy et al (2008) for the hyperspectral survey covering the Mount Isa deposit (approximate footprint shown with the yellow rectangular box). Cu (yellow) and Pb-Zn (pink) occurrences are also shown. Images are as follows: (a) false colour; (b) Ferrous iron in MgOH minerals; (c); kaolin composition; (d) hydrated silica; (e) mica crystallinity, and (f) opaques. North is to the right in each diagram.

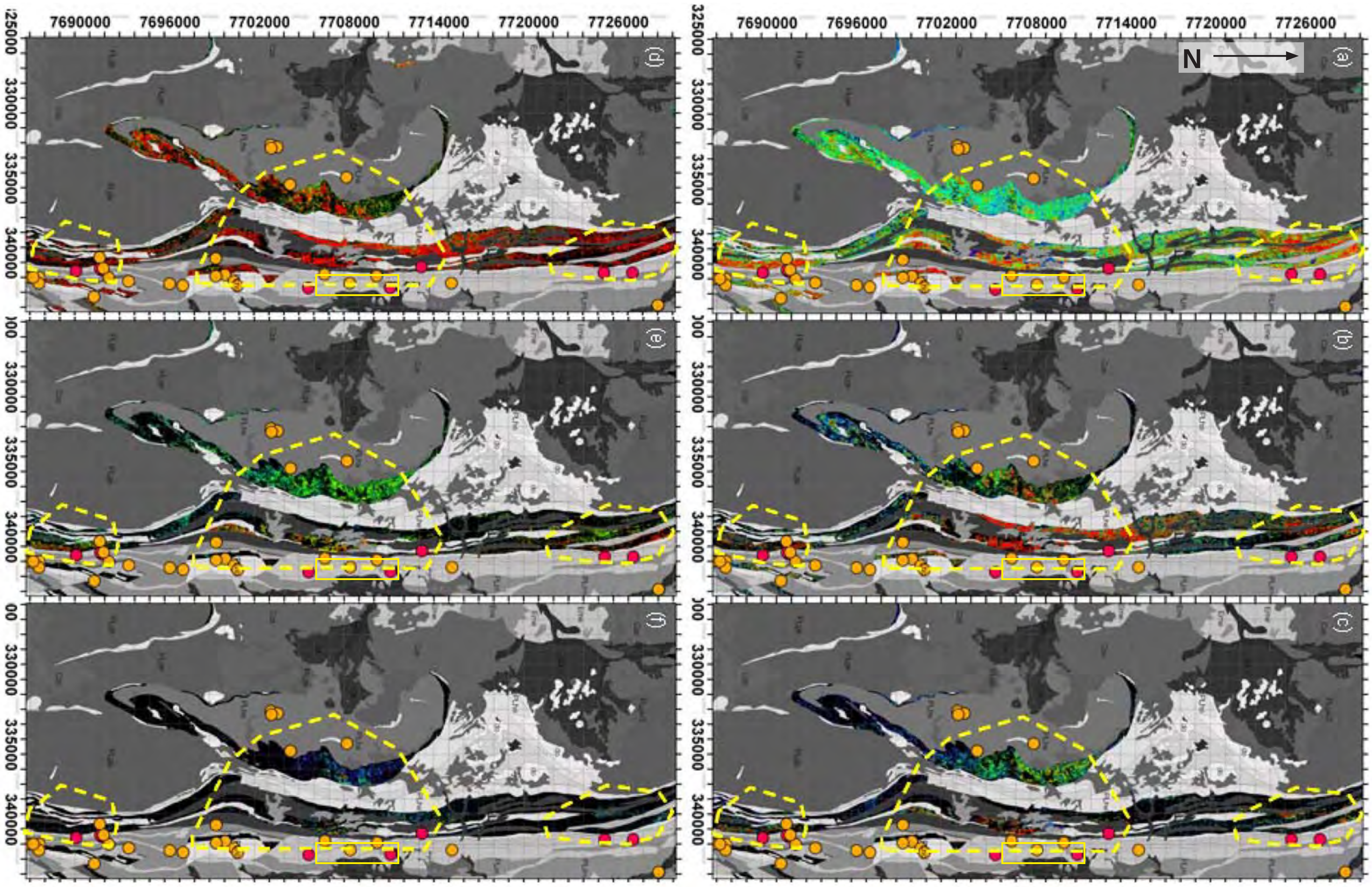

Figure 2.35. Images from Cudahy et al (2008) showing greyscale published 1:100 000 geology with quartzite units made transparent to show underlying mineral maps. Images are as follows: (a) vegetation unmixed AlOH clay content; (b) kaolin content; (c) white mica content; (d) kaolin composition; (e) white mica composition; and (f) white mica crystallinity. Interpreted mineralisation-related mineral footprints are shown with yellow dashed polygons. Yellow rectangular box - Mount Isa Cu-Pb-Zn mine footprint. North is to the right in each diagram.

REFERENCES

Betts, P. & Lister, G. (2002). Geodynamically indicated targeting strategy for shale-hosted massive sulfide Pb-Zn-Ag mineralisation in the Western fold belt, Mt Isa Terrane. Australian Journal of Earth Sciences, 49(6), 985-1010.

Carr, G.R., Sun, S-S., Page R.W., and Hinman, M., 1996, Recent developments in the use of lead isotope model ages in Proterozoic terrains:Townsville, James Cook University, Economic Geology Research Unit Contribution 55, p. 99–103.

Conaghan, E.L., Hannan, K.W. & Tolman, J. 2003. Mount Isa Cu and Pb-Ag-Zn deposits of NW Queensland, Australia. Regolith Expression of Australian Ore Systems, CRC LEME Geochemistry Special Monograph Series. 3pp

Cudahy,T., Jones,M., Thomas,M., Laukamp, C., Caccetta1, M., Hewson, R., Rodger, A., & Verrall, M., 2008 Next Generation Mineral Mapping: Queensland Airborne HyMap and Satellite ASTER Surveys 2006-2008 CSIRO report P2007/364

Davis, T. (2004). Mine-scale structural controls on the Mount Isa Zn-Pb-Ag and Cu orebodies. Economic Geology and the Bulletin of the Society of Economic Geologists, 99(3), 543-559.

Duckworth,R., 2007. Spectral and petrological study of the alteration around the Pb-Zn deposits, Mt. Isa. In. pmd*CRC I7 Final Report. Mineral system analysis of the Mt Isa–McArthur region, Northern Australia

Finlow-Bates, T. and Stumpfl, E.F., 1979, The copper and lead-zinc orebodies at Mount Isa mine, Queensland: products of one hydrothermal system: Societe Geologique Belgique Annales. v. 102, p. 497-517.

Foster, D., & Rubenach, M. (2006). Isograd pattern and regional low-pressure, high-temperature metamorphism of pelitic, mafic and calc-silicate rocks along an east – west section through the Mt Isa Inlier. Australian Journal of Earth Sciences, 53(1), 167-186.

Geological Survey of Queensland, 2011. North-West Queensland Mineral and Energy Province Report. Queensland. Department of Employment, Economic Development and Innovation, Brisbane.

Gordon, R. (2004). Isan Deformation, Magmatism and Extensional Kinematics in the Western Fold Belt of the Mount Isa Inlier. PhD Thesis, The University of Queensland. 246pp.

Gregory, M., Schaefer, J., Keays, B., & Wilde, F. (2008). Rhenium–osmium systematics of the Mount Isa copper orebody and the Eastern Creek Volcanics, Queensland, Australia: Implications for ore genesis. Mineralium Deposita, 43(5), 553-573.

Grondijs, H.F., and Schouten,C., 1937, A study of the Mount Isa ores: Economic Geology, v. 32, p. 407-450.

Hannan, K. W., Painter, M. G., Golding, S. D., & Neudert, M. K. (1999). Sedimentologic, petrographic, and sulfur isotope constraints on fine-grained pyrite formation at Mount Isa Mine and environs, northwest Queensland, Australia. Economic Geology, 94(6), 883-912.

Hannan, K., Golding, S., Herbert, H., & Krouse, H. (1993). Contrasting Alteration Assemblages In Metabasites From Mount Isa, Queensland - Implications For Copper Ore Genesis. Economic Geology And The Bulletin Of The Society Of Economic Geologists, 88(5), 1135-1175.

Heinrich, C.A., Andrew, A.S., Wilkins, R.W.T. and Patterson, D.J., 1989, A fluid inclusion and stable isotope study of synmetamorphic copper ore formation at Mount Isa, Australia: Economic Geology, v. 84, p. 529-550.

Heinrich, C.A., Bain, J.H.C., Memagh, T.P, Wyborn, L.A.I., Andrew, AS., and Waring, C.L., 1995, Fluid and mass transfer during metabasalt alteration and copper mineralisation at Mount Isa, Australia: Economic Geology, V 90, p. 705-730.

Large, R.R., and McGoldrick, P.J., 1998, Lithogeochemical haloes and geochemical vectors to stratiform sediment hosted Zn-Pb-Ag deposits; 1, Lady Loretta deposit, Queensland: Joumal of Geochemical Exploration, v . 63, p. 37-56.

Leaman, D. (1991a). Geophysical constraints on structure and alteration of the Eastern Creek Volcanics, Mt Isa, Queensland. Australian Journal of Earth Sciences, 38(4), 457-472.

Leaman, D. (1991b). Surface gravity and magnetic responses of mineralization, Mt. Isa, Northwest Queensland, Australia. Geophysics, 56(4), 542-549.

Lilly, R., & Hannan, K., 2016. Geochemistry Through Cover: Defining geochemical exploration parameters for the Cloncurry Mineral District, Queensland. Final report - Geochemistry through cover project (QDEX)

Lilly, R., Hannan, K., & Wang, M., 2014. Geochemical trials in weathered overburden: Defining exploration parameters for Mount Isa-style and IOCG mineralisation in NW Queensland, Australia. AusIMM Technical talk April 2014

Lilly, R., Taylor, D., & Spanswick, N. 2017. Mount Isa Cu-Pb-Zn deposit including George Fisher Deposit ,in Australian Ore Deposits (ed: G N Phillips), pp 473-478 (The Australasian Institute of Mining and Metallurgy: Melbourne).

Long, R.D. (2010) The Paroo Fault and the Mount Isa copper orebodies; a revised structural and evolutionary model, Mt Isa, Queensland, Australia. PhD thesis, James Cook University.

Mathias, B.V. and Clark, G.J., 1975, Mount Isa copper and silver-lead-zinc orebodies - Isa and Hilton mines: in Economic Geology of Australia and Papua New Guinea - 1. Metals, edited by CL. Knight, Australasian Institute of Mining and Metallurgy, Melbourne: Monograph No. 5, p.351-371.

McGoldrick, P.J.., 1986. Volatile and precious metal geochemistry of the Mount Isa ores and their host rocks. PhD Thesis (unpublished), The University of Melbourne.

McGoldrick, P.J. and Keays, R.R., 1990, Mount Isa copper and lead-zinc-silver ores: coincidence or cogenesis?; Economic Geology, v. 83, p. 641-650.

McGoldrick, P.J., and Large, R., 1998, Proterozoic stratiform sediment-hosted Zn-Pb-Ag deposits: AGSO Joumal of Australian Geology and Geophysics, V. 17, p. 189-196.

Miller, J.M., 2007. Structural controls on the Cu distribution at Mt Isa. pmd*CRC Project i7 report.

Neudert, M.K. and Russell, R.E., 1981, Shallow water and hypersaline features from the Middle Proterozoic Mount Isa sequence: Nature, v. 293, p. 284-286.

Page, R., & Bell, T. (1986). Isotopic and Structural Responses of Granite to Successive Deformation and Metamorphism. The Journal of Geology, 94(3), 365-379.

Painter, M. (2003). The Geochemical and Mineralogical Haloes around the Mount Isa Base Metal Orebodies. PhD thesis, U Qld

Perkins, C., Heinrich, C., & Wyborn, L. (1999). 40Ar/39Ar geochronology of copper mineralization and regional alteration, Mount Isa, Australia. Economic Geology and the Bulletin of the Society of Economic Geologists, 94(1), 23-36.

Perkins, W.G., 1984, Mount Isa silica dolomite and copper orebodies: the result of a syntectonic hydrothermal alteration system: Economic Geology, v. 79, p. 601-637.

Perkins, W.G., 1997, Mount Isa lead-zinc orebodies; replacement lodes in a zoned syndeformational copper-lead-zinc system?: Ore Geology Reviews, v. 12, p. 61-111.

Perkins, W.G., 2011. Notes on North Australia stratiform/stratabound zinc-lead-silver deposits. In: Mineralising system for stratabound sediment-hosted Zn-Pb-Ag – Western Fold Belt Province (compiled by TJ Denaro, WG Perkins & CR Dhnaram). Geological Survey of Queensland, 2011.

Russell, R.E., Cox, J.L., & Payne,L. E., 1973 Geological map of Mount Isa District. Mount Isa Mines Ltd.

Sandra Jakob, Richard Gloaguen, & Carsten Laukamp. (2016). Remote Sensing-Based Exploration of Structurally-Related Mineralizations around Mount Isa, Queensland, Australia. Remote Sensing, 8(5), 358.

Stanton, R.L., 1963. Constitutional features of the Mount Isa sulphide ores and their interpretation. Proc. Australas. Instn. Min. Metall., 205 : 131-153.

Swager, C.P., 1985, Syndeformational carbonate-replacement model for the copper mineralisation at Mount Isa, northwest Queensland: a microstructural study: Economic Geology, v. 80,p. 107-125.

Tarlowski, C.Z., and Scott, D.L., 1999 Geophysical Investigation of North Central Australia - Images, Algorithms and Crustal Models. Australian Geological Survey Organisation. AGSO Record 1998/27

Waring, C.L., 1990, Genesis of the Mt Isa Cu ore system: unpublished PhD thesis, Monash University, Victoria, Australia.

Wilde, A., Jones, P., Gessner, K., Ailleres, L., Gregory, M., & Duncan, R. (2006). A geochemical process model for the Mount Isa copper orebodies. Economic Geology and the Bulletin of the Society of Economic Geologists, 101(8), 1547-1567.